






Universitat Autònoma de Barcelona

**ADVERTIMENT.** L'accés als continguts d'aquesta tesi queda condicionat a l'acceptació de les condicions d'ús establertes per la següent llicència Creative Commons:  [http://cat.creativecommons.org/?page\\_id=184](http://cat.creativecommons.org/?page_id=184)

**ADVERTENCIA.** El acceso a los contenidos de esta tesis queda condicionado a la aceptación de las condiciones de uso establecidas por la siguiente licencia Creative Commons:  <http://es.creativecommons.org/blog/licencias/>

**WARNING.** The access to the contents of this doctoral thesis it is limited to the acceptance of the use conditions set by the following Creative Commons license:  <https://creativecommons.org/licenses/?lang=en>

**Study of Se-biofortified functional food:  
Interactions and competing mechanisms  
among different elements using  
synchrotron analytical techniques**

**Nithyapriya Manivannan**

**Doctoral thesis  
Doctoral program in Chemistry**

**Directors:  
Dr. Laura Simonelli  
Dr. Roberto Boada Romero  
Prof. Manuel Valiente Malmagro**

**Department of chemistry  
Faculty of sciences  
2021**





**Thesis report submitted in aspiration for doctoral degree by**

**Nithyapriya Manivannan**

**Director's approval**

**Dr. Laura Simonelli  
CLAESS beamline  
ALBA synchrotron**

**Dr. Roberto Boada Romero  
Department of Chemistry  
GTS group**

**Prof. Manuel Valiente Malmagro  
Department of Chemistry  
GTS group**

**Bellaterra, Barcelona  
23/09/2021**



## Acknowledgements

I would like to express my sincere gratitude to my supervisors - Laura and Roberto. Firstly, thanks for giving me this opportunity and walking me through every step along the past three years. Coming from a different background, I couldn't have survived without your constant guidance and patient teachings. I couldn't imagine my doctoral work otherwise.

Laura, thank you for your persistent support and teaching. You have always prioritized my thesis in your busy schedule and never let any obstacles get in the way of work. I have learnt a lot from you and your suggestions have always helped me to grow both professionally and personally. I have always admired your work and special thanks for all the beamtimes. I will always remember your advice to be more confident in my work and I am sure to take it along, together with your teachings.

Roberto, thank you for always being there and for your continuous teachings, encouragement and guidance. Irrespective of your schedule, you have always set out time to help from planning to following up all the work whether small or big. Always helped me in every aspect for continuous flow of work. I have always admired your work and professional ethics. It was very hard for me to catch up to your perfection. It was a good learning curve for me. Special thanks for all the hectic beamtime measurements and taking care of the plants too. I am happy to say that I have gained valuable knowledge from you, to always follow in both career and life.

Manolo, thank you for accepting me in your team and supervising my thesis. You have always encouraged me and your timely advice has helped me throughout the thesis.

Merce, thank you for all your support throughout these years. Without your guidance I wouldn't have survived in the plants' world. You have always taken time to consult and help whenever needed. Thanks for your time in reviewing and helping me understand the physiology perspective of the work.

Carlo, thank you for your support and guidance all these years. You have always been friendly and helped whenever needed. Thanks for helping me with endless scripts for data analysis. It really helped me a lot during the thesis work.

Giulio, thank you for always being friendly and encouraging. Also for helping me with my measurements during the lockdown. I can imagine how hard it would have been to find my samples.

Vlad, thank you for all your valuable advice and help. You always have something to teach and encourage.

Jose, thank you for always helping me and teaching me Spanish phrases. Thanks Nitya and Wojciech for making my initial days easy.

I am lucky to have been working with you all at CLÆSS, I will always cherish my time at ALBA. I wouldn't have survived Spain if not as a member of GTS. I always feel blessed to be part of the team. You all are life savers always having each other's back with a smile.

Mon thank you for all your help with the crazy number of ICP-MS measurements. You were always kind and ready to help. You are a positive encouragement for the team.

Thanks to the vibrant biomat team Manu, Sandra, Jorge and Manu. Manu big thanks to you, I cannot imagine my ICP-MS days otherwise. Sandra is always friendly and helpful. Jorge, always fighting for the microwave with me, thanks for always being accommodative and helpful.

Iris always a special thanks to you, the time I shared your office would be one of the good times. Thanks for helping me with my plants in late days and your conversations. Thanks Laia, it was nice to work with you in lab A and to hear about Joules too. Victor, thanks for always helping and being there.

Marcia and Marylin, I am very happy to have shared the plants lab with you two. Lou and Dong, it was nice to work along with you. Thanks for sharing your traditions among us. Maria Angels and Tingting, thanks a lot to you both for teaching me from your experience. My journey would have been hard without your help and constant support.

Thanks to Gustavo, Crisitina, Montse, Mari, Alba for their support and for welcoming me to the team. Also, thanks to all the members who have shared the time in GTS with me. Even though I missed a lot, I always liked the get-togethers with you all. Thanks for being super nice and welcoming.

People from plants always played an important role in my thesis. They were constantly encouraging. Maria, I cannot thank you enough, you have always helped me in understanding the plant world and special thanks for your constant encouragement and support. Solae, Danielle, Laura, Rosa, Silvia, thanks to you all for being supportive and welcoming.

I would also like to thank Ibraheem and Tanya from MIRAS beamline, both of you have been really supportive and helpful.

Maria del Mar, from histology, thanks to you for your initiative and help in trying the wheat sections without treatment. It was a nice experience to learn the technique under your guidance.

David, thank you for accepting me for the secondment at your lab in CRAG. It was a nice experience to work under with you and your team. Silvia, special thanks to you, for guiding me and teaching me the molecular world. Albert, thanks for teaching me the primer designing.

Thanks Stuart, from Diamond beamline for helping us with the beam time. It wouldn't have been possible to do it remotely otherwise.

Thanks to Elena from the doctoral school for help and kind replies. Pliar, thank you for helping with the in-house proposals. Thanks to Diami, Inma, Enric, Teresa secretaries at ALBA for always were processing the purchase requests on time. Thanks to Clara and Eduardo for taking care of all my paperwork. Thanks Laura Cabana for arranging the DOC-FAM events and helping us in all the processes related to the project.

I couldn't complete without thanking my family for being the backbone throughout these years. If it was not for their love, constant encouragement and immense support I wouldn't have been here.

I would like to acknowledge the in-house beamtime from CLÆSS beamline and official beamtime at CLÆSS and MIRAS beamline at ALBA. Also, I thank DOC-FAM for funding my doctoral studies and helping me to achieve it without any impediments.



## Summary

Selenium (Se) is one of the essential micronutrients needed for proper metabolic function of humans. Indeed, Se plays an active role in several functions, including antioxidant and immune responses, reproduction, cardiovascular and muscular functioning. The form of the Se species and their concentration have a key role in their bioavailability in humans. Generally, in humans the inorganic Se species (selenite, Se(IV) and selenate, Se(VI)) are less bioavailable than the organic species (e.g. selenocysteine, SeCys; selenomethionine, SeMet) which can be easily incorporated in the body to fulfil metabolic activities.

Se is incorporated into the human body from food sources. The concentration of Se in the soil where the food is produced directly correlates with the Se availability to the population in the region. In Europe, especially in the northern and western part, Se is deficient in soils, challenging the recommended intake (e.g. 55-70 µg of Se/day for adults). Se supplements are commercially available, however, prolonged dosage and toxicity effects are of high concern. Plants have the natural ability to transform inorganic Se species to more bioavailable organic Se forms which are better assimilated by humans. Indeed, in some countries like New Zealand and Finland, large scale Se biofortification of food crops were being practised. However, there are several important aspects like the total Se accumulated, tolerable limits for the plants and in turn to humans, the species of Se assimilated in the plants, environmental toxicity of Se fertilization, Se metabolism in crops, competing mechanisms with other soil pollutants that are yet to be addressed in detail. In depth knowledge in these areas will help us to better design the fortification practices and acquire improved Se-biofortification results without affecting the agronomy practices.

This study focuses on the Se-biofortification of wheat and it has two main objectives. Firstly, to analyse the competing behaviour of Se with pollutants (Cd or Hg) in hydroponic culture, and, secondly, to assess how different Se application methods (soil or foliar) affect the Se species produced by the plant in soil culture. Overall, we are aiming to understand the mechanisms affected and the possible interaction in the plants with respect to Se concentration and the chemical transformation of Se species.

In hydroponic culture, Se biofortified wheat plants were grown with and without Cd, a common agricultural pollutant. In this study, different percentage ratio of Se<sup>4+</sup>/Se<sup>6+</sup> (25/75, 50/50,

75/25) treatments were applied. The objective is to identify the Se species and their accumulation in the grains which are the final edible part and how this mechanism takes place by analysing the different parts of the plant. We have studied the plant growth characteristics, the concentration of different elements in plants and how Se species are affected under Cd pollution using X-ray absorption spectroscopy (XAS). Complementary studies with respect to sulphur (S) speciation in plants were analysed to address Se effects, as S metabolism is a direct analogous to Se assimilation pathway in plants. Fourier transform infrared spectroscopy (FTIR) experiments were carried out to study the amide band differences based on treatments along the plants. Molecular gene expression studies on short term wheat plants exposed to Cd in hydroponic culture were performed on specific genes related to S transporters, species metabolism, and stress response. In general, S transporter genes is more expressed in aerial parts and particularly in  $\text{Se}^{6+}$  treatment as they directly compete with sulfite for plant uptake. The genes indicating metabolism shows major differences in  $\text{Se}^{4+}$  treatments (also in Cd presence), as  $\text{Se(IV)}$  could be transformed to organic species more actively. The stress response genes affected by Cd presence were majorily seen in shoots and less in roots even under less Cd exposure in study. This has helped us to have a more comprehensive view in order to better understand the plant's interaction with Se under the absence and presence of pollutants. Generally, we find that Cd affects the Se biofortification process, in terms of both the Se accumulation and the species formation. In addition, getting elemental and spectroscopy maps in grains has helped us to get information about the distribution of the Se species in the different grain regions like eye, endosperm, filament and bran, which, instead, looks not strongly affected by the treatment applied.

Mercury (Hg) speciation in Se biofortified wheat plants grown hydroponically under Hg pollutant was analysed. We studied the overall protective nature of Se against Hg in plants and how it affects Hg species in the plants. XAS was used to this purpose. Irrespectively of the Se treatments applied, the plants grown under Hg pollution form toxic methylated Hg complexes which are harmful to humans. The 50/50 mixture of  $\text{Se}^{4+}$  and  $\text{Se}^{6+}$  species in the treatment reduces the accumulation of methylmercury in grains, offering protection against Hg to a certain extent.

Se biofortification in soil pot-culture was used as an intermediate step to large scale production and commercially viable cultures. Conversely to the hydroponic culture case, the interaction of Se with the growing media, i.e. soil, influences the solubility and mobility of Se

species according to the soil properties (pH, organic matter, clay content, type of soil). This study includes both either soil or foliar based Se application. Different Se treatments including, individual inorganic Se ( $\text{Se}^{4+}$  or  $\text{Se}^{6+}$ ) and a 1:1 mixture of both were used. We analysed the concentration of different essential nutrients and how the Se speciation in soil changes after a long-term cultivation of the wheat plants. The concentration of different elements in the plants was analysed together with the growth parameters to learn the effects of Se application. In addition, the speciation of Se along the plants and the spatial distribution of the elements and Se species in grain sections were studied. Complementary studies of S speciation and functional groups of proteins (amide-I:  $1600\text{-}1700\text{ cm}^{-1}$ , amide-II:  $1500\text{-}1400\text{ cm}^{-1}$ ) with the help of  $\mu\text{XRF}$ , XAS, and FTIR in grains were performed.

Generally, selenate has been identified as the best Se treatment in soils. This is based on the grain yield and Se concentration achieved in grains. On the other hand, soil application is more efficient over the foliar one, thus, considering the former methodology to be followed. Moreover, not only the application methods, but also the total Se accumulation in plants is related with the Se species formed in the grains, suggesting that attention should be paid to both parameters to control the Se biofortification process.

Globally, the here reported results help to understand the Se plant uptake mechanisms and its interaction with pollutants and permit to improve the Se biofortification practices on wheat. The thesis reports valuable information for achieving the formation of the desired Se species in wheat grains, reducing the toxicity to the plants, and to finally help the society to access an adequate Se intake which benefits the human's dietary needs.

## Resumen

El selenio (Se) es uno de los micronutrientes esenciales necesarios para las funciones metabólicas adecuadas de los seres humanos. De hecho, el Se juega un papel activo que incluye las respuestas antioxidantes e inmunes, la reproducción, el funcionamiento cardiovascular y muscular. La forma de las especies de selenio y su concentración juegan un papel importante en su biodisponibilidad en humanos. Generalmente, en los seres humanos, las especies inorgánicas de Se (selenito, Se (IV) y selenato, Se (VI)) son menos biodisponibles que las especies orgánicas (por ejemplo, selenocisteína, SeCys; selenometionina, SeMet) que se pueden incorporar fácilmente en el cuerpo para cumplir actividades metabólicas.

Se incorpora al cuerpo humano a partir de fuentes alimentarias. La concentración de Se en el suelo donde se produce el alimento se correlaciona directamente con la disponibilidad de Se para la población de la región. En Europa, especialmente en la parte norte y occidental, el Se es deficiente en los suelos, desafiando la ingesta recomendada (por ejemplo, 55-70  $\mu\text{g}$  de Se / día para adultos). Los suplementos de Se están disponibles comercialmente, sin embargo, la dosis prolongada y los efectos de toxicidad son de mayor preocupación. Las plantas tienen la capacidad natural de transformar especies de Se inorgánico en formas de Se orgánico más biodisponibles que son aceptables para los seres humanos. En algunos países como Nueva Zelanda y Finlandia, se estaba practicando la biofortificación con Se de cultivos alimentarios a gran escala. Sin embargo, existen varios aspectos importantes como el Se total acumulado, límites tolerables para las plantas y a su vez para los humanos, las especies de Se asimiladas en las plantas, la toxicidad ambiental de la fertilización del Se, el metabolismo del Se en los cultivos, los mecanismos que compiten con otros contaminantes del suelo. que aún no se han abordado en detalle. Un conocimiento profundo en estas áreas nos ayudará a diseñar mejor las prácticas de fortificación y adquirir mejores resultados de biofortificación con Se sin afectar las prácticas de agronomía.

Este estudio se centra en la biofortificación Se del trigo y tiene dos objetivos principales. En primer lugar, analizar el comportamiento competitivo del Se con los contaminantes (Cd o Hg), en cultivo hidropónico y, en segundo lugar, evaluar cómo los diferentes métodos de aplicación de Se (suelo o foliar) afectan a las especies de Se producidas por la planta en cultivo en suelo. En general, nuestro objetivo es comprender los mecanismos afectados y la posible interacción en las plantas con respecto a la concentración de Se y la transformación química de las especies de Se.

En cultivo hidropónico, se cultivaron plantas de trigo biofortificado con Se con y sin Cd, un contaminante agrícola común. En este estudio, se aplicaron diferentes proporciones porcentuales de tratamientos Se<sup>4+</sup> / Se<sup>6+</sup> (25/75, 50/50, 75/25). El objetivo es identificar las especies de Se y su acumulación en los granos que son la parte final comestible y cómo se produce este mecanismo analizando las diferentes partes de la planta. Hemos estudiado las características de crecimiento de las plantas, la concentración de diferentes elementos en las plantas y cómo las especies de Se se ven afectadas por la contaminación por Cd mediante espectroscopía de absorción de rayos X (XAS). Se analizaron estudios complementarios con respecto a la especiación de azufre (S) en plantas para abordar los efectos del Se, ya que el metabolismo del S es un análogo directo a la vía de asimilación del Se en las plantas. Se llevaron a cabo experimentos de espectroscopia infrarroja por transformada de Fourier (FTIR) para estudiar las diferencias de bandas de amida basadas en tratamientos a lo largo de las plantas. Se realizaron estudios de expresión de genes moleculares en plantas de trigo a corto plazo expuestas a Cd en cultivo hidropónico en genes específicos relacionados con los transportadores de S, el metabolismo de las especies y la respuesta al estrés en las plantas. En general, los genes transportadores S se expresan más en las partes aéreas y también en el tratamiento con Se<sup>6+</sup>, ya que compiten directamente con el sulfato por la absorción de las plantas. Los genes que indican metabolismo muestran diferencias importantes en los tratamientos de Se<sup>4+</sup> (también en presencia de Cd), ya que el Se (IV) podría transformarse en especies orgánicas de forma más activa. Los genes de respuesta al estrés afectados por la presencia de Cd se observaron principalmente en los brotes y menos en las raíces, incluso con menos exposición a Cd en el estudio. Esto nos ha ayudado a tener una visión más completa para comprender mejor la interacción de la planta con Se en ausencia y presencia de contaminantes. Generalmente, encontramos que el Cd afecta el proceso de biofortificación de Se, tanto en términos de acumulación de Se como de formación de especies. Además, la obtención de mapas elementales y espectroscópicos en granos nos ha ayudado a obtener información sobre la distribución de las especies de Se en las diferentes regiones de granos como ojo, endospermo, filamento y salvado, que, en cambio, no parece muy afectado por el tratamiento aplicado. Se analizó la especiación de mercurio (Hg) en plantas de trigo biofortificado con Se cultivadas hidropónicamente bajo contaminante Hg. Se estudió la naturaleza protectora general del Se contra el Hg en plantas y cómo se varían las especies de Hg en las plantas usando XAS. Descubrimos que, independientemente de los tratamientos con Se, las plantas contaminadas con Hg forman complejos tóxicos de Hg

metilado que son dañinos para los seres humanos. La mezcla 50/50 de especies  $\text{Se}^{4+}$  y  $\text{Se}^{6+}$  en el tratamiento reduce la acumulación de metilmercurio en los granos, ofreciendo protección contra el Hg hasta cierto punto.

Se utilizó la biofortificación en suelo en macetas como un paso intermedio para la producción a gran escala y cultivos comercialmente viables para especies de plantas superiores. A la inversa del caso del cultivo hidropónico, la interacción del Se con el medio de cultivo, es decir, el suelo, influye en la solubilidad y movilidad de las especies de Se en el suelo según sus propiedades (pH, materia orgánica, contenido de arcilla, tipo de suelo). Este estudio se dividió en aplicación de Se a base de suelo y foliar. Se utilizaron diferentes tratamientos de Se, incluyendo Se inorgánico individual ( $\text{Se}^{4+}$  y  $\text{Se}^{6+}$ ) y una mezcla 1: 1 de ambos (Semix). Analizamos la concentración de diferentes nutrientes esenciales en los suelos y cómo cambia la especiación de Se en el suelo después de un cultivo a largo plazo de las plantas de trigo. Para las plantas, se analizó la concentración de diferentes elementos junto con los parámetros de crecimiento para conocer los efectos de la aplicación de Se. Además, se estudió la especiación de Se a lo largo de las plantas y la distribución espacial de los elementos y especies de Se en secciones de grano. Se realizaron estudios complementarios de especiación S y grupos funcionales de proteínas (amidaI / 1600-1700  $\text{cm}^{-1}$ , amidaII / 1500-1400  $\text{cm}^{-1}$ ) con la ayuda de FTIR en sesiones de grano.

Generalmente, el selenato ha sido identificado como el mejor tratamiento de Se en suelos, siendo la aplicación al suelo más eficiente. Además, no solo los métodos de aplicación, sino también la acumulación total de Se en las plantas están relacionados con las especies de Se formadas en los granos, lo que sugiere que se debe prestar atención a ambos parámetros para controlar el proceso de biofortificación de Se.

Los resultados aquí reportados ayudan a comprender los mecanismos de absorción de las plantas de Se y permiten mejorar las prácticas de biofortificación de Se en el trigo. La tesis reporta información valiosa para lograr la formación de las especies de Se deseadas en los granos de trigo, reducir la toxicidad para las plantas y finalmente ayudar a la sociedad a acceder a una ingesta adecuada de Se que beneficie las necesidades dietéticas del ser humano.

## Resum

El seleni (Se) és un dels micronutrients essencials necessaris per a les funcions metabòliques adequades dels humans. De fet, el Se té un paper actiu, incloent respostes antioxidants i immunes, la reproducció, el funcionament cardiovascular i muscular. La forma de les espècies de seleni i la seva concentració juguen un paper important en la seva biodisponibilitat en humans. En general, en els éssers humans les espècies inorgàniques de Se (selenita, Se (IV) i selenat, Se (VI)) són menys biodisponibles que les espècies orgàniques (per exemple, selenocisteïna, SeCys; selenometionina, SeMet) que es poden incorporar fàcilment al cos per complir-les activitats metabòliques.

Se s'incorpora al cos humà a partir de fonts d'aliment. La concentració de Se al sòl on es produeix l'aliment es correlaciona directament amb la disponibilitat de Se per a la població de la regió. A Europa, especialment a la part nord i oest, el Se és deficient en sòls, cosa que suposa un consum recomanat (per exemple, 55-70 µg de Se / dia per als adults). Els suplementes de Se estan disponibles comercialment, però, la dosificació prolongada i els efectes de toxicitat són més preocupants. Les plantes tenen la capacitat natural de transformar espècies de Se inorgàniques a formes de Se orgàniques més biodisponibles que siguin acceptables per als humans. En alguns països com Nova Zelanda i Finlàndia, s'estava practicant la biofortificació a gran escala de Se de cultius alimentaris. No obstant això, hi ha diversos aspectes importants com el límit tolerable total de Se acumulat per a les plantes i al seu torn per als humans, les espècies de Se assimilades a les plantes, la toxicitat ambiental de la fertilització del Se, el metabolisme del Se als cultius, mecanismes competitius amb altres contaminants del sòl. que encara no s'han d'abordar amb detall. Un coneixement profund d'aquestes àrees ens ajudarà a dissenyar millor les pràctiques de fortificació i a adquirir millors resultats de Se-biofortificació sense afectar les pràctiques d'agronomia.

Aquest estudi se centra en la se-biofortificació del blat i té dos objectius principals. En primer lloc, analitzar el comportament competitiu de Se amb contaminants (Cd o Hg), en cultiu hidropònic i, en segon lloc, avaluar com els diferents mètodes d'aplicació de Se (sòl o foliar) afecten les espècies de Se produïdes per la planta en cultiu de sòl. En general, volem comprendre els mecanismes afectats i la possible interacció de les plantes respecte a la concentració de Se i la transformació química de les espècies de Se.

En cultiu hidropònic, les plantes de blat biofortificades de Se es van cultivar amb i sense Cd, un contaminant agrícola comú. En aquest estudi, es van aplicar diferents percentatges de tractaments amb  $Se^{4+}$  /  $Se^{6+}$  (25/75, 50/50, 75/25). L'objectiu és identificar les espècies de Se i la seva acumulació en els grans que són la part final comestible i com té lloc aquest mecanisme mitjançant l'anàlisi de les diferents parts de la planta. Hem estudiat les característiques del creixement de les plantes, la concentració de diferents elements a les plantes i com es veuen afectades les espècies de Se per contaminació per Cd mitjançant l'espectroscòpia d'absorció de raigs X (XAS). Es van analitzar estudis complementaris pel que fa a l'especiació del sofre (S) a les plantes per abordar els efectes del Se, ja que el metabolisme del S és una via anàloga directa a la via d'assimilació del Se a les plantes. Es van dur a terme experiments d'espectroscòpia infraroja per transformada de Fourier (FTIR) per estudiar les diferències de banda amida basades en tractaments al llarg de les plantes. Es van realitzar estudis d'expressió de gens moleculars en plantes de blat a curt termini exposades a Cd en cultiu hidropònic en gens específics relacionats amb transportadors de S, metabolisme de les espècies i resposta a l'estrès en plantes. En general, els gens transportadors S s'expressen més en parts aèries i també en el tractament amb  $Se^{6+}$ , ja que competeixen directament amb el sulfat per a la captació de plantes. Els gens que indiquen metabolisme mostren grans diferències en les tractaments de  $Se^{4+}$  (també en presència de Cd), ja que el Se (IV) es podria transformar en espècies orgàniques de manera més activa. Els gens de resposta a l'estrès afectats per la presència de Cd es van observar principalment en brots i menys en arrels, fins i tot amb menys exposició a Cd en l'estudi. Això ens ha ajudat a tenir una visió més completa per comprendre millor la interacció de la planta amb Se en absència i presència de contaminants. En general, trobem que el Cd afecta el procés de biofortificació del Se, tant pel que fa a l'acumulació de Se com a la formació d'espècies. A més, obtenir mapes elementals i d'espectroscòpia en grans ens ha ajudat a obtenir informació sobre la distribució de les espècies de Se a les diferents regions de gra com ulls, endosperms, filaments i segó, que, en canvi, no es veuen fortament afectats pel tractament aplicat. Es va analitzar l'especiació de mercuri (Hg) en plantes de blat biofortificat de Se cultivades hidropònicament amb contaminants de Hg. Es va estudiar la naturalesa protectora general de Se contra Hg en plantes i com es varien les espècies de Hg en les plantes mitjançant XAS. Vam trobar que, independentment dels tractaments amb Se, les plantes contaminades per Hg formen complexos tòxics de Hg metilats que són perjudicials per als



humans. La barreja 50/50 d'espècies de  $\text{Se}^{4+}$  i  $\text{Se}^{6+}$  en el tractament redueix l'acumulació de metilmercuri als grans, oferint en certa mesura protecció contra Hg.

La biofortificació en cultiu en test del sòl es va utilitzar com a pas intermedi per a la producció a gran escala i cultius comercialment viables per a espècies vegetals superiors. Per contra, en el cas del cultiu hidropònic, la interacció de Se amb els mitjans de cultiu, és a dir, el sòl, influeix en la solubilitat i mobilitat de les espècies de Se en el sòl segons les seves propietats (pH, matèria orgànica, contingut d'argila, tipus de sòl). Aquest estudi es va dividir en aplicacions de Se basades en sòls i foliar. Es van utilitzar diferents tractaments de Se, incloent-hi Se inorgànic individual ( $\text{Se}^{4+}$  i  $\text{Se}^{6+}$ ) una barreja 1: 1 de tots dos (Semix). Hem analitzat la concentració de diferents nutrients essencials als sòls i com canvia l'especiació del Se al sòl després d'un cultiu a llarg termini de les plantes de blat. Per a les plantes, es va analitzar la concentració de diferents elements juntament amb els paràmetres de creixement per conèixer els efectes de l'aplicació de Se. A més, es va estudiar l'especiació de Se al llarg de les plantes i la distribució espacial dels elements i de les espècies de Se en seccions de gra. Es van realitzar estudis complementaris d'especiació S i grups funcionals de proteïnes (amideI /  $1600\text{-}1700\text{cm}^{-1}$ , amideII /  $1500\text{-}1400\text{cm}^{-1}$ ) amb l'ajut de FTIR en sessions de gra.

En general, el selenat s'ha identificat com el millor tractament de Se en sòls, sent l'aplicació del sòl més eficient. A més, no només els mètodes d'aplicació, sinó també l'acumulació total de Se a les plantes estan relacionats amb les espècies de Se formades als grans, cosa que suggereix que s'hauria de prestar atenció a tots dos paràmetres per controlar el procés de biofortificació del Se.

Els resultats publicats aquí ajuden a entendre els mecanismes d'adquisició de plantes de Se i permeten millorar les pràctiques de biofortificació de Se al blat. La tesi informa d'una informació valuosa per aconseguir la formació de les espècies de Se desitjades en els grans de blat, reduir la toxicitat per a les plantes i, finalment, ajudar a la societat a accedir a una ingesta adequada de Se que beneficiï les necessitats dietètiques de l'ésser humà.



## **Table of contents**

Abbreviations .....	1
Introduction.....	2
Experimental approach .....	7
Hydroponic culture .....	8
Chapter 1 .....	8
Influence of Cd pollution in Se biofortification of wheat crops .....	8
1.1 Introduction .....	9
1.2 Experimental methods.....	11
1.2.1 Cultivation in hydroponics with and without Cd.....	11
1.2.2 Sample preparation and characterization.....	13
1.3 Results and Discussion.....	15
1.3.1 Growth parameters .....	15
1.3.2 Elemental concentration along the plant .....	18
1.3.3 Se species along plant and grains .....	26
1.3.4 Sulphur speciation along the plants .....	38
1.3.5 FTIR analysis in biofortified plant .....	43
1.4 Conclusions .....	47
Chapter 2.....	49
Gene expression analysis .....	49
2.1 Introduction .....	50
2.2 Experimental methods.....	53
2.2.1 Plant samples and growing conditions with different treatments.....	53
2.2.2 RNA extraction, cDNA synthesis and quantification.....	53
2.3 Results and discussion.....	56

2.3.1 Sulphate transporters .....	56
2.3.2 Genes related to Sulphur metabolism.....	59
2.3.3 Stress responsive genes .....	61
2.4 Conclusions.....	65
Chapter 3.....	67
Mercury speciation in selenium biofortified wheat plants grown in mercury contaminated environment .....	67
3.1 Introduction.....	68
3.2 Experimental methods.....	70
3.2.1 Cultivation under Hg pollution.....	70
3.2.2 Sample preparation and analysis .....	72
3.3 Results and discussion.....	74
3.3.1 Concentration of element of interest .....	74
3.3.2 Hg speciation and component analysis along the plant.....	76
3.4 Conclusions.....	84
Soil culture .....	85
Chapter 4.....	85
Soils and Selenium.....	85
4.1 Introduction.....	86
4.2 Experimental methodology .....	88
4.2.1 Soil pre-culturing and initial analysis.....	88
4.2.2 Soil sample preparation and characterization.....	89
4.3 Results and discussion.....	89
4.3.1 Soil elemental concentration .....	89
4.3.2 Speciation in soils.....	93

4.4 Conclusions .....	95
Chapter 5 .....	96
Se biofortification by soil and foliar application .....	96
5.1 Introduction .....	97
5.2 Experiments and methodology .....	99
5.2.1 Cultivation of plants in soils by different Se application methods .....	99
5.3 Results and discussion .....	101
5.3.1 Plant growth parameters .....	101
5.3.2 Concentration of elements in the plants .....	103
5.3.3 Se speciation and distribution in the grain: XANES and $\mu$ XRF .....	108
5.3.4 Speciation and distribution of S in grains .....	122
5.3.5 FTIR in grain sections .....	126
5.4 Conclusions .....	128
Conclusions .....	131
References .....	137
ANNEX .....	1

## **Abbreviations**

**SeCys** : Selenocysteine

**SeCyst** : Selenocystine

**SeMet** : Selenomethionine

**SeMeCys** : Selenomethylcysteine

**XAS** : X-ray Absorption Spectroscopy

**XANES** : X-ray Absorption Near Edge Structure

**EXAFS** : Extended X-ray Absorption Fine Structure

**μXRF** : Micro X-ray Fluorescence

**FTIR** : Fourier Transform Infrared spectroscopy

**ICP-MS** : Inductively Coupled Plasma Mass Spectroscopy

**qPCR** : Quantitative Polymerase Chain Reaction

## Introduction

Micronutrients are essential elements necessary for humans and other living organisms in trace amounts. Generally, they include vitamins and minerals, which play an important role in a whole series of physiological functions essential for the metabolism. Food is the primary source of micronutrients for living organism, as they cannot be produced in their system.

Selenium (Se) is one of these essential micronutrients. Humans need Se in varying amounts depending upon their age group and nutritional needs (Brown and Arthur, 2021). Kids of 1 to 3 years or 4 to 13 years need 15-20 µg/day or 30-4 µg/day, respectively. Adults from 14 to 50 yrs. need 55-70 µg/day, while above 51 years, 70-100 µg/day of Se is needed. The recommended value of pregnant women is around 65 µg/day, and of 75 µg/day for the period of lactation (Brown and Arthur, 2021; Kieliszek, 2019).

The importance of Se in the human biological functions was discovered in 1957 (Brown and Arthur, 2021; Gupta and Gupta, 2017). Se is one of the crucial elements for proper functioning of the human metabolism. Indeed, in the mammalian genes, there are 30 different selenoproteins which take part in the formation of various needed metabolites to regulate the body functioning (Brown and Arthur, 2021). Glutathione peroxidase, selenoprotein P, selenoprotein W, iodothyronine deiodinases and thioredoxin reductase are some of the most prominent selenoproteins and its containing enzymes in humans (Brown and Arthur, 2021; Rayman, 2000), where Se acts as an antioxidant and reduces free radical formation, thus helping against cancer formation and aging. More in particular, thyroid functioning is related to Se which, with other elements, affects the growth of hormones. In reproduction, Se also plays an important role in fertility, embryonic implantation, and placental retention. In addition, Se is highly necessary to maintain and permit a proper functioning of muscles especially that of skeletal and cardiovascular wellbeing (Brown and Arthur, 2021; Kieliszek, 2019). Some of the known Se deficiency related endemic was Keshan and Kashin-Beck diseases (Brown and Arthur, 2021; Gupta and Gupta, 2017). The former caused cardiomyopathy and the later reported cartilage softness in arms and legs (Kieliszek, 2019). The Se level in the body is also related with diseases like Alzheimer's, depression, reduction in virulence of HIV, and fetal development (Kieliszek, 2019).

On the other end, upper tolerable limits of Se for adults is considered to be 300-400  $\mu\text{g}/\text{day}$  (Boyd, 2011; Kieliszek, 2019). In particular, it has been reported that an oral intake of 5 mg/day or inhalation exceeding 0.2 mg/cm<sup>3</sup> (volcanic eruption and organic matter decomposition) causes heavy selenium poisoning (Kieliszek, 2019; Koller and Exon, 1986). In fact, both inorganic and organic Se can cause the toxicity effects based on the organism and the Se concentration and species consumed. Se poisoning by acute toxicity leads to, among others, hair loss, tachycardia, hypotension, garlic breath, dry cough, anemia, hyper salivation, kidney malfunction. Moreover, too high Se level distorts and accelerates the sulphur metabolism leading to damage in biochemical functions of cells by over production of enzymes and proteins (Kieliszek, 2019).

In terms of Se species, Se has four different oxidation states (-2, 0, +4, +6). In nature, it is found in both organic and inorganic forms. Some of its organic forms biologically relevant are selenomethionine (SeMet) and selenocysteine (SeCys), selenodiglutathione, dimethylseleniumsulfide, dimethylselenide, while the inorganic forms include selenite ( $\text{SeO}_3^{-2}$ ), selenide ( $\text{Se}^{2-}$ ), selenate ( $\text{SeO}_4^{-2}$ ) and the elemental selenium (Se) (Fernández-Martínez and Charlet, 2009; Kieliszek, 2019). Inorganic selenium species, as selenite (Se(IV)) and selenate (Se(VI)), or organic Selenocystine (SeCyst) can be assimilated into the human system but cannot be easily incorporated into proteins. Therefore, they are less bioavailable than other selenoamino acids such as selenomethionine (SeMet), selenocysteine (SeCys), and methyl selenocystine (SeMeCys), which are instead efficiently absorbed for the needs of the metabolic activities in humans (Roman et al., 2013).

One of the major sources of bioavailable Se for humans are edible plants, since plants are able to convert inorganic Se species to bioavailable organic forms. The Se level in plants is determined by the soil properties and type of plant, with a higher concentration in leafy and grasses than in leguminous plants. The plants which can tolerate, and then accumulate, higher amount of Se are seleniferous plants (e.g., *Astragalus* species from Fabaceae family and *Stanleya pinnata* from Brassicaceae family) typically found in USA and China. In seleniferous plants, the Se accumulation ranges from 70 to 20,000  $\mu\text{g}/\text{g}$  depending on the plant species. Plants that can accumulate Se but not as a nutritional requirement for the plant are often termed as secondary accumulators. Cereal crops are considered good secondary accumulators, which typically store Se



in their seeds in a range of 0.1-0.5  $\mu\text{g/g}$ , where above 5  $\mu\text{g/g}$  of storage is toxic for the plant (Gupta and Gupta, 2017).

Generally, in soils under normal conditions plants uptake selenate form better than selenite (Lara et al., 2019; Qin et al., 2017; Ros et al., 2016; Wang et al., 2017). Selenate is absorbed by sulphate transporters, while selenite is taken up, especially in acidic soils where they are in the form of selenic acids, mainly by phosphate transporters. Organic species are taken up by amino acid transporters, however this mechanism is not yet well understood. The Se species are further reduced in the plant. In particular, selenate is reduced into selenite by ATP sulphurylase, and catalyzed with ATP reductase and GSH, it is forming organic species. Anyway, the amount of selenate accumulated is a rate limiting step in the process of Se transformation in plants. In addition, with the help of O-acetyl serine enzymes and reductase, cysteine reductase, selenite further forms SeCys. Alternatively, with the help of semethyltransferase, inorganic species can be directly converted into organic SeCys species. Further methylated species such as Semethionine (SeMet), Seleno-methylmethionine or Se-methylselenocysteine (Se-MSC) are formed from mechanisms like SeCys methyl synthase, cysteine reductase. SeMet and SeMeCys can be incorporated into proteins with the release of dimethyl selenide or dimethyl-diselenide (Ellis and Salt, 2003; Schiavon et al., 2020; Zhou et al., 2020).

The level of Se in foods is then directly related to the soil characteristics, therefore, Se-poor soils around the world (Koller and Exon, 1986) results in the production of Se-deficient food lacking of the essential seleno-aminoacids for humans. Indeed, the Se amount is widely distributed along the earth crust, but its concentration critically varies with soil type and texture, organic matter content, climatic factors, and with certain anthropogenic activities. For example, the Se soil content can be increased with fertilization rich in selenium, crude oil refining, and coal combustion (Boyd, 2011; Dinh et al., 2017; Qin et al., 2017; Shamberger, 1983; Sharma and Singh, 1983). Se-rich soils are present mainly in Northern parts of America, China, Australia, Ireland, while Se-poor areas include New Zealand and a wide part of Northern Europe (Gissel-Nielsen et al., 1984; Gupta and Gupta, 2017; Tóth et al., 2016).

Biofortification has been proposed to overcome such Se-deficiency in diets due to Se-poor soils. Biofortification is a process by which the plants' nutritional properties are improved by increasing the presence of the desired elements in their system either via genetic modification

(Malagoli et al., 2015) or agronomy practices (Boldrin et al., 2016; Curtin et al., 2006; Schiavon et al., 2020; Subirana, 2018; Xiao et al., 2020). Agronomical biofortification is advantageous since it is cost-effective and it can be performed in large scale applications. Currently, the most commonly practiced method consists on applying inorganic selenium species in the field as fertilizers within the approved limits (Curtin et al., 2006; Xiao et al., 2020). In Europe there is no general consensus, respect to limits and, selenium feeding is preferred in the form of sodium selenate (EFSA Journal 2017).

Current efforts are devoted to find the most effective Se application methodology to get Se-biofortification of crops with less long term effects in the agricultural land and without altering the other nutritional benefits of the plants. Two main approaches exist to provide inorganic Se species to the plants: by directly irrigating the soils, or by foliar application spraying the fertilizer over the leaf surface. In addition, the biofortification process should be optimized considering different parameters including the crop variety, the Se species used (species solubility in soil, organic matter content in soil, pH related uptake, uptake and breakdown pathways in plants), time of application, other fertilization practices during Se application (e.g. nitrogen application before fortification process increases the Se yield), and frequency of application (Curtin et al., 2008, 2006; Dinh et al., 2017; Lara et al., 2019; Z. Li et al., 2017; Lidon et al., 2019). Such parameters affect the Se assimilation pathway and the final Se species provided by the plant in the final product, the edible part of the plant. On the contrary, controlled hydroponics culture plays a vital role in understanding the mechanism of Se uptake in plants, making it the first step prior to address soil cultures (soil and foliar applications) and to pass to large scale applications (Sambo et al., 2019; Verdoliva et al., 2021).

Other factor to take into consideration is that the Se-biofortification process can be hindered by soil pollutants, which could compete with Se in the elemental soil accumulation, complex formation, and plant uptake. This is often the case of pollutants which share the same Se metabolic pathways, reducing the Se concentration and affecting the Se species distribution along the plant. Therefore, it is also essential to address the role of different pollutants in the biofortification process. Many previous works have reported antagonism behavior of selenium towards mercury, cadmium, lead, and arsenic which are some common agricultural pollutants delivered to the medium by anthropogenic activities (Dong et al., 2019; Huang et al., 2017; Tóth

et al., 2016; Zhou et al., 2020; Punshon and Jackson, 2018; Tangahu et al., 2011; Wang et al., 2014). In that respect, information regarding the major mechanisms affected by the Se biofortification practices and environmental pollutants, especially in terms of species which form in major part in successful biofortification, has not been reported yet.

In this work, we have studied the Se-biofortification of wheat as it is one of the three major cereals crops consumed and produced around the world along with rice and maize. They are used for both human food and livestock feed. The starch content in wheat is higher compared to proteins at 60-80% however, the 10-20% protein content present is essential of human metabolism (Shewry, 2009). Wheat production is the second largest cultivar in Europe (Brisson et al., 2010; Poblaciones M.J et al., 2014) being the average production about 10 tons per ha (Gupta and Gupta, 2017). In addition, wheat can be easily harvested in large scale and the grains can be stored for a long time without losing their nutritional and breeding properties.

The understanding of Se formation under pollutants, by speciation studies and gene expression analysis reveals the Se metabolism and factors influenced in the plants. This helps us to address the knowledge gap in the literature in terms of species accumulation distribution and plant tolerance. In addition to the application methods in soil culture, foresee strategies in large scale agronomic practices.

## Experimental approach

The main aims of this work are to biofortify wheat with Se and to understand the Se accumulation mechanism and the fate of Se in the plants, and, in addition, to analyse the influence of common pollutants like Cd and Hg into the biofortification process. Respect to the biofortification, parameters like Se treatment applied, growth medium, Se application method and, influence of pollutants were studied to compare, understand and choose the best conditions for performing the most effective and sustainable biofortification process.

Thus, the work was broadly divided into two sections based on the growth medium

### 1) Hydroponics

- Long term wheat plants were grown under different ratio of inorganic Se mixture ( $\text{Se}^{4+}/\text{Se}^{6+}$ ) treatments applied at the vegetative stage, with or without Cd pollution. The elemental concentration, Se species and their spatial distribution in grains, Cd speciation, S speciation and distribution in grains, FTIR of bulk samples were analyzed.
- qPCRs of genes related to S and Se metabolism were performed in short term wheat plants grown with individual inorganic Se treatments and Se mixture with or without Cd, to understand the uptake, distribution and speciation mechanisms of Se to easily exploit the knowledge in soil-based cultures.
- Also, the Hg speciation in Se biofortified wheat plants under Hg pollution was studied and analysed.

### 2) Soil cultivation

- Long term wheat plants were cultivated in soil medium, and biofortified with Se by direct soil application or by foliar application. Individual inorganic Se species ( $\text{Se}^{4+}$  and  $\text{Se}^{6+}$ ) and mixture of both (applied at fluorescence stage) were used in the study.
- Plant samples (divided as roots, stems, leaves and grains) were analyzed for their elemental concentration, Se speciation along different parts of the plant, Se species and spatial distribution in grains, S speciation and distribution in grains, FTIR in grain sections were studied.

**Hydroponic culture**

**Chapter 1**

**Influence of Cd pollution in Se biofortification of wheat crops**

## 1.1 Introduction

Soil pollution, especially with heavy metals is a growing environmental concern (Motuzova et al., 2014). In agriculture, the presence of pollutants in the soil could affect the Se-biofortification process. In fact, the antagonism between Se and other heavy metals (e.g. Hg, Cd, Pb) and their effects on plant functioning and elemental uptake must be considered (Chen Shan et al., 2009; Landberg and Greger, 1994; Tóth et al., 2016). Among the most common pollutants, cadmium (Cd) is a non-essential toxic compound for both plants and humans, that cause damage to lungs, liver functions, lead to cancer, and induce kidney diseases (Johri et al., 2010). Cd can occur naturally in agricultural soils, although recent reports warn about the increase of Cd on soils due to the continuous use of phosphate based fertilizers (Roberts, 2014). Despite the fact that several restrictions have been implemented in different European countries from 1970s (Ulrich, 2019), Cd concentrations in agricultural soils of around 10-20  $\mu\text{g/g}$  have been reported (Tóth et al., 2016), whereas the EU regulation recommend a Cd limit of 1-3  $\mu\text{g/g}$  (Commission Regulation (EC) No 1881/2006, n.d.; Council Directive 86/278/EEC of 12 June 1986, n.d.). Hence, it is necessary to study the influence of Cd in the Se biofortification process, to adapt the developed methodologies to large scale production (2020 (EU), n.d.) (Boldrin et al., 2016; Brown and Shrift, 1982; Ellis and Salt, 2003; Gupta and Gupta, 2017; Chen et al., 2002; Wang et al., 2013, Mehes-Smith et al., 2013;).

Previous studies, reported that a 1:1 molar concentration mixture of  $\text{Se}^{4+}/\text{Se}^{6+}$  (herein referred as 50/50 or Semix) has less toxic effects in wheat plants grown hydroponically (Guerrero et al., 2014), and it forms more beneficial species in grains (Subirana, 2018). Hence, in our study different mixture ratios of selenite and selenate were used. We have performed the Se biofortification of wheat crop in hydroponic culture to have a better control of the cultivation parameters (e.g. nutrients availability) and to have a simple environment in which the interaction of Se with other factors, like in the presence of agricultural pollutants, and their effect in the biofortification process can be studied.

The term hydroponics was coined from merging two Greek words meaning “working” and “water” (*hydro* means “water”, and *ponics* means “working”). Hydroponic systems are also termed as “soilless” cultures, as plants need only water, essential nutrients at proper proportion, and

enough time for getting a successful growth. Although the use of hydroponics dates far back in history (Babylon gardens), it started to gain renewed attention in the 1930's. However, the better adaptability of the soils respect to more sensitive and care demanding hydroponic systems lead to a decrease in its commercialization despite that over decades different growing methods based in the soil-less culture were developed.

In soilless culture, the roots of the plants are either suspended freely in the nutrient solution (open systems) with static or continuous aeration, or submerged in a substrate (either organic, e.g., moss; or inorganic, e.g., perlite) with continuous or occasional addition of nutrient solution. The open systems are mainly referred to as hydroponics among the soilless systems.

The major advantages of hydroponic systems include the ability to grow plants in diseased or nutrient poor regions, the manual labouring of soil preparation is reduced, the nutrient and water requirement are more controlled and readily available to plants in the production. This leads to less waste, reduced pollution and increased productivity by reducing the effects of soil borne diseases and, more importantly, it can be adapted to any region and size with better cultivation. The major disadvantages are the initial construction cost of the system for large scale production, and it needs proper monitoring with skilled personnel (“Hydroponics: A Practical Guide for the Soilless Grower - J. Benton Jones Jr.,” n.d.).

In today's growing demand for food for increased population and the amount of agricultural land conditions and availability across globe, vertical farming is considered a better solution for filling the gap. Also, especially in aerospace studies to fulfil the dietary need of astronauts, different hydroponic systems were being studied. Moreover, in research, hydroponic cultivation helps to understand the plant metabolism due to the highly controlled parameters.

Here we report, the Se species evolution along Se-biofortified wheat plants, grown under hydroponic medium with and without Cd. We have analysed the effects of Cd interaction with Se and overall effects in plants with respect to different ratio of Se biofortication treatments. Direct Se speciation has been obtained by means of X-ray absorption spectroscopy at the Se K-edge. Complementary species studies respect to Cd and S were reported. The elemental concentration and the functional groups present in the plant samples obtained from Ion coupled plasma mass spectroscopy (ICP-MS) and Fourier infrared spectroscopy (FTIR) respectively are reported.

## 1.2 Experimental methods

### 1.2.1 Cultivation in hydroponics with and without Cd

Wheat (*Triticum aestivum*) seeds were procured from Fito S.A. (Barcelona, Spain). Seeds of similar size and no visual fungal infection were selected and germinated using moistened filter paper at 25°C, 7 days in dark and 4 days in light, until they had a shoot of 6-7 cm in length. Afterwards, the plants were pre-cultured in pots for 30 days with 0.5L of ½ strength Hoagland solution per plant before applying Se and/or Cd. The formulation of the Hoagland solution is described in Table 1.1. The nutrient solution was buffered using MES (2-morpholinoethanesulphonic acid) at pH 6.0 and renewed once a week.

For the Se biofortification, sodium salts of selenite ( $\text{Se}^{4+}$ ) and selenate ( $\text{Se}^{6+}$ ) were used to form the  $\text{Se}^{4+}/\text{Se}^{6+}$  mixture in the ratios 25/75, 50/50 and 75/25. The total Se concentration was set to 0.78  $\mu\text{g/g}$  following the best results from previous studies regarding the optimization of Se dosage in wheat plants (Subirana, 2018). Cadmium chloride ( $\text{CdCl}_2$ ) was used to introduce the Cd pollution in the system at the concentration of 0.1  $\mu\text{g/g}$  which is well below the upper limit set by the European regulation for agricultural soils (Council Directive 86/278/EEC of 12 June 1986, n.d.). The treatments were applied weekly and every time the nutrient medium was renewed.

The treatments applied along with their naming are summarized in Table 1.2 for the sake of clarity. Six plants per pot with two pots per treatment of 10L capacity were studied in order to provide replicates, where a total of 16 pots and 72 plants were cultivated.

The plants were grown until they were completely mature and harvested for further characterization. After the harvest, the plants were divided into roots, shoot (leaves and stems) and grains. Roots were cleaned with ice cold 2 M  $\text{CaCl}_2$  to remove surface impurities. Roots and shoots were lyophilized at -80 °C for 12 h and dry weights were measured. Grains were stored at -4°C in sealed paper bags. Figure 1.1 reports the pictures from the cultivation. The samples were powdered using an automatic agate mortar and pestle grinder, and stored in airtight tubes until further processing for performing ICP-MS elemental analysis and for XAS direct speciation studies.



Table 1.1: Hoagland solution (half strength)

		Stock solution (M)	Stock concentration (g/L)	Final Volume added (ml/L)
Macronutrients	KNO <sub>3</sub>	1	101.1	3
	Ca(NO <sub>3</sub> ) <sub>2</sub>	1	236.16	2
	NH <sub>4</sub> H <sub>2</sub> PO <sub>4</sub>	1	115.08	1
	MgSO <sub>4</sub> · 7H <sub>2</sub> O	1	246.49	0.5
Micronutrients		Stock mM		
	KCl	50	3.728	0.5
	MnSO <sub>4</sub> · H <sub>2</sub> O	2	0.338	0.5
	ZnSO <sub>4</sub> · 7H <sub>2</sub> O	2	0.575	0.5
	CuSO <sub>4</sub> · 5H <sub>2</sub> O	0.5	0.125	0.5
	(NH <sub>4</sub> ) <sub>6</sub> Mo <sub>7</sub> O <sub>24</sub> · 4H <sub>2</sub> O	0.5	0.088	0.5
	H <sub>3</sub> BO <sub>3</sub>	3	1.546	0.5
	Fe-EDTA	20	7.341	0.5

Table 1.2: Se biofortification with Cd pollution treatments

Without Cd	With Cd
<b>Control</b>	<b>Cd</b>
<b>25/75:</b> (25% Se <sup>4+</sup> , 75% Se <sup>6+</sup> )	<b>25/75+Cd:</b> (25% Se <sup>4+</sup> , 75% Se <sup>6+</sup> ) + Cd
<b>50/50:</b> (50% Se <sup>4+</sup> , 50% Se <sup>6+</sup> )	<b>50/50+Cd :</b> (50% Se <sup>4+</sup> , 50% Se <sup>6+</sup> ) + Cd
<b>75/25:</b> (75% Se <sup>4+</sup> , 25% Se <sup>6+</sup> )	<b>75/25+Cd:</b> (75% Se <sup>4+</sup> , 25% Se <sup>6+</sup> ) + Cd

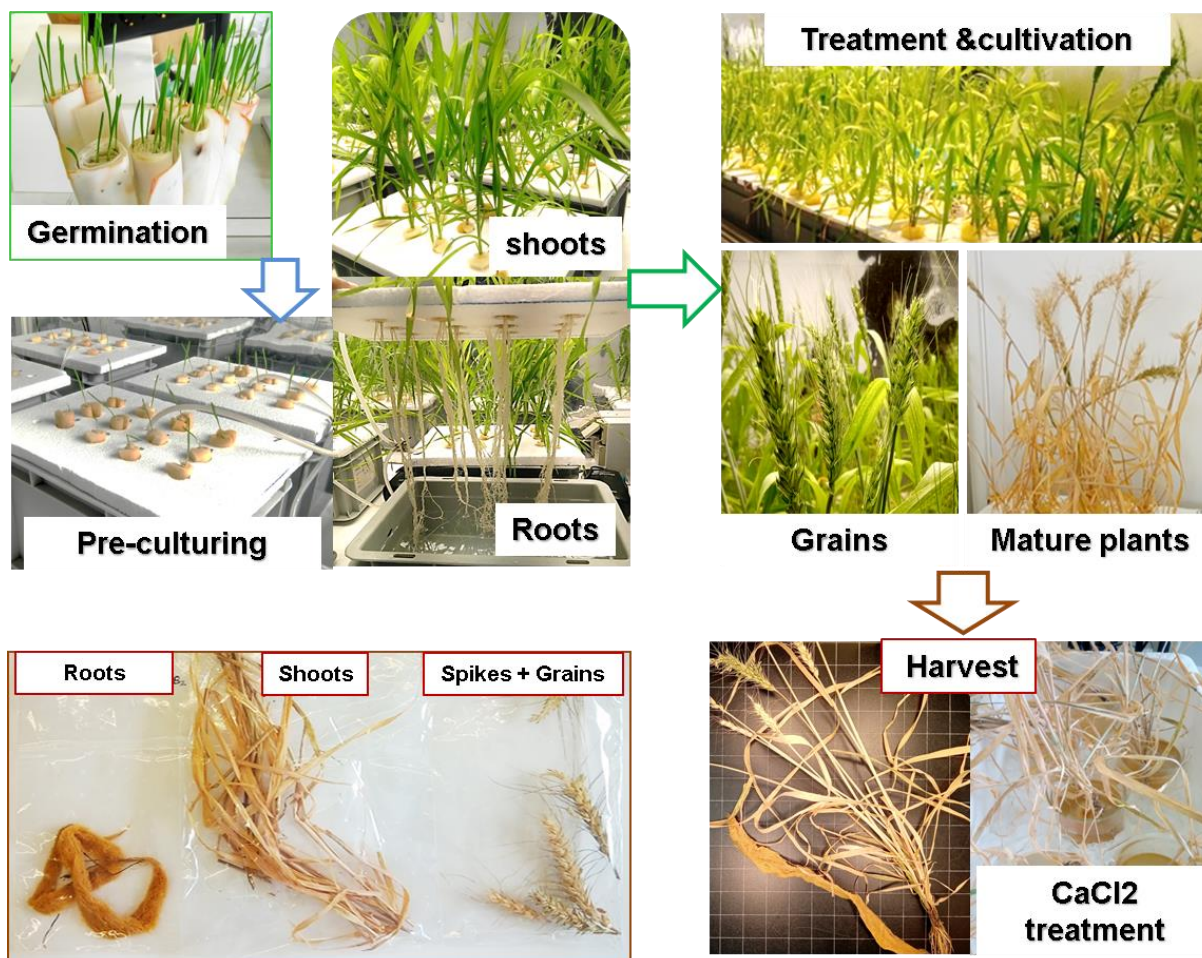


Figure 1.1: Stages of the Se biofortification under Cd pollution cultivation.

### 1.2.2 Sample preparation and characterization

To analyze the elemental concentration by means of ICP-MS, an average of three plants per treatment were grouped and microwave digested using 10 ml HNO<sub>3</sub>:H<sub>2</sub>O<sub>2</sub> (3:1) mixture. The digested samples were filtered using 0.22 μm syringe filters before further dilution. The samples were diluted according to the set calibration range of the desired elements and most of the major elements were analyzed. The results obtained were checked for statistical differences using one-way ANOVA and compared with student t-test distribution with each pairs of all possible individual comparison, with no adjustments for multiple tests in JMP pro 13 software. The statistical significance was denoted by compact letter display of LSD ( $\alpha$  - 0.05) based on

treatments. Translocation factor was calculated as the ratio between the Se concentrations of the sample from initial to final part in the study.

X-ray absorption near edge structure (XANES) spectra were measured at CLÆSS beamline (Simonelli et al., 2016) at the Se, Cd, and S K-edge. The synchrotron radiation emitted by a wiggler source was monochromatized using a double crystal Si(311) monochromator. The rejection of higher harmonics was done by choosing proper angles and coatings of the collimating and focusing mirrors. Powdered plant samples (combination of three plants), ~21 mg, were pressed into 5 mm pellets using a hydraulic press. The appropriated amount of inorganic and organic reference compounds was mixed with cellulose and pelletized. The K-edge absorption spectra of plant samples were collected in fluorescence mode using a multi-element silicon drift detector with Xspress3 electronics, while the reference spectra were measured in transmission mode using ionization chambers. High energy resolution Se K-edge XANES (HERFD-XANES) spectra were collected using the CLEAR emission spectrometer available at the beamline based on Johansson-like dynamical-bent diced-analyzer Si crystals for scanning-free energy dispersive acquisition. The Se  $K\alpha_1$  emission line was collected using the Si(444) reflection of the analyzers working in back-scattering geometry. The energy resolution estimated from the FWHM of the quasi-elastic line was around 0.8 eV. All the measurements were carried out at liquid nitrogen temperature to minimize radiation damage. The data were processed and the linear combination fitting (LCF) analysis was performed using Athena software of the Demeter package (Ravel and Newville, 2005). The goodness of the fit was obtained by the R-factor ( $\frac{\sum(data-fit)^2}{\sum data^2}$ ), which is a measure of the mean square sum of the misfit at each data point.

Spatial distribution of Se and other elements in grain sections (half grain) was determined collecting micro-focused beam X-ray fluorescence ( $\mu$ XRF) maps using a pinhole of 50  $\mu$ m diameter. In each grain, around 100 points were selected for collecting  $\mu$ XANES spectra at the Se K-edge. After an exploratory assessment, a linear combination fitting (LCF) analysis of the maps with the most appropriated set of references was carried out using an in-house developed software (Marini et al., 2021). Moreover, the complementary spatial distribution of some selected sulphur species has been studied in the grains.

The functional groups present in the different parts of the plant were characterized with Fourier infrared spectroscopy (FTIR) using a globar source in transmission mode. The samples were prepared by homogenizing 1 mg of plant samples in 99 mg of potassium bromide (KBr), from Sigma Aldrich IR grade and made into 13 mm thin pellets. The background was subtracted using pure KBr pellet during the analysis. The measurements were carried out in transmission mode, at 36x with 30x30  $\mu\text{m}$  aperture. A total of 3 points per sample at different locations in the pellet with three replicates were collected (256 scans per point) in the range of 400-4000  $\text{cm}^{-1}$ . The measurements were pretreated and analyzed using unscrambler software. The spectra collected were baseline corrected using a linear baseline transformation and normalized using unit vector normalization followed by smoothing of spectra with 2<sup>nd</sup> order and 7 points smoothing using Savitzky-Golay Smoothing transform.

## 1.3 Results and Discussion

### 1.3.1 Growth parameters

The dry weight (DW) of the different parts of the plants gives information about the biomass produced by the plant and allows us to assess factors in the biofortification treatment that influence the plant's growth. Figure 1.2 shows the DW of different parts of the plant for the treatments applied.

In roots, respect to the Se treatments, the dry weight changes with 75/25 having less DW compared to 25/75 and 50/50. Then for the case in which only Cd is added to the feeding, Cd treatment, the DW increases respect to the Control. When adding Se and Cd, Se+Cd treatments, there is an overall decrease of the DW respect to the Se treated plants except for the 75/25+Cd. Statistically, the decrease of the DW for the treatments with higher  $\text{Se}^{6+}$  ratio, 25/75+Cd and 50/50+Cd, is significant from other treatments.

In shoots, the presence of Se in the treatment reduces the shoots biomass respect to the control sample. There is no appreciable effect of the selenium species used in the Se treatment. When adding Cd, the DW decreases noticeably, and for the Se+Cd treatments there is dependence with the ratio of the Se species being the DW lower for the treatments with higher  $\text{Se}^{6+}$  content,

25/75+Cd and 50/50+Cd. Statistically, Se treated samples, with treatments of different ratios (except 50/50) are significantly different from Control however, they share the components with 50/50 treatment. The changes observed for the Cd addition is significant respect to Control, and similar to roots,  $\text{Se}^{6+}$  higher treatments are significant compared to other treatments.

In case of spikes, the addition of Se, Cd or both dramatically decreases the DW respect to the Control. Although the DW is rather similar for all treatments in the Se and Se+Cd groups, overall, the DW for the Se group is higher, compared to Se+Cd one. For the Se group, the DW decreases when increasing  $\text{Se}^{4+}$  in the treatment. On the other hand, in the Se+Cd group there is not a clear trend, but the 25/75+Cd displays the lowest DW among all treatments. Statistically, the differences found for Control and Cd treatments are significant among each other and respect to 25/75+Cd treatment, however, the rest of the treatments do not show statistically significant differences among them.

For the grains, in the case of the Se group, the DW is higher in case of 25/75 treatment respect to Control, whereas the 50/50 and 75/25 treatments display the lowest grain weight among all the treatments. Upon the addition of Cd, the highest grain weight is obtained for the Cd treatment, whereas for the Se+Cd group, the trend regarding the  $\text{Se}^{4+}/\text{Se}^{6+}$  ratio is inverted respect to the Se group being 75/25+Cd the treatment which displays the highest DW. Control and treatments in Se and Se+Cd groups are statistically not fully significant whereas, Cd treatment is significantly different from all the treatments.

The Figure 1.2 panel (e) shows the total number of grains produced. Among all the treatments, Control produced the highest number of grains, however, respect to the standard deviation (SD) of total grains produced in two pots, Cd is almost similar to Control. In Se group, the grain production decreases with the increase of  $\text{Se}^{4+}$  in the treatment. In Se+Cd group, 50/50+Cd has the lowest grain production respect to the other two ratios which are almost similar among them. This also correlates with the average weight of the grains produced.

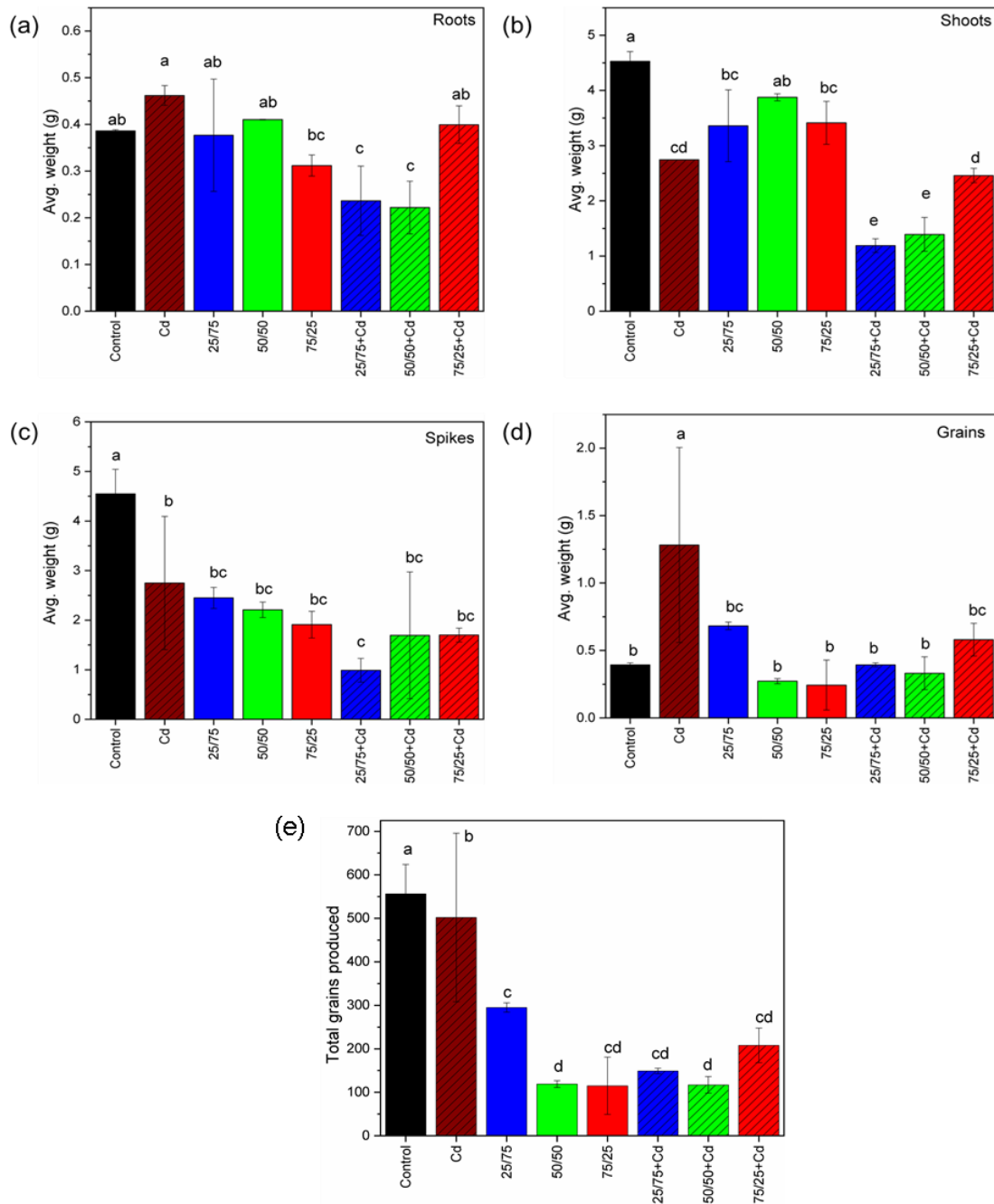


Figure 1.2: Biomass of different parts of the plant (DW), roots (a), shoots (b), spikes (c) and grains (d) and total number of grains (e). The treatment groups are represented as control (black), Cd (brown), 25/7 (blue), 50/50 (green), 75/25 (red), Control and Se group (no pattern), Cd and Se+Cd group (diagonal pattern). The statistical significance between different treatments based on means comparison of technical replicates was shown by student t-test with significance  $\alpha=0.05$ . Different letters define the level of significance.

In summary, our results show that, respect to the Control, the addition of Cd has a significant effect in the plant's development affecting differently the different parts of the plant. In terms of Se application, respect to the Control, along the plants the treatments do not significantly affect the biomasses, whereas in grains the total DW clearly increases when increasing in Se<sup>6+</sup> content in the treatment. In terms of Cd treatment along with Se, Se+Cd group, globally less biomass was produced respect to the Se group and an increase of Se<sup>4+</sup> in the treatment increases the total grain DW. Moreover, 25/75+Cd and 50/50+Cd show the lowest DW in roots and shoots compared to 75/25+Cd. This could be due to the presence of more Se(IV) in the plant, which helps to overcome the stress induced by Cd.

### **1.3.2 Elemental concentration along the plant**

The Se concentration found in the different parts of the plants (roots, shoots and grains) is displayed in Figure 1.3(a). Overall, considering all the parts of the plant, the Se concentration decreases in the presence of Cd. In addition, the amount of Se accumulated in the roots is higher than in the aerial parts (shoots and grains). The Se concentration in roots significantly increases when increasing the ratio of Se<sup>4+</sup> in the treatment both with and without Cd.

Instead, in shoots, the Se accumulation decreases with the increase of Se<sup>4+</sup> in the ratio, whereas the Cd presence does not noticeably influence the trend. In terms of significance, regarding the Se and Se+Cd groups, the individual Se treatments are significant among each other.

In grains, the Se concentration in the presence of Cd gets reduced, with slightly higher values toward higher Se<sup>4+</sup> amount, with values which are consistent with previous results reported in the literature (B Bisbjerg, 1969; Curtin et al., 2006; Gissel-Nielsen et al., 1984; Stroud et al., 2010). Interestingly, for the grains grown without Cd, the 50/50 treatment has a slightly higher Se concentration among all treatments (156 µg/g). This enhancement is statistically significant respect to all the rest of the treatments.

These results highlight the strong influence of Cd on the Se bioaccumulation process.

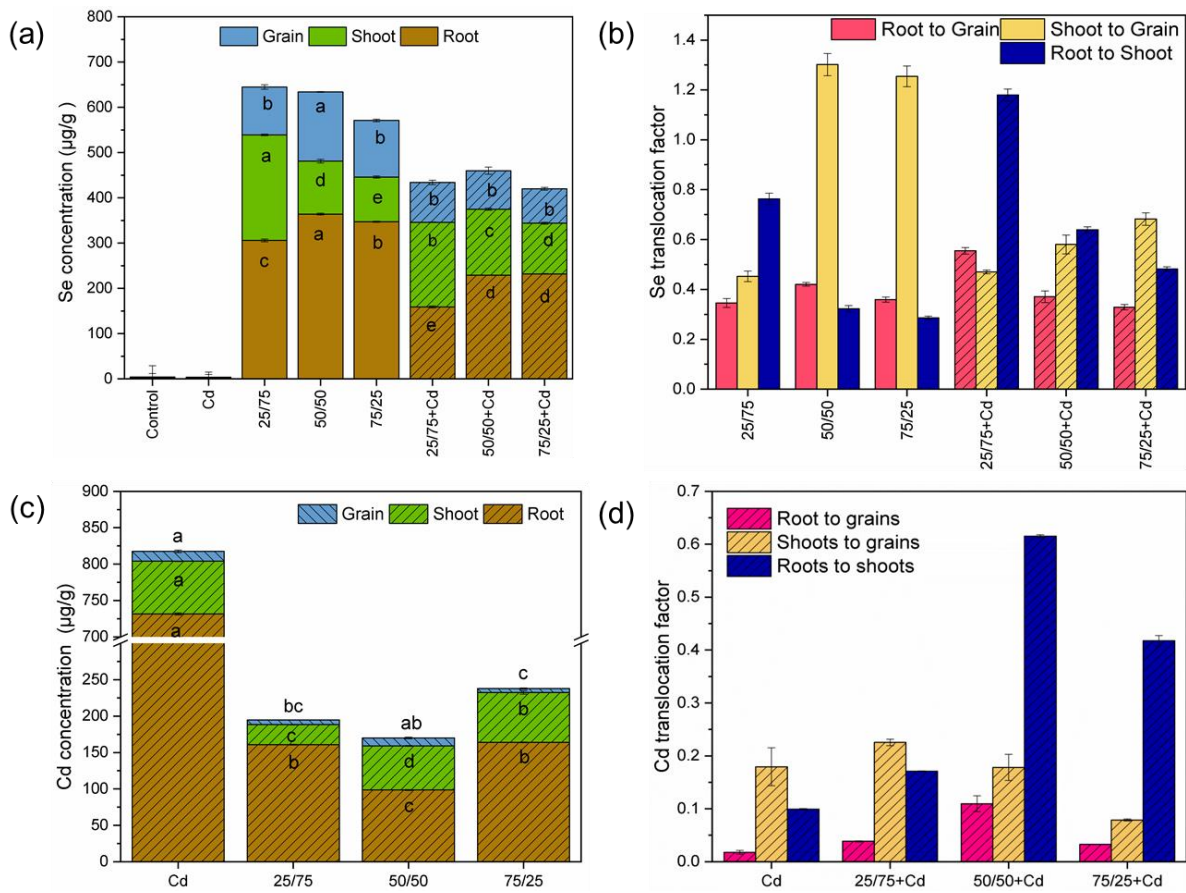


Figure 1.3: Elemental concentration and translocation factor for selenium (a, b) and cadmium (c, d). For the concentrations (a, c): roots (brown), shoots (green) and grains (blue). For the translocation factor (b, d): roots-to-grains (pink), shoots-to-grains (yellow) and roots-to-shoots (blue). Bars for Control and Se group have no pattern, and for Cd and Se+Cd group have diagonal pattern. Error bar represents the %RSD of the measurement. The statistical significance between different treatments based on means comparison of technical replicates was shown by student t-test with significance  $\alpha=0.05$ . Different letters define the level of significance.

The translocation factor (TF) is described as the ratio of elemental concentration between the destinations to origin of the part of the plants. The TF of a heavy metal should be more than 1 to consider that the mobility and the accumulation of that element is successful along the plant (Usman et al., 2019). Figure 1.3(b) shows the translocation of Se along the plants under different treatments. Se TF from roots-to-shoots is higher in the Se+Cd group treatments respect to the Se



group treatments. This suggests that under Cd pollution the translocation of Se to the shoots is favoured. Among the Se treatments, the TF decreases with  $\text{Se}^{4+}$  ( $25/75 > 50/50 > 75/25$ ). In contrast, the shoots-to-grains TF is lower for the Se+Cd group and increases with the  $\text{Se}^{4+}$  content. This trend is better defined under Cd pollution, while along the Se group, the shoots-to-grains TF looks to reach a plateau already at the 50/50 treatment. Finally, the roots-to-grains TF change marginally in the purely Se treated samples, with a maximum for the 50/50 ratio. The Cd looks to increase the roots-to-grains TF when  $\text{Se}^{6+}$  is applied in higher amount. The better TF in bio fortification was seen in root-to-shoot in 25/75 treatment and from shoots-to-grains in 50/50 and 75/25 treatment, for the latter with  $\text{TF} > 1$  for purely Se treated samples. Hence, these results indicate that the Cd application hinders the Se translocation during the biofortification process respect to only Se treated plants, with a major effect found for the treatments involving a significant  $\text{Se}^{4+}$  amount.

The Cd concentration under the Se treatments is depicted in Figure 1.3(c). Respect to the Cd treatment, roots and shoots of Se+Cd group plants show reduced Cd concentration. Slight changes are found in roots in terms of the Se treatments applied with 50/50 having the minimum concentration ( $98 \mu\text{g/g}$ ). Instead, in the case of shoots, the Cd concentration shows pronounced dependence as a function of the Se treatment applied, having higher Cd concentration for the treatments with higher  $\text{Se}^{4+}$  content. 25/75+Cd displays the lowest Cd concentration ( $27 \mu\text{g/g}$ ), while 75/25+Cd has more than twice ( $68 \mu\text{g/g}$ ). In grains, we observe that the Cd concentration is overall very small, and it less affected by the Se treatment applied. The highest Cd concentration is found for 50/50+Cd ( $11 \mu\text{g/g}$ ), in contrast with the opposite trend displayed by roots.

When assessing the results of the TF of Cd, see Figure 1.3(d), the shoots-to-grains TF follow an opposite trend respect the Se TF, with increase of  $\text{Se}^{4+}$  concentration that correspond to Cd TF decrease. Roots-to-shoots and roots-to-grains Cd TF show a maximum translocation at 50/50+Cd treatment, with all Se treatments having a better translocation than the Cd treatment sample. However, the overall translocation of Cd in the plant system is systematically below 1, thus limiting the Cd accumulation.

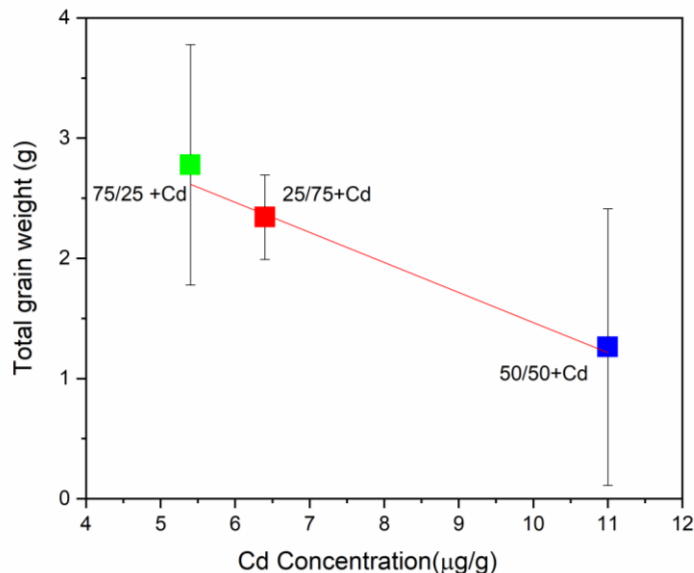


Figure 1.4: Total weight versus Cd concentration in grains. The line represents the linear fit with  $R^2=0.969$ . The  $Se^{4+}/Se^{6+}$  ratio corresponding to different treatments is reported close to the experimental points.

The plot reporting the average grain weight as a function of the Cd concentration is shown in Figure 1.4. The linear correlation found together with the data reported in Figure 1.2 d-e suggest a combined toxicity effects from Cd and Se, which causes the reduction of the grain weight.

The Se and Cd interaction affecting their accumulation and translocation is similar to previous findings in rice (B. Huang et al., 2017), where Se hinders excessive Cd accumulation in the grain. In our case, depending on the treatment, Cd accumulation in the Se+Cd group decreased from 80% (50/50+Cd) to 30% (25/75+Cd and 75/25+Cd) respect to the Cd treatment. Moreover, Cd affects the biofortification process by significantly reducing the concentration of Se. For both Se and Se+Cd groups, the higher Se concentration in roots is found in treatments towards higher  $Se^{4+}$  in the ratio. This could be ascribed to the higher solubility of  $Se^{4+}$  in water than  $Se^{6+}$ , which makes  $Se^{4+}$  more available for plants in hydroponic systems (Meltzer et al., 1993).

It is important to assess the concentration of other elements like zinc (Zn), molybdenum (Mo), copper (Cu), manganese (Mn) and boron (B) which are essential for protein synthesis, proper enzymatic reactions and affect plant antioxidant behaviour. The concentrations of these elements

along the different parts of the plant are reported in Figure 1.5. The statistical significance analysis among treatments with significance 0.05 under student t-test respect to comparison of each pair among the treatments is detailed in the figure as letters on top of the column bars. As seen from the figures, all the elements concentration was affected respect to the Se treatments and the presence of Cd.

Regarding the Mn concentration, see Fig. 1.5(a), shoots contain higher amount of Mn than grains and roots. In roots, the Mn concentration decreased among all treatments except 25/75, respect to Control treatment. Se groups have higher concentrations compared to Se+Cd groups. Except for 25/75 treatment and Control, all other groups display significant differences among them. In shoots, all treatments show higher Mn content respect to the Control treatment. Selenium group has less Mn concentration compared to Se+Cd group. 25/75 treatment has more Mn in Se group and significant than other two ratios. In contrary, 25/75+Cd has less Mn in the Se+Cd group. Cd and 50/50Cd are similar and significant among all the other treatments.

In grains, the concentration of Mn was higher in Cd treatment respect to Control. Opposite to shoots, Se group has higher Mn than Se+Cd groups. 50/50 treatment has less Mn in Se group, whereas 50/50+Cd has higher Mn in Se+Cd group. In addition, respect to Control and Cd treatment, the differences observed for Se and Se+Cd groups are statistically significant.

Mo is an important micronutrient that, as Se follows the sulphate transporters and takes part in related to antioxidant defense activity in wheat plants and also in general in amino acid synthesis. The Mo concentration is shown in Figure 1.5(b). The results show that Mo is more present in roots and shoots than in grains. In roots, overall concentration of Mo is higher in Se group compared to Se+Cd. Control has less Mo than Se groups, similar to Cd treatment being less than Se+Cd groups. 50/50 is higher in Mo content compared to other ratios in Se group and in contrary 50/50+Cd is the lowest in case of Se+Cd group. In shoots, Se group has less concentration of Mo compared to Se+Cd group. Control has less concentration compared to all the treatments. The 25/75 treatment had more Mo in Se group and 50/50+Cd have more Mo in case of Se+Cd groups in shoots. In grains, the overall concentration is more or less similar. However, respect to Control and Cd treatment, the differences found for Se and Se+Cd groups are statistically significant.

The concentration of Cu along the parts of the plant is given in Figure 1.5(c). Roots show higher concentration of Cu compared to the shoots and grains. In addition, respect to the Control, except 25/75 treatment, all the rest have less Cu and this change is statistically significant. Similarly, Cd treatment has higher Cu concentration than Se+Cd treatments. In general, in roots, Se treatments have higher Cu than Se+Cd groups. 25/75 show the highest concentration among all treatments and within Se group, while 75/25+Cd has high concentration in case of Se+Cd group. In shoots, all Se treatments are higher in concentration than Control treatment and similar among Se group. Cd treatment shows higher concentration among all treatments, also compared to Se+Cd groups. In case of Se+Cd group, 25/75+Cd has less concentration compared to the other ratios. Generally, in grains, Se group has higher levels of Cu compared to Se+Cd group. The 25/75 has higher concentration among all. The Cd treatments have higher concentration than Se+Cd treatments.

Zn concentration shown in Figure 1.5(d) suggests that, generally, the concentration of Zn in roots is lower than in shoots. In roots, the Control and the Cd treatments are higher in concentration compared to Se and Se+Cd groups. The concentration decreases with increase in  $Se^{4+}$  in the treatment ratio in Se and Se+Cd groups. The Cd and 25/75+Cd have same concentration and not significant while other treatments show significance. In shoots, Se+Cd group has higher concentration compared to the Se group, which is also more or less similar in grains. In shoots, respect to Control and Cd treatments, Se and Se+Cd groups have higher Zn concentration. The 50/50 treatment has lower concentration in Se group whereas 50/50+Cd has higher concentration in Se+Cd group. This trend is also similar between the shoots and grains. All treatments show significance among each other.

Concentration of B is shown in Fig 1.5(e). In general terms, shoots have lower concentration of B than roots, and the highest concentration is found for grains. In roots, respect to control, all treatments are lower in concentration, also compared to Cd treatment Se+Cd group is lower. The Se group 50/50 have the lowest concentration compared to other two ratios. In case of Se+Cd group, the concentration decreases with increase in  $Se^{4+}$  in the treatment. The treatments are significant among each other. In shoots, less difference among treatments are seen unlike roots, the control being highest in concentration similar to Cd and 25/75 in Se group. 50/50 and 75/25 are similar in case of Se group. In Se+Cd 50/50+Cd is higher compared to others and significant

compared to the other two ratios. In grains, 50/50+Cd has the highest concentration followed by Control, Cd and 25/75. The concentration in 50/50 and 75/25 is significantly lower than in the other treatments.

The results from the microelements in the plants help us to understand the effects of Se and Cd. The lower concentration of Mn in grains respect to shoots can be attributed to the plants hindering capacity against Mn. It has been reported that, in some cases, Se application lowers the Mn accumulation in sunflower plants to prevent Mn induced toxicity due to metal related elements antioxidant activity of plants (I. Saidi et al., 2014). Previous work on lettuce also reported a decrease in Mn concentration linked to an increase in the Se level (Kleiber Tomasz et al., 2018).

Similar to Se, Mo follows the sulphate transport in plants. Overall plant growth seems affected by the coexistence of Mo, Se, and S in the growing media because of their competition in the uptake. In Shoots, we find more Mo in the Se+Cd group. This could be due to the lower accumulation of Se and due to the Cd presence, which increases the Mo. As the presence of Se or the concomitant anomalous S level tends to affect Mo in the plant tissues. This effects among elements were reported in sulfur presence and absence in wheat. (Shinmachi et al., 2010) . Also protective effect of Mo and Se are reported to reduce the stress induced by Cd in plant (Ismael et al., n.d.).

On the other hand, the Cu level is generally affected by the plant uptake pathway in terms of ion exchange since its primarily role in the production of enzymes. This may explain the higher Cu level found in roots, where the major elemental uptake takes place (Hou et al., 2006).

The interaction between Cd and Zn was reported to affect the accumulation of both elements in some small herbs (*Festuca arundinacea*) (Dong et al., 2019). Some works report that the presence of Cd and Zn reduces the Cu uptake (Adamczyk-Szabela et al., 2020) which was not true in our case. The B changes respect to Se and Cd interaction in plants were not reported in literature. Thus, in general, micronutrients are affected by the presence of Se treatments and pollutants in the growing medium. Despite the significance of the results clear trends were difficult to identify, implying that further studies are necessary to increase the data set to further address correlations.

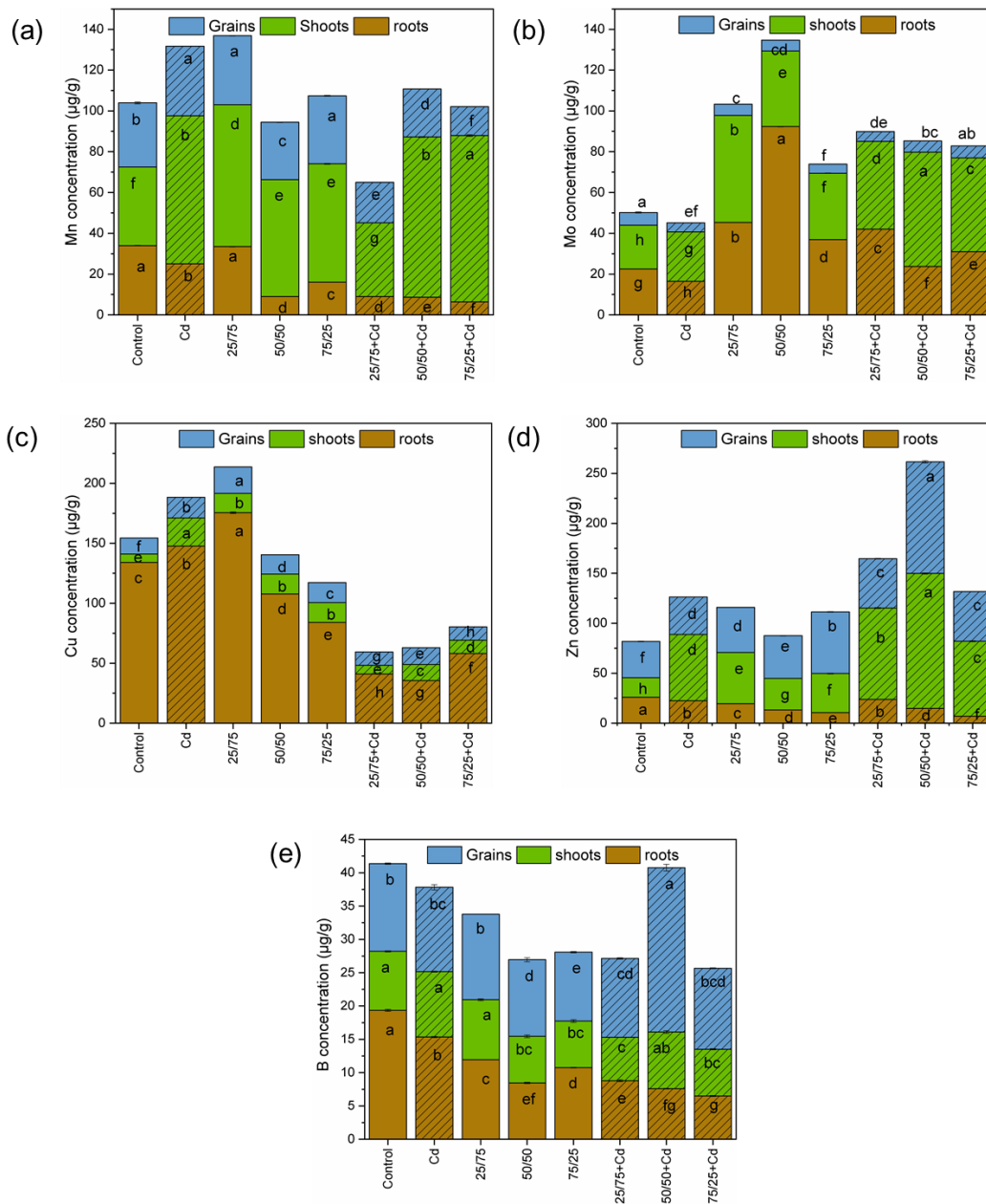


Figure 1.5: Elemental concentration of Mn (a), Mo (b), Cu (c), Zn (d), and B (e). The stacked plot represents roots (brown), shoots (green) and grains (blue) of control and Se group (no pattern) and Cd and Se+Cd group (diagonal pattern). The error bar denotes the RSD of the measurements. The statistical significance between different treatments based on means comparison of technical replicates was shown by student t-test with significance  $\alpha=0.05$ . Different letters define the level of significance.

### 1.3.3 Se species along plant and grains

To assess the evolution of the different Se species along the plant, XANES was used as a direct speciation technique. This allows us to study the Se species present in the wheat plants without having to destroy the sample nature with other chemical treatments as occurs with other indirect speciation techniques such as HPLC-ICP-MS. Figure 1.6 shows the Se K-edge XANES spectra collected on roots 1.6(a), shoots 1.6(b) and grains 1.6(c) samples. By direct comparison, of the XANES spectra of the plant samples with those of the Se references the main Se species can be qualitatively assessed.

In the case of roots, the spectral profile of the Se treated samples resembles mostly the one of the Se organic species having the white-line (first resonance feature after the absorption rising edge) at similar energy (12660.4 eV) then SeMet and SeMeCys references, in which the coordination of Se is in the form of C-Se-C. It is worth noticing that the white-line is wider in the plant samples than in the Se standards. This can be attributed to a more distorted local environment of the Se present in the plants or coexisting phases. Overall, no major spectral differences regarding the Se<sup>4+</sup>/Se<sup>6+</sup> ratio in the treatments were observed, except for the 25/75+Cd sample, where there is a clear rise of spectral weight at higher energies respect the main common white line. Such higher energy feature may correspond to intermediated Se species. According to the energy position at which it appears (between C-Se-C and Se(IV) references), it might be compatible with selenide intermediate species, formed as a residue during the breakdown of Se(VI) to Se(IV) using ATPSulphurylase, or further breakdown using cysteine synthase complexes in plants reduction of Se(VI) and Se(IV) assisted by S-containing thiol compounds like gluathionine reductase. This is expected to occur in roots due to the presence of sulphur assimilators and transporters (Ellis and Salt, 2003; Schiavon et al., 2016). Moreover, a slightly shift of the white-line towards lower energy was found in the case of 75/25 sample (with and without Cd), most likely reflecting the presence of a small amount of Se bound to cysteine (e.g. SeCyst, in the form of C-Se-Se-C bonding structure).

On the other hand, XANES spectra of shoots show a major contribution of selenide intermediated species the which presence is reduced in favour of Se(VI) contribution upon increasing the Se<sup>6+</sup> ratio in the treatment. With the addition of Cd that trend is less marked.

Interestingly, both with and without Cd, the evolution of this intermediated species as a function of the Se treatment looks inverted respect to the roots case. The presence of Se(VI) in shoots was also reported in by Xiao and coworkers (Xiao et al., 2021) and it could be attributed to oxidative processes within the plants leading to the conversion of Se(IV) to Se(VI).

The conversion of Se(VI) to SeCys or SeMet in plants has been reported to occur in shoots, where major transformation of organic species takes place with the help of O-Acetyl serine complexes, Seleno methyl transferase, Cysteine reductase and other Se reducing enzymes. This process is normally less efficient for Se(VI) than from Se(IV), since Se(VI) needs a prior conversion to Se(IV). This limits the conversion of Se inorganic species in the organic ones through ATPSe reductase and transferase (Ellis and Salt, 2003; Schiavon et al., 2020). The Se(VI) transformation along this process seems to be slowed down by the presence of Cd in the treatment. The release of selenide from Se(VI) conversion can form organic bonds with Cd, making Se and Cd less bioavailable. The formation of selenide bonded to Cd in roots was reported among other species of plants like kidney beans (Shanker et al., 1995).

Similar to roots, the Se species present in grains do not differ much respect to the treatment applied, however, the spectral profiles are much similar to the one from the selenoamino acid references than in the root case, and less broadening of the white-line intensity is found. This indicates that the Se species have reached a more stable organic form at the end of the translocation process. The 25/75 treatment displays an enhancement of the second spectral feature at higher energy, where the Se(VI) contribution appears.

To get a better understanding of the different Se species coexisting in grains, a linear combination fitting (LCF) analysis was performed using selected Se reference spectra: Se(IV), Se(VI), SeMet, SeCys, and SeMeCys. The best fit provides semi-quantitative information of the combination of references that reproduce the grain Se K-edge XANES spectra, see Fig. 1.6(d). The R-factor of the fitting is reported in Table 1.3.



Table 1.3: R-factor of LCF of grains

	Se		Se+Cd
25/75	0.0014	25/75+Cd	0.001
50/50	0.0014	50/50+Cd	0.002
75/25	0.0016	75/25+Cd	0.002

The results from the LCF analysis confirm the observations discussed above, by directly comparing the spectra collected in the grains with the references. The Se(VI) feature has been found only in the 25/75 samples (with and without Cd), while organic SeMet and SeCys resulted to be the main species in all the Se treated samples, being SeMet the dominant one, in agreement with the literature (Schiavon et al., 2020). For the Se+Cd treatments, mainly the dominant SeMet species reduce in favour of SeMeCys, which was negligible for the treatments without Cd. 50/50 have slightly higher SeMet component than the other two Se treatment ratios applied. Instead, SeCys is slightly suppressed in 50/50 Se treatment, while both trends are reversed under Cd application. It resulted then that the presence of Cd changes the SeCys and SeMet accumulations and, more importantly, it helps in the conversion and accumulation of SeMeCys compound.

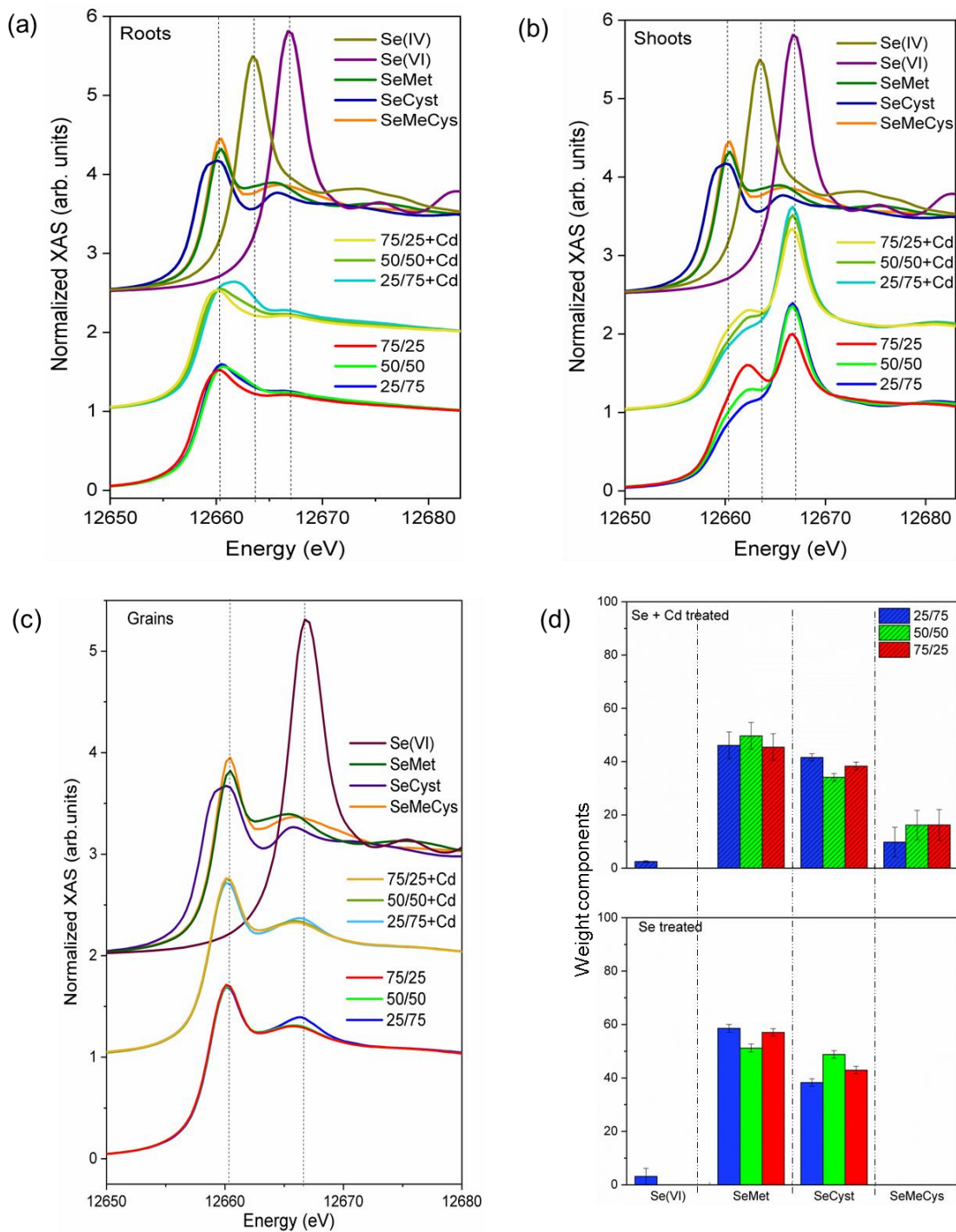


Figure 1.6: Se K-edge XANES spectra collected over roots (a), shoots (b), and grains (c). Se species weight components resulting from the linear combination fitting analysis of the grain spectra (d). The vertical dashed lines are guides for the eyes. In panel (d) the  $\text{Se}^{4+}:\text{Se}^{6+}$  treatment ratios were given by 25/75 (blue), 50/50 (green), 75/25 (red), Se treated group (no pattern), Se+Cd treated group (diagonal pattern).

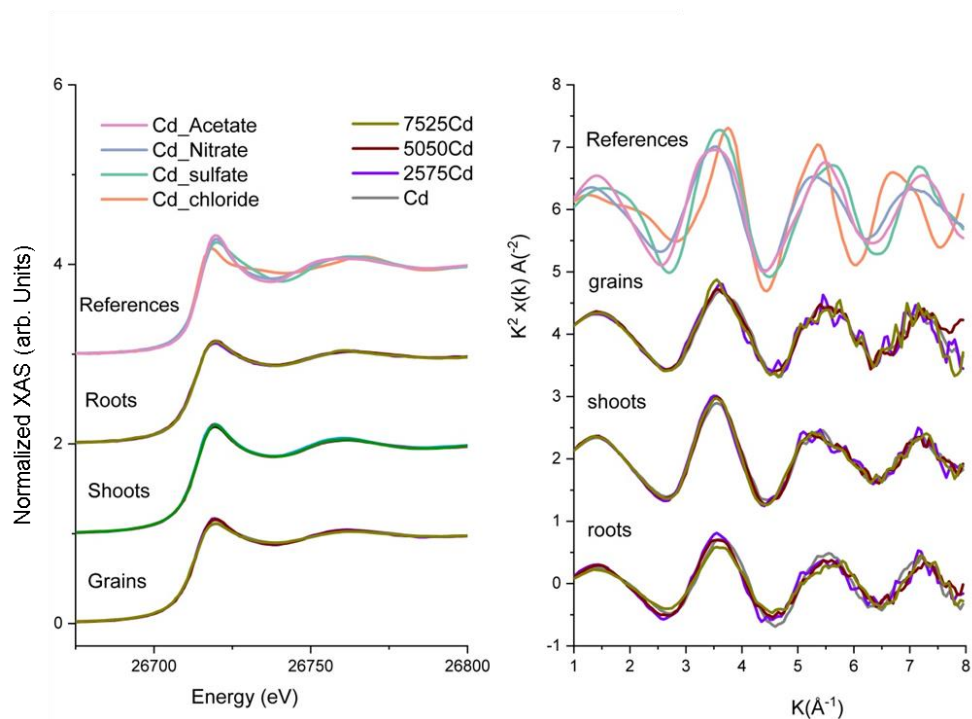


Figure 1.7: Cd K-edge absorption spectra collected over plants grown under Cd pollution. The panel on the left shows the XANES region, while the right one the EXAFS region. The spectra of references, roots, shots and grains (from top to bottom) are shown.

Cd K-edge XAS measurements performed along the different parts of the plants, is shown in Figure 1.7. It shows a similar spectral profile regardless the Se treatment applied. Both the profile of the samples Cd K-edge XANES spectra, as well as the corresponding EXAFS Fourier transform resembles Cd nitrate reference. It could be due to the presence on amine groups as Cd complexes, which could form as defense mechanisms with the help of phytochlelatin reductase and gluathionine reductase while accumulating Cd in cell vacuoles, imobilizing it in the plants.

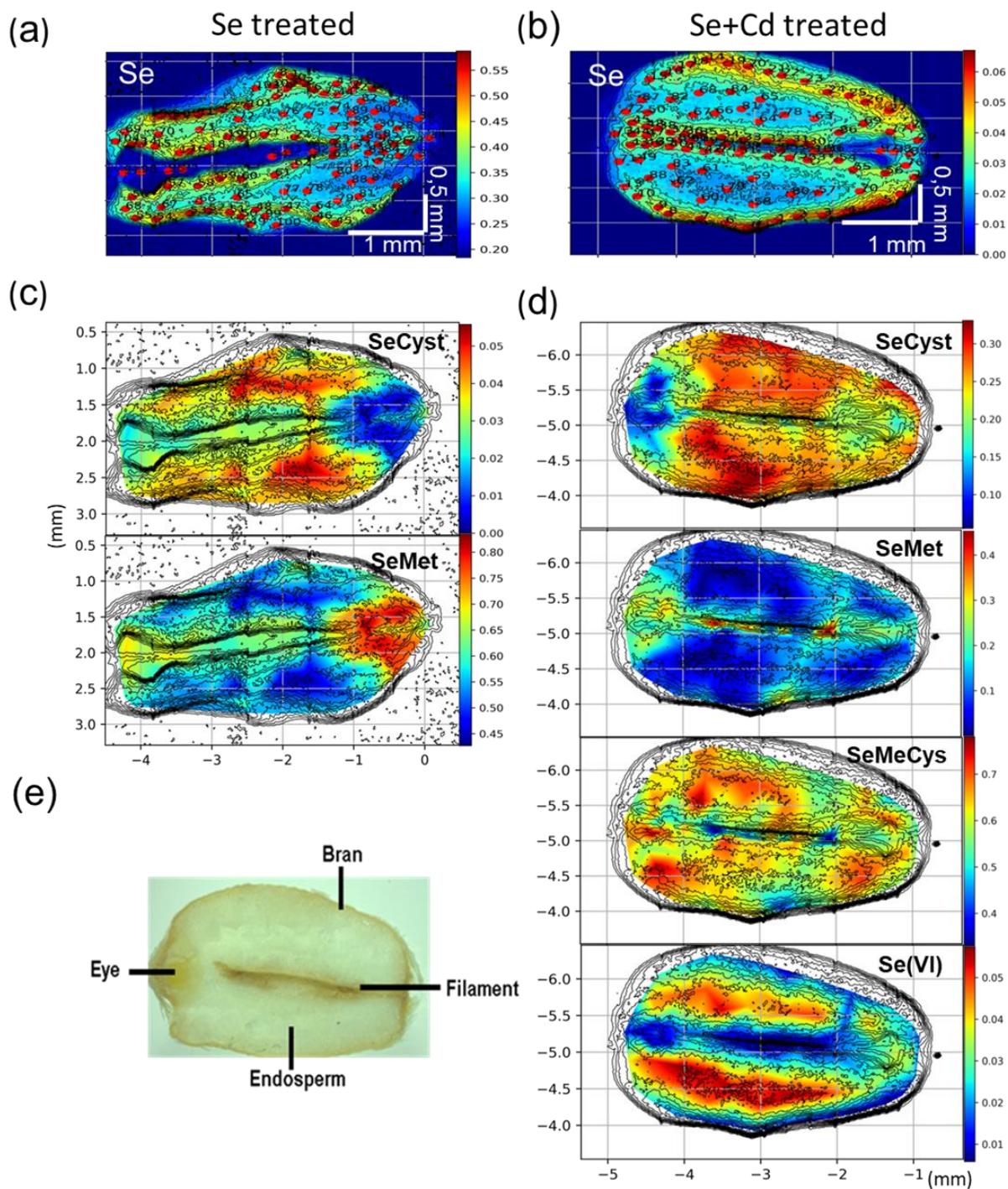


Figure 1.8: Selenium (a, b) and Se species distribution (c, d) along the wheat grains. Two representative grains have been selected: Se treated 50/50 (a, c), and 25/75+Cd (b, d). The red dots in panel a and b represent the positions where the Se K-edge  $\mu$ XANES spectra have been acquired. The contour plots in panels c and d report the Se species distribution in the grains. Sketch of the different grain regions (e).

The spatial Se distribution along the grain sections was obtained by  $\mu$ XRF mapping with a resolution of 50  $\mu$ m. Being the mapping results independent by the Se feeding mixture, in Fig.1.8 are reported only the representative Se distribution maps for samples grown without (panel a) and with (panel b) Cd. Se rich regions appear in warmer colours (red maximum, blue minimum). The main grain regions of interest are eye, endosperm, bran and pigment as represented in the picture displayed in Fig. 1.8(e). Our results show that Se is more concentrated in the bran, eye and filament regions. The Se distribution for the rest of the samples is reported in Figure 1.9(a) without and 1.9(b) with Cd left.

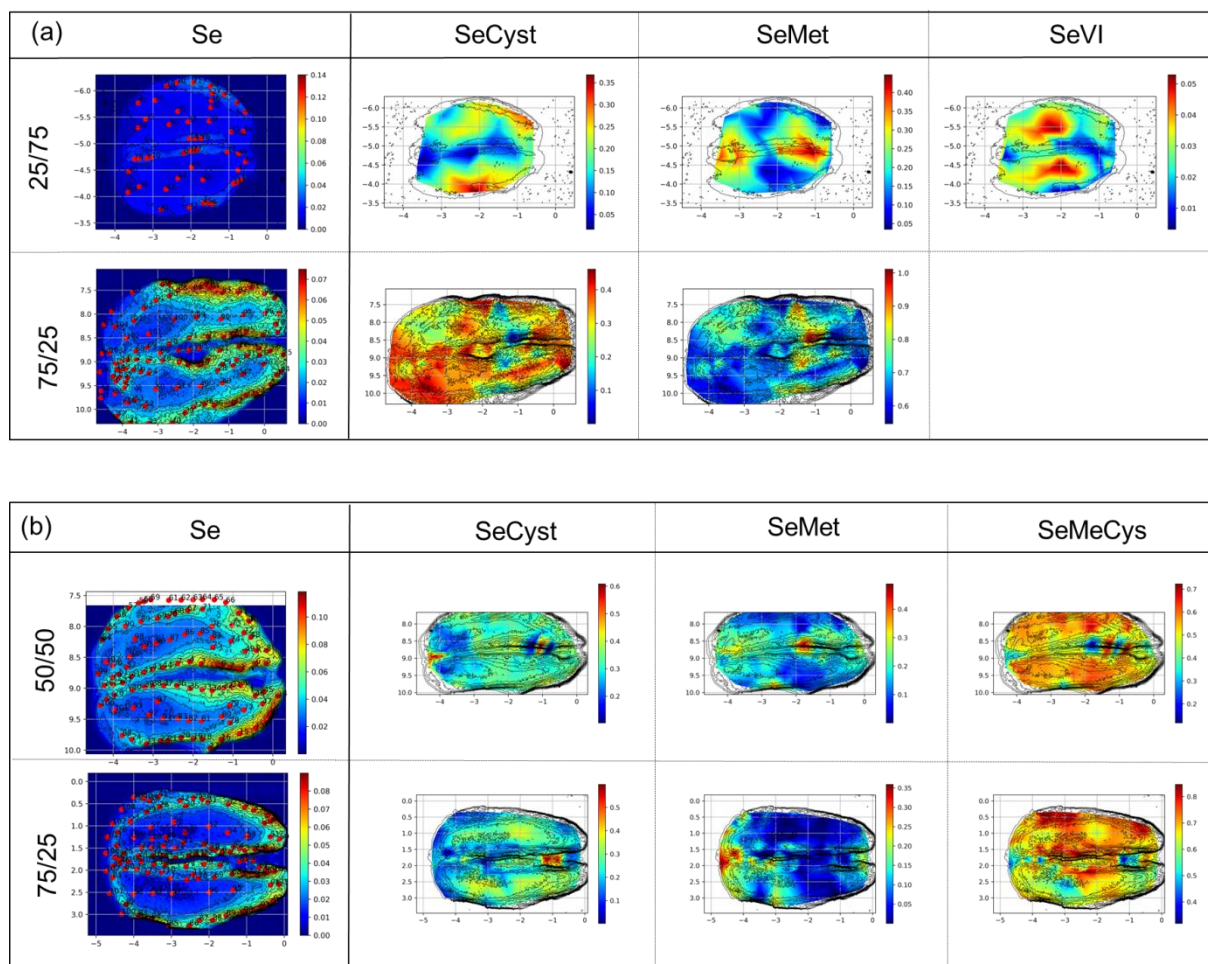


Figure 1.9: Se and Se Speciation Spatial distribution on grains produced by wheat plants grown without (a) and with Cd (b). The red dots represent the positions where the Se K-edge  $\mu$ XANES spectra have been acquired. The contour plots report the Se species distribution in the grains.

Se K-edge  $\mu$ XANES spectra were collected at different positions to determine the Se species along the grains. To be able to retrieve a chemical picture of the grain section, we performed an LCF analysis of each  $\mu$ XANES measured and then re-built the map of the Se species distribution (Fig 1.8(c) and 1.8(d), and Fig 1.9 right side) by applying a linear interpolation among the measured points (red dots on the Se maps in Fig 1.8(a, b), and Fig 1.9 left). As it is possible to quickly visualize, the results are irrespective of the Se applied treatment. The Cd presence promote the SeMeCys formation and Se(VI) species are present in minor amount for Se treatment with higher  $\text{Se}^{6+}$  fraction. From, the Se species distribution, we can identify that SeMet is mainly accumulated in the filament and eye region of the grain. SeMeCys and Secys are commonly distributed in the endosperm of the grain, with the SeMeCys showing not negligible also in the eye region. Finally, Se(VI) is accumulated in the endosperm. In samples with reduced  $\text{Se}^{6+}$  feeding ratio it could be found in the endosperm, near bran, mostly as concentrated regions, as shown in Figure 1.8 and 1.9 of Se mapping of grains from different treatments.

To support these observations, the  $\mu$ XANES spectra within each grain region were averaged and the resulting spectra reported in Figure 1.10. The results from the LCF analysis of the merged spectra are displayed in Figure 1.11. The results clearly correlate with the reconstructed chemical images of the grain maps. The presence of SeMet is enhanced in the eye and filament region, and with higher weight in purely Se treated samples than under Se+Cd treatments. The SeCys is generally more present in the endosperm and bran of purely Se treated samples, while its distribution looks more homogeneous along the grain on the Cd treated ones, even if globally within a similar total amount. SeMeCys is distributed among the regions only under Cd pollution and more prominently visible in endosperm region. Se(VI) is present in 25/75 at the endosperm region both with and without Cd pollution.

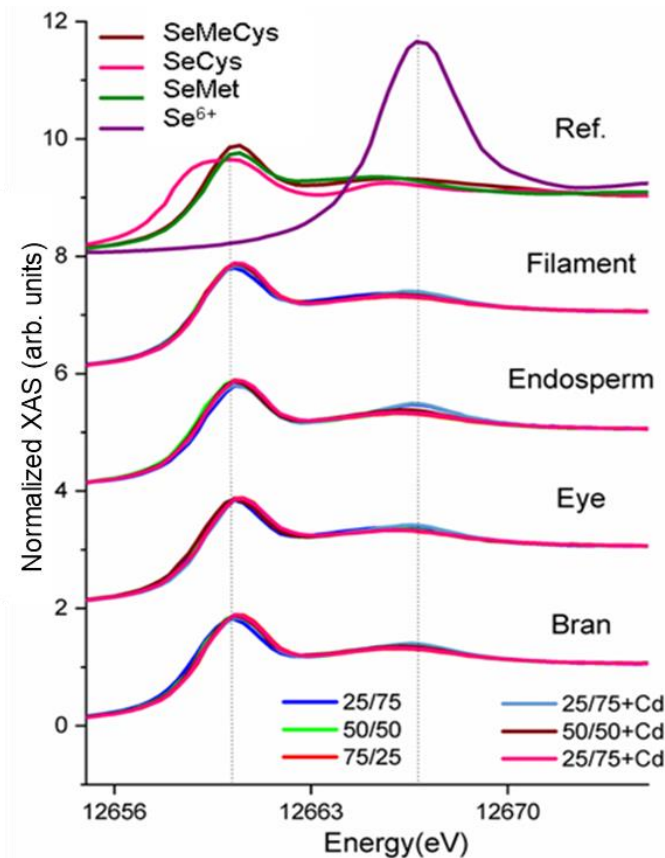


Figure 1.10: Se K-edge  $\mu$ XANES spectra collected along different grain regions. The spectra represent references, merged spectra collected along the filament, endosperm, eye and bran regions (from top to bottom).

Inorganic Se species  $\text{Se}^{4+}$  and  $\text{Se}^{6+}$  compounds enter the plant system through the sulphur pathway (Ellis and Salt, 2003).  $\text{Se}^{6+}$  reduce into selenide and selenite respectively, by different mechanisms and other enzymes of thiol groups in plants. Accumulation and further breakdown of inorganic Se species in plants, helps their transformation into Se organic compounds. Selenite breakdowns to form SeCyst, with the main help of O-AcetylSerine, cysteine syntheses, and glutathione reductase. SeCyst further convert into SeMet, with the release of selenide as exchange and different intermediate compounds are normally formed. In addition, SeMet is also methylated into volatile dimethyl selenium compound with an intermediate SeMeCys and release of other volatile elements.

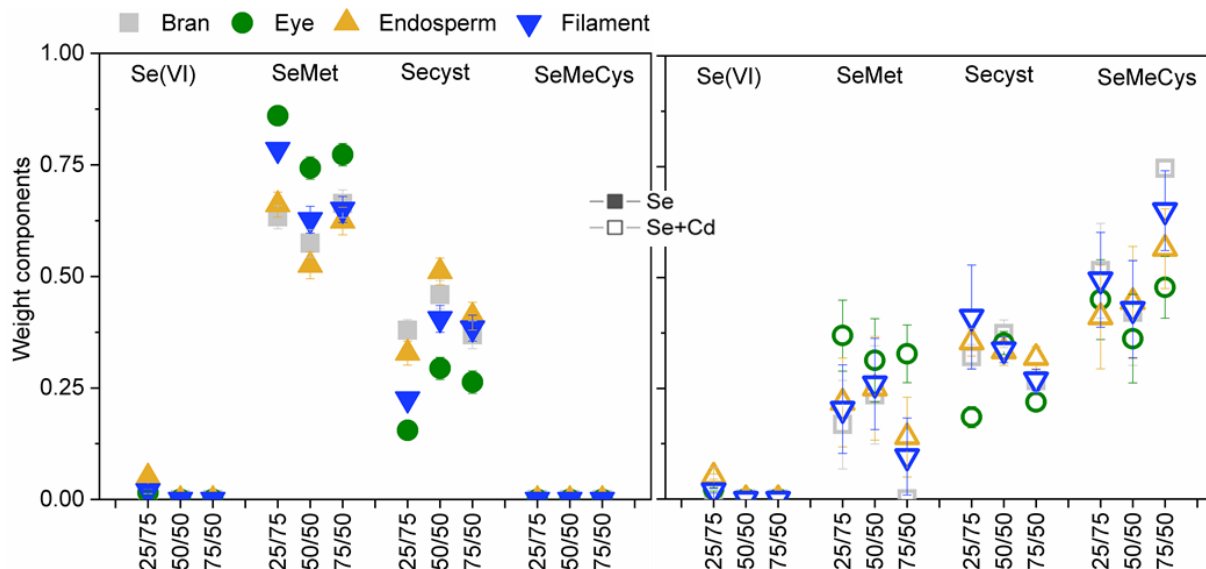


Figure 1.11: LCF of Se K-edge  $\mu$ XANES spectra collected along the grains. The results correspond to average values obtained on the three different Se treatments. Left panel shows the Se treated—closed symbols and right panel shows Se+Cd treated—open symbols. The error bars represent the variations of the results obtained for the different Se treatments.

The change in the plants' response, especially under stress, concerns these metabolic pathways, altering the Se accumulation patterns. For example, it has been reported that Cd stress can affect the sulphur pathway and glutathione assimilations in different organisms including plants (Mendoza-Cózatl et al., 2005). In wheat, Cd induces more stress compared to Se into the sulphur assimilation pathway and S containing thiol compounds, potentially affecting the Se speciation in grains (Harada et al., 2002; Nocito et al., 2007). In the present work, we detected the intermediate SeMeCys forming in the grain under Cd condition at the expenses of SeMet species. This indicates how the stress induced by Cd can affect the Se transformation in wheat.

In summary, the major Se species found in the wheat grains, as products of Se biofortification, are SeMet, SeCyst, SeMeCys, and Se(VI). SeMet and SeCyst are found to be the major components in Se group, while the presence of Cd promotes as well a significant SeMeCys fraction. Se(VI) is present independently by the Cd presence in minor quantity and only



corresponding to a high fraction of  $\text{Se}^{6+}$  in the treatment. SeMet and SeMeCys have the highest absorption capacity in the human system, similarly to Se(IV), of 95-98%. It is important to highlight that Se(IV) is more toxic to humans than SeMet since it cannot be readily incorporated, and it makes its formation not as desirable as the other species. SeCyst cannot be accumulated in the body since it needs to be reduced to SeCys to be incorporated in the selenoproteins. Instead, SeCys, similar to cysteine in S species, could be easily incorporated as functional proteins for metabolic functions in humans (Fox et al., 2004). As proposed previously (Xiao et al., 2020), the presence of SeCyst could be directly related to sample handling, where SeCys could oxidize to SeCyst. However, the not systematic presence of this species in all the samples suggests that it did not occur in the present case.

These common factors make the Se species obtained from the proposed Se biofortification beneficial for food resources. Respect to the treatments, in Se group there were no major differences the in species formed, however, the total Se in grains is higher in 50/50 treatment compared to 25/75 and 75/25. In Se+Cd group, species composition and the total Se where less affected by the Se treatments. However, the presence of Se(VI) in 25/75 and 2575+Cd is not good in terms of biofortification, as it can be absorbed by the human system but it cannot be incorporated into the metabolic functions. Considering, the studies carried out in hydroponic culture and its affinity to Se(IV) species in plants, it is more reliable to say that the 50/50 treatment is better in terms of biofortification.

The distribution of other essential micronutrients like zinc (Zn) and iron (Fe) of different treatments are shown in the Figure 1.12 and 1.13, respectively. They have been acquired simultaneously to the Se distribution by selecting the corresponding  $K\alpha$  emission line of the element of interest detected by the fluorescence detector. The distribution of these elements does not differ among treatments. Zn is seen to be mostly concentrated in the filament strand and the eye region followed by the bran. In the case of Fe, it is also present in filament and eye however, its distribution is more homogenous respect to the concentration. The presence of Zn and Fe in these regions coincides with the natural presence of wheat proteins, as these elements are mainly involved in enzymatic mechanisms in plants.

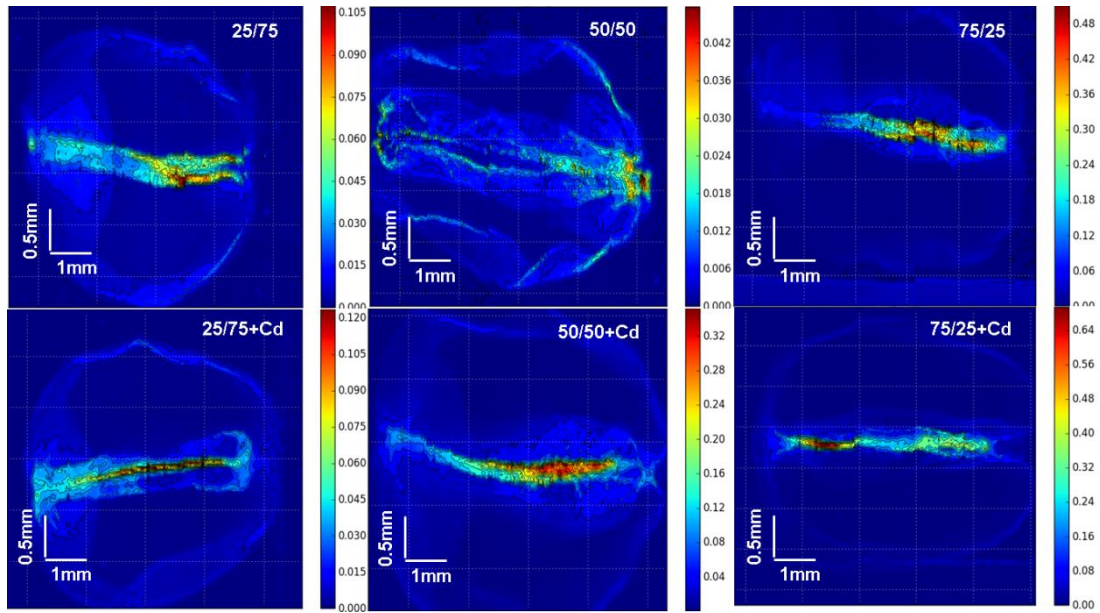


Figure 1.12: Spatial distribution of Zn among different treatments. The top layer represents the Se group and bottom layer represents the Se+Cd group.

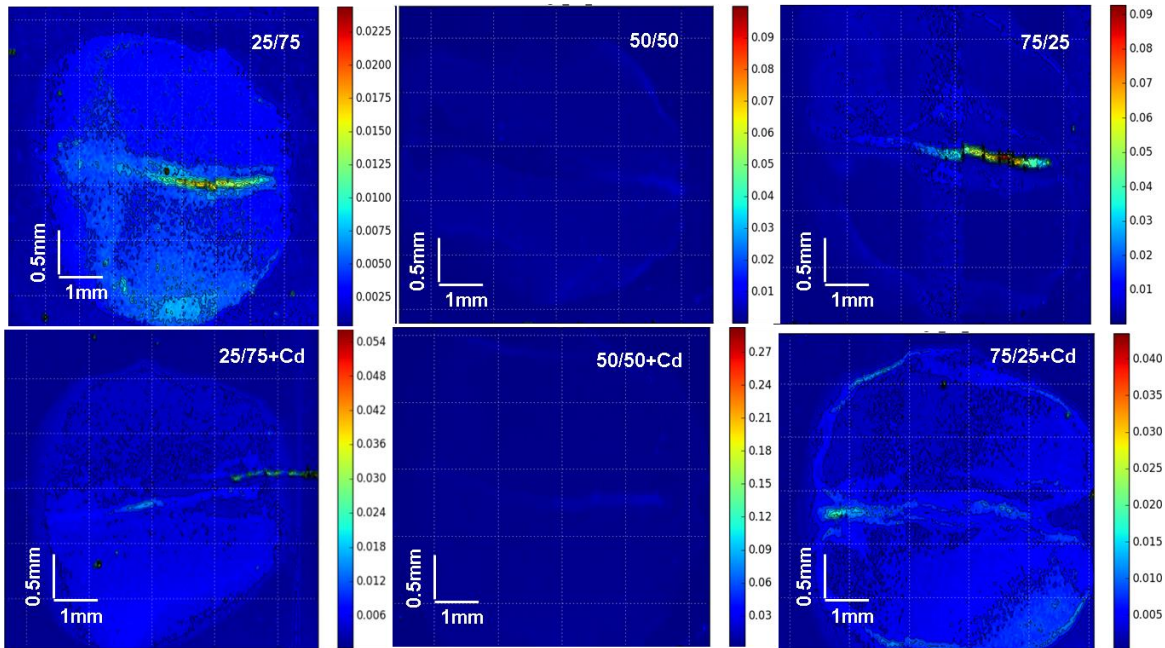


Figure 1.13: Spatial distribution of Fe among different treatments. The top layer represents the Se group and bottom layer represents the Se+Cd group.

### 1.3.4 Sulphur speciation along the plants

Sulphur speciation in plants, provides complementary information to address the Se biofortification processes since S and Se (especially selenate) share the same sulphate uptake and transformation pathways as plants cannot differentiate between these two elements. Selenate share similar characteristics with sulphate and are easily available for plants. Different Se treatments are expected to affect the sulphur speciation either by starving the essential amount needed by the plants or by hindering the process of conversion of other essential sulphur related organic species like cysteine and methionine, with the help of enzymes like glutathione peroxidases, phytochelatins, phytoalexins and glucosinolates. These enzymes and their conversion process are also affected by heavy metals entering the plant systems, eg. Cd and Se, as they form chelating compounds as glutathione (GSH) bounded, for example, to Cd or Se by peptide chain, and restrict their transformation. Characterizing the S speciation helps in identifying the Se and S interactions, by which their effects in the Se biofortification process.

The S speciation is directly accessible by S K-edge XAS. The corresponding spectra collected on different parts of the plants are shown in Figure 1.14, together with the spectra of the reference compounds (glutathione, thiophene, cysteine, cystine methionine sulfoxide, methionine, sulfonate (V), sulfone (IV) and sulphate (VI)). The reference spectra, of sulfonate, sulfone, cystine and sulphate were taken from the ESRF database. All the spectra show contributions in the low and high energy side in different extent. The low energy feature, located around 2472.5 eV, is compatible mainly with cysteine (S-C) contribution, however, that broad feature could also contain minor contributions from GSH (N-S=O, contributing around 2472.5 eV), methionine (C-S-C, contributing around 2472.9 eV) and thiophene (C-S-C, contributing around 2473.2 eV) references. At higher energies, main contributions can be identified around 2480.5 and 2481.5 eV, corresponding to the S(V) (sulfonate), and S(VI) (sulphate) oxidation state, respectively and intermediates among them based on treatments.

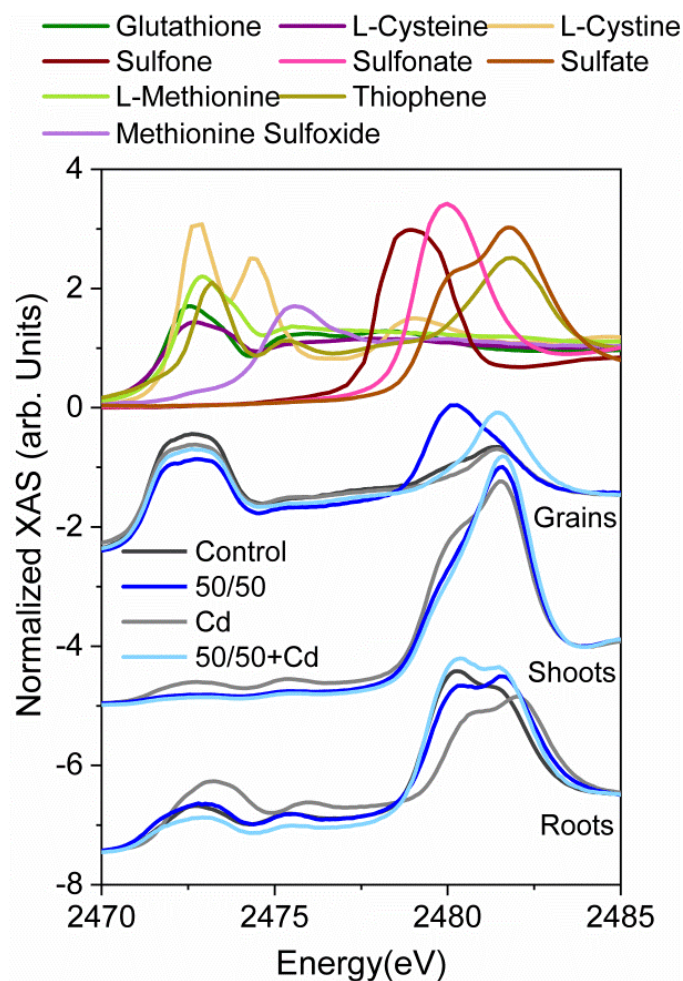


Figure 1.14: S K-edge absorption spectra collected over roots, shoots and grains samples (from bottom to top) compared with references (top).

In the roots, the S species are varying among treatments especially in higher energy. Comparing the Control to the 50/50 of Se group, the lower spectra energy range (cysteine, S-C) is relatively similar, while differences appear in the higher energy side, where S(VI) decreases and S(V) increases. Around 2475.5 eV, close to the methionine sulfoxide white line and the second absorption peak of all the references having a white line at lower energy, a bump clearly appears on the root spectra at slightly different energies for the different treatments, suggesting the presence of overlapping contributions in this energy range.

On the other hand, the application of Cd has a more severe effect on the spectral profile and the contributions at low energy increase whereas those at high energy decrease and both shift towards higher energy. The 50/50+Cd treatment, instead, recall more the Se group. It induces a slight depletion of the components contributing at lower energy, while the components at higher energy slightly increases.

In shoots, among 50/50 and 50/50+Cd treatments there were not spectral differences, while Cd have slightly different spectra. The components at higher energy dominate the spectral profile and the component at low energy (cysteine, S-C) is only significant for the Cd sample. Differently from roots the S(VI) contribution dominates the spectra and S(V) is rising only in the case of the Cd sample.

For the grains, the spectra are similar in shape among treatments at lower energy, where only small intensity changes can be appreciated. Indeed, the contributions at low energy (cysteine, S-C) show a slight depletion when adding 50/50 or Cd to the system, but the relative distribution of the species does not change. Instead, at higher energy 50/50 is clearly different compared to 50/50+Cd, Cd, and the control, showing a marked S(V) contribution, which is absent in the other samples. The S(VI) contribution is more pronounced in 50/50+Cd respect all the other treatments.

The major S species present in the plants are organic, at lower energy and highly oxidized species at higher energy. Organic species are expected as the results of the plant metabolism, which convert inorganic S to organic S species (Dall'acqua et al., 2019; Rüdiger Hell et al., n.d.; Yarmolinsky et al., 2013). The reducing intensity in the organic contributions respect to treatments could indicate their replacement or interaction of Se as competing systems, forming Seleno amino compounds. The latter could be the case in grains, where control has the highest intensity compared to the other treatments.

As previously mentioned, the spectral contribution at lower energies, is compatible with a minor contribution of glutathione and L-methionine. Glutathione is also an important species seen in plants. It helps in the intermediate compound formation (GRX glutathione reductase activity), antioxidant response induced in plant stress, to form peptide complexes with heavy metals. It acts as a bridge between cysteine reduction and further metabolism (Rey and Tarrago, 2018).

Moreover, L-methionine is a common product of S transformation in plants formed from methylation of cysteine.

Further, mainly for the root samples, a thiophene contribution is compatible in the low energy side. It is expected that thiophene is produced in the plants as a chemical defense mechanism, especially in plant species where organic substances were stored in different parts of the plant (Ibrahim et al., 2015).

In the medium energy range, relatively lowmethionine sulfoxide components could be present, mainly in the roots spectra. Unfortunately overlapping contributions do not really permit to clearly recognize its contribution. Methionine sulfoxide reductase has a major role in antioxidant response in plants and it is for this of interest in the present case. Methionine and sulphur containing amino acids can reduce to form methionine sulfoxide (reversible) and methionine sulfone (irreversible) (Rey and Tarrago, 2018).

Finally, S(VI) contribution is present in most of the spectra in the high energy side, especially in shoots and grains. It is expected to be related to the detoxification process (Yarmolinsky et al., 2013).

S(IV) can be further reoxidized to S(VI) species or assimilated in S reductive pathway. The reoxidation is normally catalyzed by sulphite oxidase. The reoxidation normally takes place as a protective mechanism against plants sulphite toxicity (Yarmolinsky et al., 2013).

The spatial distribution of organic and oxidized sulphur species has been studied in the grains. The grains were spatially scanned by selecting the S  $K\alpha$  emission line with the fluorescence detector and setting the incoming energy at selected energies, corresponding to organic and oxidized species and to an isosbestic point above the XANES region for normalization purposes. The beam size defined the spatial resolution around 150  $\mu\text{m}$ .

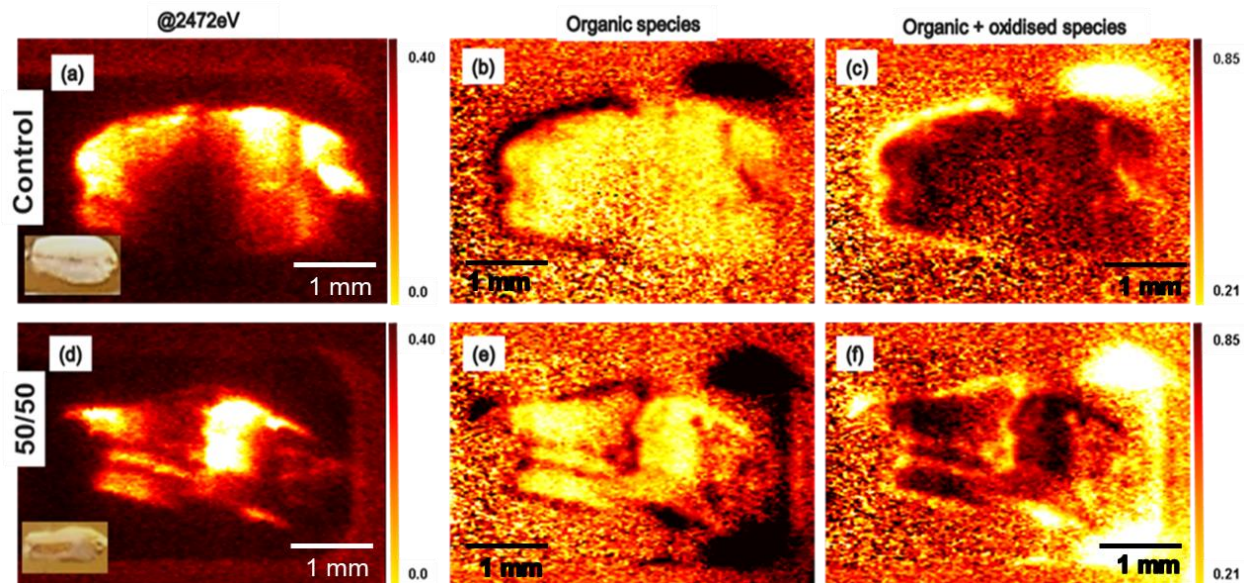


Figure 1.15: Sulphur species distribution in grains from control and 50/50 Se treatment. The first column (a) and (d) represents the total S, second column (b) and (e) represents the organic species distribution and column (c) and (f) represents the highly oxidized species distribution. The intensity of the maps is represented by the scale bar.

The incoming energy have been set at 2472.5 (organic species white line) and 2481.5 eV (S(VI) white line), to characterize the distribution of the organic and highly oxidized S species distribution. The S distribution has been collected as well fixing the incoming energy to 2491.6 eV (isosbestic point) for normalization purposes. Figure 1.15 depict the corresponding relative species distribution obtained by normalizing each map respect the isosbestic point ( $yn_i$ ) and dividing a particular normalized map (for example  $yn_{Cys}$ ) per the sum of all the normalized maps ( $Y_{Cys} = yn_{Cys} / (yn_{Cys} + yn_{S(VI)})$ ). It can be seen that the S organic species look present in the endosperm, while the higher S oxidized species are concentrated in the bran, eye, and filament regions.

From, the literature, generally in biological systems S and Se occur in proteins as constituents of the amino acids as cysteine, methionine, selenocysteine, and selenomethionine. Their redox activity can allow an amazing variety of post-translational protein modifications, metal free redox pathways, and unusual chalcogen redox states. Unlike any other amino acid, the “redox

chameleon” cysteine can participate in several distinct redox pathways, including exchange and radical reactions, as well as atom-, electron-, and hydride-transfer reactions. It occurs in various oxidation states in the human body, each of which exhibits distinctive chemical properties (e.g. redox activity, metal binding) and biological activity, and are then of interest in the present study (Jacob et al., 2003).

Comparison between the main Se and S species distribution in grains, for the Control and 50/50 treatment shows that both SeMet and highly S oxidised species are located in the eye and filament regions. Instead, the endosperm contains mainly Secys species and S organic species, as it could be expected, confirming both the reported results as in general Se is replaced by S in cysteine and methionine. Interestingly, the bran seems to present mainly a coexistence of SeMet, SeCys, and highly S oxidated species. However, the thickness of the samples, around 0.5 mm, should be considered, having S and Se K-edge absorption energies different penetration depths.

### **1.3.5 FTIR analysis in biofortified plant**

Complementary information to the Se and S speciation can be obtained by Fourier transform infrared spectroscopy (FTIR), giving it access to the functional groups present in the plant samples, identifying the protein bonds present in the plants. The IR fingerprints of different regions of the plant were given in the Figure 1.16. In general, amide I band ( $1700-1600\text{ cm}^{-1}$ ) which represents mainly C=O stretching and CN stretching and NH bending vibrations of peptide linkage. This amide region is very sensitive to protein secondary structures, with alpha helix and beta sheets at  $1645-1640\text{ cm}^{-1}$  Amide II which can be seen around  $1600-1500\text{ cm}^{-1}$  presentation of combined peptides with CN stretching and NH bending vibrations. Amide III, which is also sensitive to secondary protein structure and a less pronounced mostly seen in lower wavelength at  $1130-1175\text{ cm}^{-1}$  suggesting CN stretching and NH bending vibrations, CC stretching and CH bending. In some case the amide I and III are studied complementary to each other to analysed the protein conformational changes (Samargandi et al., 2014).

Table 1.4: FTIR wavelength and respective functional group found in the samples.



Wavelength (cm <sup>-1</sup> )	Roots	Shoots	Grains	
3400-3700 3300-3500	3382	3396	3367	O-H stretching N-H stretching (amides)
2850-2975	2927	2917.7, 2873	2929	C-H stretching(aldehydes)
1650-1750	1733.6	1729.8		C=O stretching
1600-1700	1641, 1602.5	1644.9	1654.6	C=O stretch (amide I)
1500-1600	1515		1540.8	C-H stretching and N-H bending amide II
1387	1384.6	1384.6		C-H methyl
1274	1253		1240	C-N stretch amide III
1000-1400	1049	1112, 1079	1155, 1024	C-O stretching

In the roots samples on panel (a) of Figure 1.16, the absorbance spectra respects to treatments are seen. The main peaks related to amine C=O stretching at 1641 cm<sup>-1</sup>, sharp peak in all samples and N-H stretching shifted to 1515 cm<sup>-1</sup> at lower region. Also 1604 cm<sup>-1</sup>, C-C stretching of aromatic compounds, with 1255 cm<sup>-1</sup> amide III seen in all Cd treated samples as a small peak, and mainly by control group and less pronounced in Se treatments. Similarly, the amide peaks were seen in present in shoots Figure 1.16(c) at slightly shifted positions 1644 cm<sup>-1</sup> of amide I, amide II and III is not present in shoots. In grains, Figure 1.16(e) amide I at 1654.6 cm<sup>-1</sup> and amide II at 1540.8 cm<sup>-1</sup> were more pronounced in all the samples. This could represent the more functional groups representing proteins in the grains than roots and shoots.

The peak at  $1387\text{ cm}^{-1}$  could be due to C-H bending, of methyl species, and they are only seen in roots and shoots. As seen from the left panel (b) and (d) of roots and shoots, they are more prominent in Se treatments and Cd group compared to Se with Cd treatments. This contribution could be either from a methyl, an aliphatic C-H stretching of methyl and phenolic compounds (Bulgariu et al., 2019; Samargandi et al., 2014). Also, the amide I and II peaks of grains can be visualized clearly in left panel (e), where in Se treatments and Se with Cd treatments the intensity of the bands is reversed, with 75/25 higher in Se group and lower under presence of Cd. It could be due to more selenite in the plants affects the protein contribution.

The contribution at lower energy  $1049\text{ cm}^{-1}$  is C-O stretching, broad range at  $3382\text{ cm}^{-1}$  O-H stretching of alcoholic compounds and C-H stretching of aldehydes at  $2927\text{ cm}^{-1}$ . They were also seen in shoots 1.16(c) and grains 1.16(e) at slightly shifted positions. However, the  $3330\text{-}3500\text{ cm}^{-1}$  also represents N-H stretch in amides in general, they don't attribute to protein bonding. These were not important in our study and not directly related to the proteins or peptide chains of enzymes and they won't be discussed further. The fingerprints of the IR respect to the samples were given in Table 1.4.

The selenium treatments have minor effects in the protein accumulation in the grains, they have reverse trend under the presence of Cd, moreover the amide II peak is not seen in the shoots and only in the roots and shoots rather methyl and phenolic compound is dominant in these parts of the plant.

In plants, the amide functional groups are main contribution of selenoproteins and suflur bound proteins. From, the results presented, we can see the presence of distinctive functional groups present and how the peaks vary according to treatment. Quantitative analysis based on amides present in the samples was not possible with the small set of data.

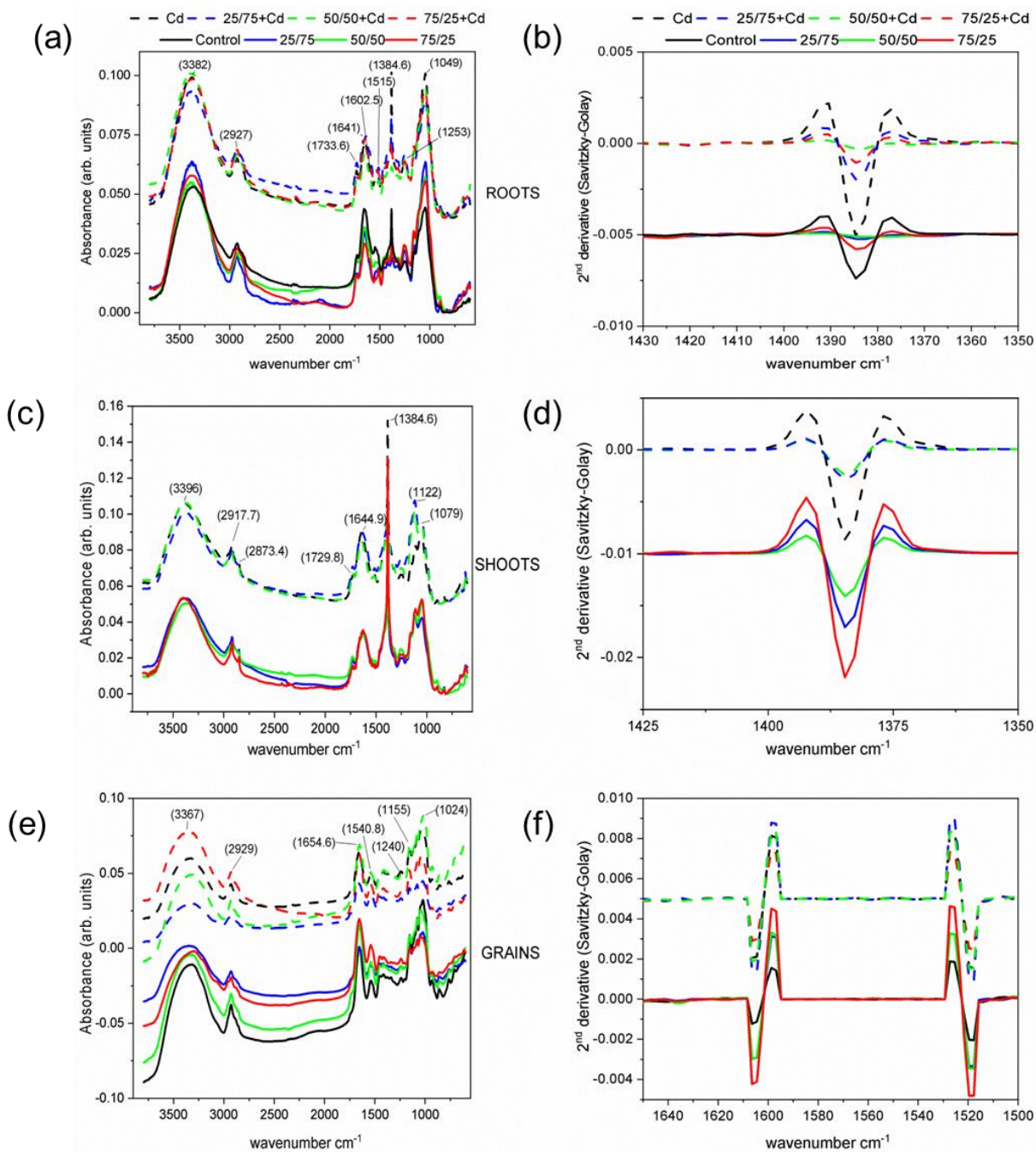


Figure 1.16: FTIR along different parts of the plant respect to treatments; (a), (c) and (e) represent the whole absorbance range of the spectra and (b), (d), and (f) represent the second derivative in different amide regions respect to roots, shoots and grains of different treatments. Continuous lines of spectra represent control and Se treatments, while dashed lines of spectra represent Cd and Se +Cd treatment group.

## 1.4 Conclusions

Se biofortification with different ratio of  $\text{Se}^{4+}$  and  $\text{Se}^{6+}$  in the treatments was studied in hydroponically grown wheat plants, in the absence and the presence of Cd.

The biomass and grain yield were reduced by the Se biofortification process, as well as by the Cd application. The total number of grains produced under Cd treatments were not significantly different from the Control, but it got reduced in the presence of Se. The Se uptake and translocation was reduced by 50% under Cd pollution, with a maximum of Se accumulation in grains for the 50/50 treatment. Instead, the Cd translocation from roots to grains increased in the presence of Se, with a maximum for the 50/50+Cd treatment. The average grain weight was linearly reduced when the Cd accumulation was higher. This suggests a combined toxicity effect from Cd and Se applications. Se and Cd treatments affect the uptake and storage of the essential micronutrients as Mo, Zn, Cu and Mn because of the competing uptake mechanisms.

SeMet and SeCyst are the major Se species found in Se biofortified grains, approximately 73% and 37%, respectively. In the presence of Cd, SeMeCys is forming while the amount of SeMet species gets reduced. The effect of Cd on the Se speciation does not affect the Se biofortification process as SeMet and SeMeCys are both directly bioavailable for human body, while SeCyst is less desired.

In a similar way to Se case, S K-edge XAS study showed how the Cd and Se interactions in the plant metabolism affect as well the coexisting sulphur species. Both organic and highly oxidized S species coexist along the plant and in the grains. SeMet and highly S oxidised species are mainly located in the eye and filament regions, while the SeCyst and S organic species are present in the endosperm. Instead, SeMet, SeCyst, and highly S oxidated species are present in the bran region of the grains. This is in accordance with the known natural distribution of wheat proteins.

The FTIR results show that the presence of Amide protein, which could be linked to seleno aminoacid, varies slightly depending upon the treatments. In roots and shoots, the peaks of methyl and phenolic compounds are more prominent, but only in shoots highly oxidized Se and S species are found, where all are expected to be related to the Se-induced stress.

Considering the Se speciation and total Se accumulation reported, the 50/50 treatment is better in terms of Se-biofortification of wheat plants grown in hydroponic media.

## **Chapter 2**

### **Gene expression analysis**

## 2.1 Introduction

Plant molecular studies focus on genes related to the elemental transportation pathways, adaptability of plants to different environments and defensive responses, for example against heavy metals and helps in optimizing the plant production in an effective way.

The stress responses of plants vary within plant genera, species, and cultivars (Gaudet et al., 2011). Moreover, plants have the ability to interact with different chemical species differently. For example, the  $\text{Se}^{4+}$  uptake is more diffusion based, mainly by phosphate transporters. Instead,  $\text{Se}^{6+}$  uptake is mainly due to sulphate transporters and follow, the sulphur metabolism in the plant system.(Ellis and Salt, 2003; Schiavon et al., 2020) In addition, it is well known that Se and Cd are reciprocally affecting their uptake and accumulation by plants (Affholder et al., 2019; Zhu et al., 2020). So, to address the sulphur pathway is a strategy to understand the effect of Se treatments and the possible Cd interference on the plant's metabolism and heavy metals accumulation.

In wheat, an adequate supply of sulphur is required for optimum growth and grain yield and quality. Sulphur is a constituent of amino acids, redox compounds, and many secondary metabolites contributing to both abiotic and biotic stress responses (Zhao et al., 1999). Sulphur transporters are responsible for trans-membrane transport of sulphate and other oxy-anions (Buchner et al., 2004) among them Se whose rate of uptake is likely to be influenced by both transporter expression levels and competition with bio-available sulphate (Hawkesford and Zhao, 2007).

In the present study, we quantify the expression of several genes related to sulphate transport and metabolism, and the antioxidant activity of the cell (Table 2.1) to assess how Cd-induced stress affects the Se biofortification process in wheat plants.

Up to now, similar studies have been done mainly on rice (Cui et al., 2018; Wan et al., 2016; Wu et al., 2021) and in less extent concerning other crops like broccoli (Pedrero et al., 2007), rape (Zembala et al., 2010), and wheat as well (Li et al., 2020; Zembala et al., 2010; Zhu et al., 2020), but as far as we know there is no information available respect the above mentioned genes expression comparing different Se forms ( $\text{Se}^{4+}$ ,  $\text{Se}^{6+}$  and the mixture of them) combined or not with Cd exposure.

Table 2.1: Genes of interest and their function

Wheat gene acquisition Database (IWGSC)code /(Gramene.org)	Gene name	Function
TraesCS4A02G043400	SULTR 1:1	<ul style="list-style-type: none"> <li>• high affinity sulphur transporter in plasma membrane, roots guard cells</li> <li>• uptake of sulphate from roots as an anion transporter</li> </ul>
TraesCS5B02G228500	SULTR1:3	<ul style="list-style-type: none"> <li>• high affinity sulphur transporter in plasma membrane</li> <li>• source to sink sulphate translocation in roots</li> </ul>
TraesCS5A02G166400	SULTR4:1	<ul style="list-style-type: none"> <li>• Low affinity sulphate transporter, found in tonoplast of vacuoles</li> <li>• facilitates the efflux of sulphate from the vacuole into the cytoplasm, influencing the capacity for vacuole storage of sulphate mainly in roots(Kataoka et al., 2004)</li> </ul>
TraesCS5A02G382900	APS	<ul style="list-style-type: none"> <li>• ATP sulphurylase (ATPS), involved in the sulphate activation, first step in S metabolism.</li> <li>• ATPS forms adenosine phosphosulphate (APS) from ATP and sulphate, further reduced into sulphide by APS reductase to be incorporated into cysteine.</li> </ul>



TraesCS5A02G022200	OASTL	<ul style="list-style-type: none"> <li>• O-acetylserine(thiol)lyase, a catalyzer in the synthesis of cysteine by condensation of O-Acetyl serine and sulfide.</li> <li>• Involved in the S reduction assimilation pathway.</li> </ul>
TraesCS7A02G272200	PCS2	<ul style="list-style-type: none"> <li>• Mainly seen in vascular plants, in both roots and shoots. Phytochelatins, are small peptides synthesised for heavy metal detoxification.</li> <li>• It is synthesised non-ribosomically, from GSH by PC synthetase (PCS).</li> </ul> <p>Mainly expressed in Cd<sup>2+</sup> tolerance, known to form Cd-GSH complexes (Kumari et al., 2015).</p>
TraesCS4A02G025200	APX	<ul style="list-style-type: none"> <li>• Ascorbate peroxidase – induced by antioxidant defense response.</li> <li>• It regulates various biological pathways by maintaining H<sub>2</sub>O<sub>2</sub> homeostasis within the plant cell (Kumari et al., 2015).</li> </ul>
TraesCS1A02G020500	Actin	<ul style="list-style-type: none"> <li>• Essential component of cell cytoskeleton</li> <li>• Plays an important role in cellular functions involving, cytoplasmic streaming, cell shape determination, cell division, organelle movement and extension growth.</li> </ul> <p><b>Housekeeping gene</b> of the study (gene expression remains stable as not affected among treatments)-</p>

## 2.2 Experimental methods

### 2.2.1 Plant samples and growing conditions with different treatments

The experimental conditions of the cultivation of short term plants were same as reported in section 1.2. For the gene expression studies the treatment groups used were shown in the Table 2.2.

Table 2.2: Se biofortication with Cd pollution treatment groups gene expression studies

<b>Control</b> (No treatment)	<b>Cd</b> (Cadmium)
<b>Se<sup>4+</sup></b> (Selenite)	<b>Se<sup>4+</sup> + Cd</b> (Selenite + Cadmium)
<b>Semix</b> (1:1 ratio of Se <sup>4+</sup> /Se <sup>6+</sup> )	<b>Semix + Cd</b> (1:1 ratio of Se <sup>4+</sup> /Se <sup>6+</sup> + Cadmium)
<b>Se<sup>6+</sup></b> (Selenate)	<b>Se<sup>6+</sup> + Cd</b> (Selenate + Cadmium)

Note: The treatments were mentioned in the figures, with oxidation state inside brackets rather than in superscript as shown in the table and the text follows.

The treatment concentration (Se10  $\mu$ M and Cd1  $\mu$ M) and the application time (vegetative) were same as well as given in section 1.2, under experimental methods. The plants were harvested just before the flowering stage. Pool of three plants (roots and shoots) from each group along with two replicates were immediately frozen in liquid nitrogen and stored at -80°C for further studies.

### 2.2.2 RNA extraction, cDNA synthesis and quantification

RNA of root and shoot (leaves, stem, and nodes) samples were extracted following the protocol of the plant extraction kit (Maxwell© RSC from Promega) and the concentration measured using a nanodrop (Thermofisher). cDNA of the samples was retrotranscribed with the help of Invitrogen-SuperScript Double-Stranded *cDNA Synthesis Kit* from Thermofisher. The obtained cDNA was diluted 10 times and used for quantification of genes of interest. Primers for the targeted genes were designed in the 5'-UTR or 3'-UTR of the mRNA sequence of each gene, obtained from Gramene wheat genome database using NCBI primer blast tool. The primer

sequences are listed in Table 2.3. Each 10  $\mu$ l qPCR reaction was composed of 1x LightCycler® 480 SYBR Green I Master (Roche), 10% of cDNA diluted 1:10 and gene-specific primers at a final concentration of 250 nM. Three biological replicates and two technical replicates were used for each treatment. The qPCR amplification program was set as: 1 cycle of pre-incubation at 95°C for 5 minutes, 45 cycles of amplification at 95°C for 10 seconds, 58°C for 15 seconds and 72°C for 10 seconds, 1 cycle of melting at 95°C for 5 seconds, 65°C for 1 minute, and a final cycle of cooling at 40°C. The actin gene was used as internal reference (or housekeeping) gene, as it showed the most stable expression among all the treatments. Normalization of qPCR data was done by calculating the gene copy numbers from the Ct values and dividing for a normalization factor based on the primer efficiency. Then the relative gene expression was calculated by comparing the values to the control treatment, whose expression was set as equal to 1. The primers amplification efficiencies were calculated using the raw amplification data in LinRegPCR software and used to adjust the normalized expression value.

Table 2.3: Primers for the targeted genes

Wheat gene acquisition Database (IWGSC) code / (Gramene.org)	Gene name	Forward primer 5' - 3'	Reverse primer 5' - 3'
TraesCS4A02G043400	SULTR 1:1	GCATCAGGTTCG CAAGAT	ACCTCCATCCAACTGC T
TraesCS5B02G228500	SULTR1:3	AGCCGAGATCGG TATAAGCA	ACAAGCTTGGCTTTTG CTTCA
TraesCS5A02G166400	SULTR4:1	CCATCGCTTGAG TAGGAC	GAGGATGTGGGGAGCA AG
TraesCS5A02G382900	APS	TGGTGCCAATAA GGATGG	GTGCTCCAGTGAAAAA TATAACACC
TraesCS5A02G022200	OASTL	GTCCATATGTCA GCCAGTG	CCGACGGTCCAGATTG A
TraesCS7A02G272200	PCS2	TGTTATGGATCG GAGGGAC	TAGGGAGCTTCAGAAG ACC
TraesCS4A02G025200	APX	GAACCCTCTGAA GATGTACG	CATGAATAGCAGATGG GGG
TraesCS6D02G012200	TaFNRII	TGTAGCGATGAG TGAGTGG	ACGACCAGAAGACGAT CGAG
TraesCS1A02G020500	Actin	CCCTAGCATAGT TGGTCGCC	TCACGATACCGTGCTC GATG

## 2.3 Results and discussion

### 2.3.1 Sulphate transporters

The expression of several sulphate (SULTR1:1, SULTR1:3, and SULTR4:1) transporter genes in relation to ACTIN in roots and shoots of wheat plants under different Se and Cd treatments (Figure 2.1) shows that the S transport in the aerial part of the plants is statistically (Table 2.4) more active than in the roots, most likely to facilitate the distribution of nutrients, while they are not overexpressed or suppressed in the roots, probably as a natural plant defense in front of a possible Se or Cd toxicity.

The expression of SULTR1:1 in roots (Figure 2.1(a)) is not affected by the exposure to Cd neither Se, except for Se<sup>6+</sup>. However, when plants are grown in the combined presence of Se+Cd, the expression of this gene is altered, being repressed with Se<sup>4+</sup> and induced with Se<sup>6+</sup>, showing intermediate values the Semix treatment. The uptake of sulphate from roots as an anion transporter, which is represented by the SULTR1:1 gene expression, seems not altered under the presence of Cd alone, while the Se<sup>6+</sup> treatments, both with and without Cd, enhance this process, indicating that the Se<sup>6+</sup> species tend to activate and probably follow the sulphate uptake pathway. Higher activity of SULTR1:1 in the presence of Se<sup>6+</sup> was also seen in the literature among different wheat species (Ciaffi et al., 2013; Dall'acqua et al., 2019). Interestingly, the combination of Se<sup>4+</sup> and Cd seems to reduce such uptake. In the presence of Cd SULTR1:1 and SULTR1:3 root expressions (Figure 2.1(b)) are highly correlated. Instead, contrary to SULTR1:1, the expression in roots of SULTR1:3 are highly repressed by all Se and especially Cd treatments. When Cd is present, Se<sup>4+</sup> strongly repressed the expression of SULTR1:3 while the supplementation with Se<sup>6+</sup> tends to ameliorate the repression of this gene caused by Cd. Again, the Semix treatment shows intermediate expression values between both Se forms. Instead, in shoots the expression level of SULTR1:3 (Figure 2.1(c)) is not altered by any of the Se treatments, but it is significantly increased up to 6-fold by Cd compared to control and even more, up to 12-fold, by the combination of Se treatments with Cd.

The sulphate translocation, represented by the SULTR1:3 gene expression, looks reduced by Se and Cd in the roots, while is strongly enhanced by their combination in the shoots. It could be due to the nature of the gene as SULTR 1:3 is a high affinity transporter localized in phloem

and important for source–sink redistribution of sulphate (Gigolashvili and Kopriva, 2014). This trend is also seen in SULTR 1:3 expression in other wheat species (Ciaffi et al., 2013). In particular, the very strong up-regulation of this gene for the Semix with Cd seems to correlate with the enhancement of the Cd TF from roots-to-shoots reported above (Figure 1.3(d)). It could correspond to the final higher Cd contamination in the wheat produced grains, when the wheat plant are Se biofortified with a 50:50 mixture of  $\text{Se}^{4+}$  and  $\text{Se}^{6+}$  species in the presence of Cd, which need to be considered for applications.

The expression of SULTR4:1 in roots (Figure 2.1(d)) is downregulated by  $\text{Se}^{4+}$  and it seems to progressively increase by increasing the  $\text{Se}^{6+}$  fraction in the treatment. In the presence of Cd, SULTR4:1 expression seems repressed by this metal, and significantly enhanced only by the  $\text{Se}^{6+}$  treatment. In shoots (Figure 2.1(e)) Se treatments caused no significant change in the expression level of SULTR4:1 but Cd treatments significantly increased this gene expression. The SULTR4:1 expression is expected to facilitate the efflux of sulphate from the vacuole into the cytoplasm, influencing the capacity of sulphate storage, mainly in roots. Its general stronger expression in roots for  $\text{Se}^{6+}$  respect to  $\text{Se}^{4+}$  treatment suggest a higher sulphate storage capability in the latter case, confirmed by the corresponding smaller Se TF capabilities from roots to shoots (Figure 1.3(b)) Interestingly for the shoots it looks the contrary, with  $\text{Se}^{4+}$  treatment which shows a lower sulphate storage capability, confirmed by the increased Se TF from shoots to grains with increasing the  $\text{Se}^{4+}$  fraction in the treatment (Figure 1.3(b)).

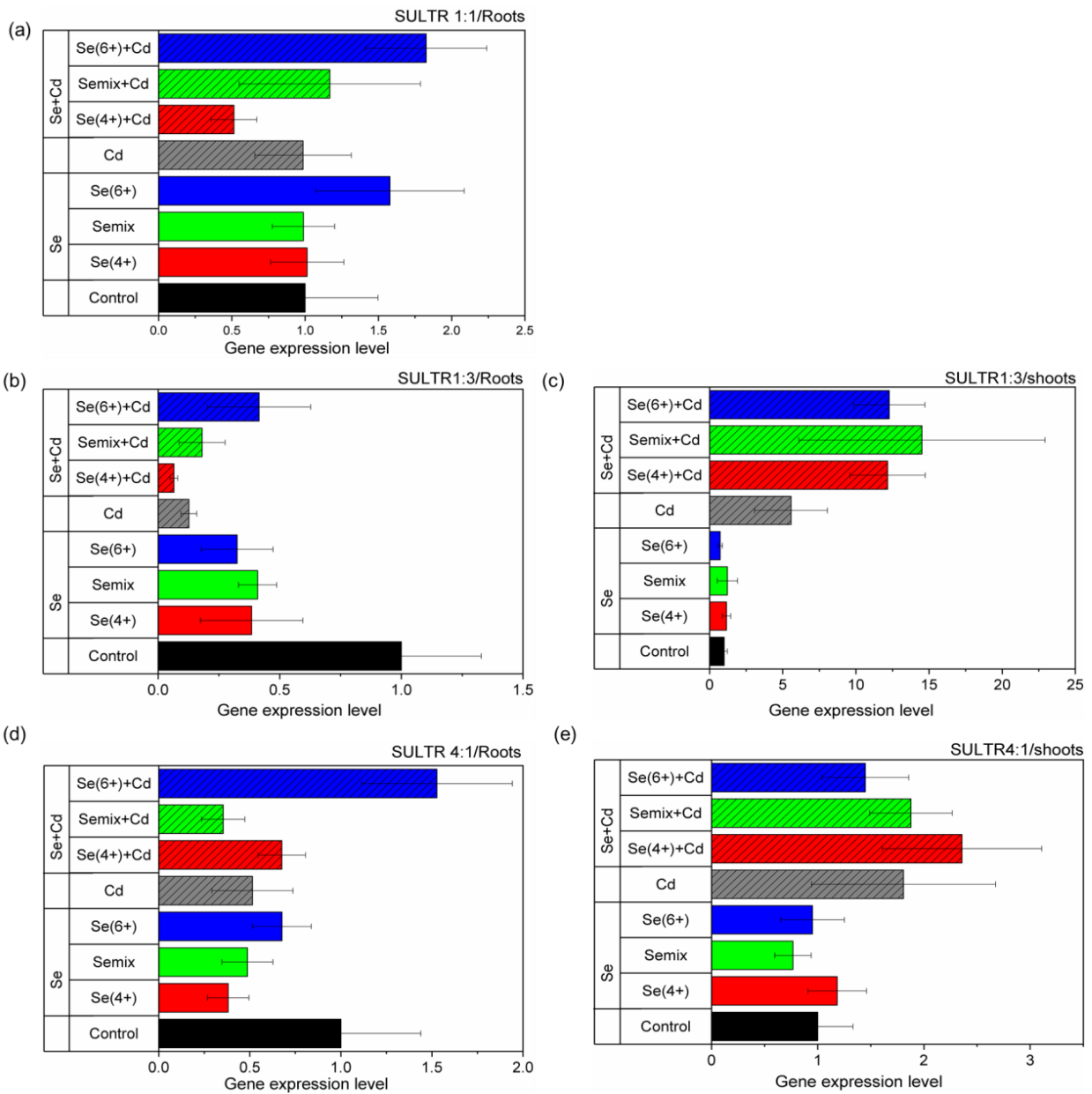


Figure 2.1: Expression of sulphate transporter genes (SULTR) in relation to ACTIN in roots (a, b, d) and shoots (c, e) of wheat plants under different Se (10  $\mu$ M no pattern bars) and Cd (1  $\mu$ M diagonal pattern) treatments. Control (black), Cd (grey), Se $4^+$  (blue), Semix (green) and Se $6^+$  (red). Values are means  $\pm$  SE (n=3).

Table 2.4: Statistical analysis of sulphate transporters by the non-parametric comparison Dunnet test pair joint ranking respect to the control sample (P value 1). The score mean of comparison is given in brackets. The groups are ordered from higher mean score ranking to the lowest based on the expression obtained respect to control. The treatments statistically not significant respect to control were given the same mean score.

<b>Roots</b>			<b>Shoots</b>	
<b>SULTR 1:1</b>	<b>SULTR 1:3</b>	<b>SULTR 4:1</b>	<b>SULTR 1:3</b>	<b>SULTR 4:1</b>
Se(6+)+Cd (3)	Cd (5)	Cd (2)	Semix+Cd (5)	Se(4+)+Cd (4)
Se(6+) (2)	Se(6+)+Cd (0)	Se(6+) (0)	Se(6+)+Cd (4)	Semix+Cd (3)
Cd (1)	Semix (-1)	Se(6+)+Cd (0)	Se(4+)+Cd (3)	Se(6+)+Cd (1)
Semix+Cd (1)	Se(4+) (-2)	Se(4+)+Cd (-1)	Semix (1)	Se(4+) (0)
Se(4+) (0)	Se(6+) (-3)	Semix (-3)	Se(4+) (0)	Se(6+) (0)
Semix (0)	Semix+Cd (-4)	Se(4+) (-4)	Se(6+) (0)	Semix (-1)
Se(4+)+Cd (-2)	Se(4+)+Cd (-6)	Semix+Cd (-5)	Cd (-2)	Cd (-2)

### 2.3.2 Genes related to Sulphur metabolism

Figure 2.2 depicts the expression of the APS (panel (a)) and OASTL (panels (b), (c)) genes related to ACTIN, both involved in the sulphur metabolism. The statistics is given in Table 2.5. In roots without Cd, the expression of APS seems slightly repressed by Se<sup>4+</sup> and upregulated by Se<sup>6+</sup> treatment. Anyway, the absence of a clear trend and the small amount of the variations once compared with the error bars request a further confirmation to validate this result. Instead, when Cd is present, the expression level of APS is strongly downregulated, indicating smaller sulphate activation in the presence of this pollutant. Only the combination of Se<sup>4+</sup> and Cd ameliorates the expression of APS above the values found for Cd alone, suggesting that the particular combination of Se(IV) species and Cd could help the formation of organic species. Such organic species could link to Se to form SeCyst species at least, as shown by the increase of spectral weight at lower energy in the previously reported Se K-edge absorption spectra (Figure 1.6). Instead, the



expression of OASTL in roots is repressed similarly for the different Se treatments, both in the presence and absence of Cd. However, all Se treatments in the presence of Cd have slightly higher expression of this gene compared to Cd alone, highlighting possible synergies in between Se and Cd to favor the organic species formation. Again, in shoots, the expression of OASTL seems slightly enhanced in the presence of  $\text{Se}^{4+}$ , in agreement with the higher detected SeCyst content when increasing the  $\text{Se}^{4+}$  fraction in the treatment (Figure 1.6). Cd alone has no effect on the expression of OASTL compared to the control level, but  $\text{Se}^{6+}$  and  $\text{Se}^{4+}$  together with this metal downregulate and upregulate the relative expression of this gene once compared to both Cd and control treatments, respectively.

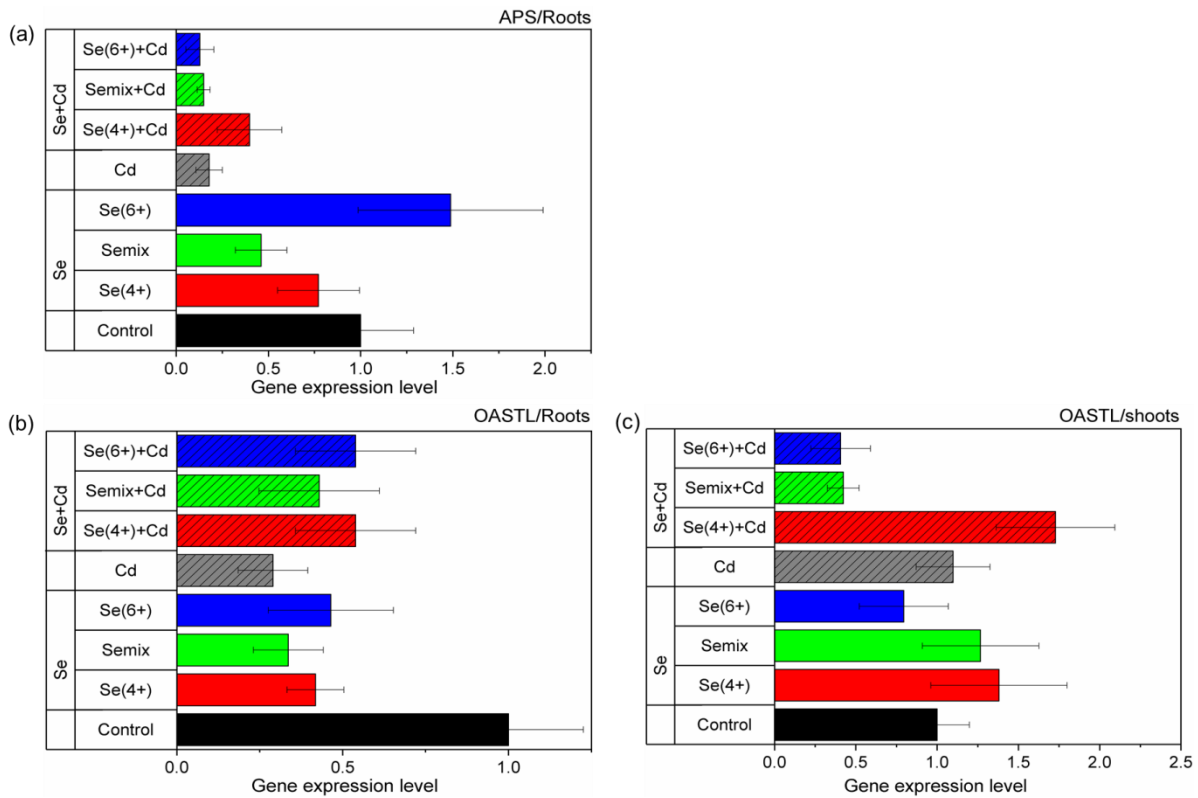


Figure 2.2: Expression of the sulphate metabolism genes, (a) APS and (b, c) OASTL, related to ACTIN in the roots and shoots of wheat plants under different Se ( $10 \mu\text{M}$  no pattern bars) and Cd ( $1 \mu\text{M}$  diagonal pattern) treatments. Control (black), Cd (grey),  $\text{Se}^{4+}$  (blue), Semix (green) and  $\text{Se}^{6+}$  (red). Values are means  $\pm$  SE ( $n = 3$ ).

Table 2.5: Statistical analysis of sulphate metabolic genes by the non-parametric comparison Dunnet test pair joint ranking respect to the control sample (P value 1). The score mean of comparison is given in brackets. The groups are ordered from higher mean score ranking to the lowest based on the expression obtained respect to control. The treatments statistically not significant respect to control were given the same mean score.

<b>Roots</b>		<b>Shoots</b>
<b>APS</b>	<b>OASTL</b>	<b>OASTL</b>
<b>Cd (3)</b>	<b>Cd (2)</b>	<b>Se(4+)+Cd (3)</b>
<b>Se(4+) (0)</b>	<b>Se(4+)+Cd (-1)</b>	<b>Se(4+) (2)</b>
<b>Se(6+) (0)</b>	<b>Se(6+)+Cd (0)</b>	<b>Semix (1)</b>
<b>Semix (-1)</b>	<b>Se(6+) (0)</b>	<b>Cd (0)</b>
<b>Se(4+)+Cd (-2)</b>	<b>Semix+Cd (-5)</b>	<b>Se(6+) (0)</b>
<b>Semix+Cd (-4)</b>	<b>Se(4+) (-4)</b>	<b>Semix+Cd (-1)</b>
<b>Se(6+)+Cd (-5)</b>	<b>Semix (-3)</b>	<b>Se(6+)+Cd (-2)</b>
<b>Cd (3)</b>	<b>Cd (2)</b>	<b>Se(4+)+Cd (-3)</b>

### 2.3.3 Stress responsive genes

Finally, the expression of APX and PCS genes in relation to heavy metal detoxification can be used to characterize the Cd-induced stress response in wheat plants (Figure 2.3 and Table 2.6). In roots, both genes are repressed by the presence of Se and Cd alone or in combination respect to the control, suggesting a reduced stress response in the Se biofortified roots plants. This result is in contrast with the literature found (Kumari et al., 2015), but the discrepancy could be due to the difference in concentration used by the authors, 200 mg Cd Kg<sup>-1</sup> (1.7 mM) of soil respect to 1 µMCd L<sup>-1</sup> of solution in our study. The higher threshold value in European agricultural soil is

0.17mM (Tóth et al., 2016). Indeed, the root DW in the present study is not affected by the Cd concentration applied (Figure 1.2 (a)).

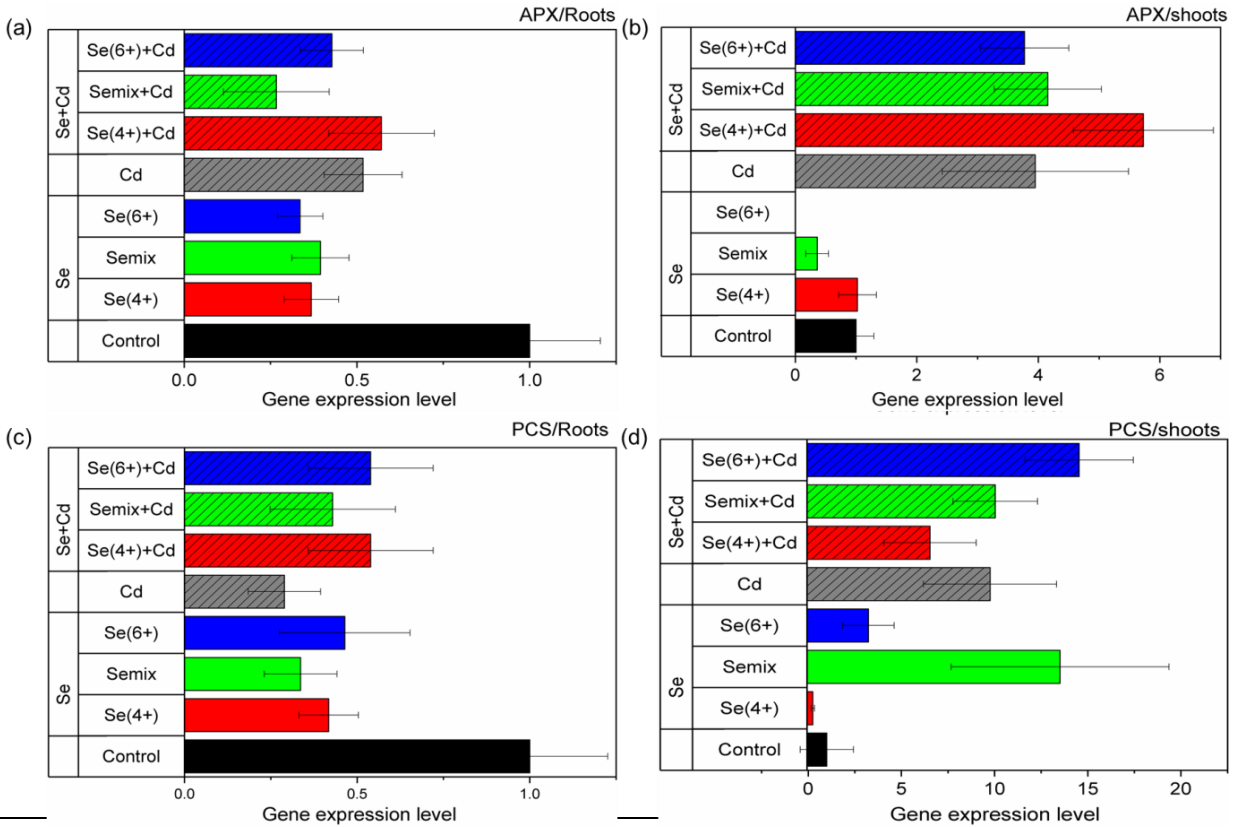


Figure 2.3: Expression of stress responsive genes (a, b) APX and (c, d) PCS related to ACTIN in roots and shoots of wheat plants under different Se (10  $\mu$ M no pattern bars) and Cd (1  $\mu$ M diagonal pattern) treatments. Control (black), Cd (grey), Se<sup>4+</sup> (blue), Semix (green) and Se<sup>6+</sup> (red). Values are means  $\pm$  SE (n = 3).

In shoots (Figure 2.3(b) and (d)), the presence of Cd strongly increases both the APX and PCS expression in a significant way. This is in accordance with the results from Kumari et al., 2015, suggesting a tight control of such element in the above part of the plant where the most sensitive metabolism is present. Moreover, in the presence of Cd, the APX expression seems strongly correlated with the expression of SULTR4:1, which has low affinity to sulphate transport. The Cd detoxification in shoots seems related to its storage in the vacuole. In the presence of Se,

such a mechanism seems affected by the Se species with Se<sup>4+</sup> which is favouring it. Still in shoots, in the absence of Cd, the increase of Se<sup>6+</sup> fraction in the treatment is progressively downregulating up to the full suppression the APX gene expression.

Table 2.6: Statistical analysis of stress responsive genes by the non-parametric comparison Dunnet test pair joint ranking respect to the control sample (P value 1). The score mean of comparison is given in brackets. The groups are ordered from higher mean score ranking to the lowest based on the expression obtained respect to control. The treatments statistically not significant respect to control were given the same mean score.

<b>Roots</b>		<b>Shoots</b>	
APX	PCS	APX	PCS
Cd (1)	Cd (2)	Se(4+)+Cd (4)	Se(6+)+Cd (5)
Se(4+)+Cd (0)	Se(6+)+Cd (1)	Semix+Cd (3)	Semix (4)
Se(6+)+Cd (-2)	Se(4+) (0)	Se(6+)+Cd (1)	Semix+Cd (3)
Semix (-3)	Se(4+)+Cd (0)	Se(4+) (0)	Se(4+)+Cd (1)
Se(4+) (-4)	Semix (-1)	Semix (1)	Se(4+) (0)
Se(6+) (-5)	Se(6+) (-3)	Se(6+) (-1)	Se(6+) (0)
Semix+Cd (-6)	Semix+Cd (-4)	Cd (-2)	Cd (-2)

Interestingly, in the same conditions, the PCS expression is strongly enhanced by Semix, in agreement with the stronger wheat resistance to such treatment (Subirana, 2018). Always in the presence of Cd, while the Se<sup>4+</sup> treatment is increasing the APX, it is decreasing the PCS gene expression respect the Se<sup>6+</sup> treatment, with the Semix systematically in the middle. These reported trends unveil the competing plant detoxification mechanism and their sensitivity to particular chemical species. The results show that in shoots, the systematic transformation of inorganic to organic species is altered among the presence and absence of Cd in the selenium treated samples, suggesting that particular Se and Cd combinations can influence the formation of organic

complexes and affect the final growing parameters. In the present case the shoots DW tend to increase without Cd or Se treatment, while in Cd presence by increasing the  $\text{Se}^{4+}$  fraction in the treatment, plants have positive effect against the Cd and Se toxicity indicating involvement of both Cd and  $\text{Se}^{4+}$  species in plant stress reduction.

## 2.4 Conclusions

The expression of the selected genes, characterizing the sulphate transport and metabolism, and the plant stress response in young wheat plants grown under different Se treatments in the presence and absence of Cd has been addressed.

The sulphate transporter genes, which are expected to affect the Se and Cd mobility, are more active in the aerial parts of the plants for SULTR1:3 and SULTR4:1, while they are suppressed in the roots. However, the major root transporter SULTR1:1 is seen active in roots.

In the roots, in most of the cases, the sulphate transporter genes are upregulated by the Se<sup>6+</sup> treatments, independently of the Cd presence, but Se<sup>4+</sup>+Cd downregulate them. Interestingly this is not in accordance with the amount of Se and Cd detected in the roots for the different treatments. It is more related to the uptake mechanism, as Se(VI) inhibits S uptake in the roots which results in the gene expression upregulation for Se<sup>6+</sup> and downregulation in the presence of Se<sup>4+</sup>. This could be related with the previously reported general increase of other nutrients (Zn, Mo, Cu, Mn, and B) by Se<sup>6+</sup>, caused by influence in uptake.

The expression of the genes related to the sulphur metabolism is, in most of the cases, repressed by the Cd and Se treatments. However, most Se+Cd treatments show slightly higher expression of these genes compared to Cd alone, highlighting possible synergies in between Se and Cd in favouring the formation of organic species. As they could affect the gene expression resulting in transportation of S and organic S compounds involved in the metabolism. This effect is recognised by S starvation due to competition with Se and possibly Cd. Such organic species seems partially to link to Se to form organic Se species, as shown in the previously reported results from the Se K-edge XAS study.

In brief, both the stress responsive gene expressions in roots are suppressed by the presence of Se and Cd respect the control sample, suggesting a reduced stress response in the Se biofortified wheat roots, and look no correlated to the plant growing parameters. Just the combination of Cd and Se<sup>4+</sup> seems to slightly upregulate the APX gene in the roots.

In shoots, the expression level of the sulphate transporter genes is not strongly altered by any of the Se treatments, but they are increased for the Cd treatment respect to the control and even more by the combination of Se treatments with Cd. This is in accordance with the translocation factors reported previously, which are affected by the Se and Cd combination. In particular, the very strong up-regulation of the SULTR1:3 gene for the Semix with Cd seems to correlate with the enhancement of the Cd TF from roots-to-shoots and it could correspond to the higher Cd accumulation in the shoots. Moreover, SULTR4:1 (controlling the efflux of sulphate from the vacuole into the cytoplasm, influencing the capacity of sulphate storage) is slightly upregulated by  $\text{Se}^{4+}$ , which may correspond with the increased Se TF from shoots to grains observed when  $\text{Se}^{4+}$  fraction was higher in the treatment.

In addition, OASTL (catalyse the synthesis of cysteine) in shoots, is upregulated in the presence of  $\text{Se}^{4+}$ , in agreement with the higher detected SeCyst content when increasing the  $\text{Se}^{4+}$  fraction in the treatment, as visible from the previously reported Se K-edge XAS spectra. Cd alone has no effect on its expression compared to the control level, but  $\text{Se}^{6+}$  and  $\text{Se}^{4+}$  together with Cd downregulate and upregulate the relative expression of this gene once compared to both Cd and control treatments, respectively. Cysteine also affected by the antioxidant stress induced in plants, which is could be activated more in the presence of both Se and Cd.

Moreover, the presence of Cd increases significantly the stress responsive gene expression for both APX and PCS in shoots, suggesting a relative tolerance to such element at low concentration. This can be related to the fact that the APX expression is strongly correlated with the SULTR4:1 response.  $\text{Se}^{4+}$  enhances the availability of sulphate in the cytoplasm, but decreases the expression of PCS which might be involved in the Cd detoxification mechanism. In contrast, in absence of Cd, such correlations disappear. The increase of  $\text{Se}^{6+}$  fraction in the treatment is progressively downregulating up to the full suppression the APX gene expression, while the PCS expression is strongly enhanced by Semix, in agreement with previous results showing the enhanced resistance with Semix.

In conclusion, the selected genes expression looks affected by the different Se and Cd treatments, even at realistic concentrations for practical applications. The presence of Cd and of different Se species influences the plant metabolism and affects the Se biofortification process, with the different chemical species competing in the sulphate pathways and transformation.

## **Chapter 3**

### **Mercury speciation in selenium biofortified wheat plants grown in mercury contaminated environment**



### 3.1 Introduction

Mercury (Hg) is an element that has been traditionally used in different activities ranging from mining to medicine (coal mining, (Hylander and Goodsite, 2006) gold mining, (Esdaile and Chalker, 2018) dental amalgams, (Faheem Maqbool et al., 2014) pharmaceutical industry (Vries et al., 2015)). Unfortunately, the release of Hg as a result of anthropogenic activities causes harmful effects on the environment and to the human health (Nica et al., 2017; Sánchez-Báscones et al., 2017) .

Hg species can easily transform and form complexes making Hg contamination a cyclic process in the environment (Álvarez-Fernández et al., 2014; Arif et al., 2016; Singh et al., 2016; Tangahu et al., 2011). Among all, methylated Hg species cause the major threat due to their high toxicity. The ability of the methylated group to cross the blood brain barrier makes it more prone to the development of nervous and nephron pathologies in humans (Sharma et al., 2019). Moreover, in pregnant women, methylmercury species may affect the foetus development and may lead to congenital neural disorders (Humaira, 2016; Karita et al., 2016; Nica et al., 2017) .

Hg concentration above 2 µg/g in soils is considered an ecological risk (Tóth et al., 2016). However, detailed surveys carried out across Europe, sampling mostly agricultural and grazing soils, have found that Hg concentration ranges from 0.003 to 3.12 µg/g and it accumulates in those areas of northern Europe where a wet and cold climate favours the build-up of soil organic material (Ottesen et al., 2013). The Hg species present in soil depend on soil characteristics (pH and moisture of the soil, the presence of sulphur reducing bacteria, organic matter content, etc...). In general, there is a conversion of the most soluble and rather unstable  $\text{Hg}^0$  and  $\text{Hg}^{2+}$  species to organic complexes. The combination of environmental and geological factors together with the plant species define both the level of Hg and its chemical state present in food (Humaira, 2016). Organic forms and methyl complexes formed by bacterial methylation ( $\text{Hg}^{2+}$  species in case of methyl group) are usually absorbed by plants over  $\text{Hg}^0$  at suitable acidic pH and Hg species mobility conditions (Arif et al., 2016; Hylander and Goodsite, 2006; Tangahu et al., 2011). Methylmercury species commonly bioaccumulate and biomagnify in the food chain mostly in polluted aquatic ecosystems and in food crops and fodder produced from contaminated soils (Andrews, 2006; Navarro et al., 2006; Sysalová et al., 2017) which is a major health concern.

Heavy metal absorption by plants is mainly due to the ability of roots to exudate chelates to form metal complexes, to induced pH changes and redox reactions to solubilize them or simply by diffusion of ions into the cells driven by concentration gradients (Álvarez-Fernández et al., 2014; Arif et al., 2016; Tangahu et al., 2011). On the other hand, the plant metal uptake pathway occurs through a series of chemical breakdowns which normally affects the main uptake of nutrient elements, potentially modifying the efficiency of the absorption mechanism (Arif et al., 2016; Dubey et al., 2018). Regarding Hg, different species of plants may have different Hg uptake mechanisms as reported for grains like rice, wheat and maize (Dubey et al., 2018; Krupp et al., 2009; R. Li et al., 2017; Sahu et al., 2012; Shumaker and Begonia, 2005). The forms in which metal ions are transported from the roots to the shoots and grains are not well known. In cereal crops, Hg accumulates more in roots whereas its concentration gets reduced in the plant system along shoots and in the final amount stored in the grains (Dang et al., 2019; Li et al., 2019; Meng et al., 2011; Y. Wang et al., 2016). Hg has the effect to reduce the chlorophyll synthesis activity in the plants and to interfere with the nutrients uptake mechanisms (Dubey et al., 2018; Liu et al., 2010). In addition, Hg generates oxidative stress and affects the plant root formation, biomass, and grain yield (Sahu et al., 2012).

The antagonism between Hg and Se (Dang et al., 2019; Li et al., 2019) have been widely studied in animals, (Cuvín-Aralar and Furness, 1991; Khan and Wang, 2009) and aquatic life (Gailer et al., 2000; George et al., 2011). In case of plants, Hg and Se antagonism is gaining attention for varying applications including bioremediation and nutritional enrichment (Chang et al., 2020; Li et al., 2019). In plants, the sulphur pathway is the most affected under the presence of Se and Hg as the accumulation of heavy metals causes stress in the sulphate transporters and other redox reactions and in turn there reduction pathways along the plants (Álvarez-Fernández et al., 2014; Li et al., 2019; Singh et al., 2016). Hence, this competing mechanism may have a direct effect on the final Hg concentration and on the ratio of chemical species found in crops grown in Hg polluted soils, as well as, on the outcome of the Se-biofortification process. Heavy metal accumulation varies from plant to plant; anyway some common behaviour can be identified. For example, Se uptake has been found to reduce the Hg concentration by modifying the uptake of other essential nutrients in rice grains (Li et al., 2019). Similarly, in vegetables like radish Se helps in circumventing Hg uptake (Shanker et al., 1996).

However, in most cases, the speciation of Hg in plants, which is intrinsically linked to its toxicity, is overlooked or performed via indirect speciation techniques, e.g. HPLC-ICP-MS, that require harsh sample treatment which may influence the chemical state of the species under study.

In this work, we report a study on the Hg speciation in Se-biofortified wheat. Wheat was chosen since it is one of the crops most widely consumed over a wide range of population in Europe (Eurostat, 2020) and secondary Se accumulator. In addition, wheat is one of the cereal crops which is most largely affected by heavy metal contamination due to its physiological nature (R. Li et al., 2017; Liu et al., 2009; Meng et al., 2011; S. Wang et al., 2016). We used hydroponic cultivation system to be able to decouple the influence of the soil parameters over the Hg and Se interactions. The aim of the present work is to study the influence that the different inorganic Se chemical species used for Se-biofortification of wheat crops (selenite and selenate) have over the concentration and speciation of Hg in the different parts of the plant (roots, shoots, grains). X-ray absorption spectroscopy (XAS) has been used as a direct speciation technique to get information about the chemical state and local coordination structure of Hg.

## **3.2 Experimental methods**

### **3.2.1 Cultivation under Hg pollution**

Common wheat (*Triticum aestivum* L. cv. Pinzon) plants were grown in hydroponic culture to have a precise control of nutrient availability. Seeds (purchased from Semillas Fito, Barcelona) were germinated in tap water damped filter paper for around 7 days. Afterwards, seedlings were transferred to 12 L opaque containers (6 plants per container). Half strength Hoagland nutrient solution buffered with MES (2-(N-morpholino) ethanesulfonic acid) to maintain a pH around 6.0 was used (details can be found in Table 3.1). Se and Hg treatments were applied as described in the Table 3.2. For our study, 0.5  $\mu\text{M}$  (0.1  $\mu\text{g/g}$ ) Hg was chosen which is well below the concentration limit imposed for agricultural soils by the current regulations, 1.5  $\mu\text{g/g}$  (Commission Regulation (EC) No 1881/2006,.; Council Directive 86/278/EEC of 12 June 1986.). However, in our hydroponic culture study, all the Hg was available for the plant whereas not all Hg in soils is

bioavailable for the plants. This is expected to be reflected in the results and it will be discussed later.

Table 3.1: Half strength Hoagland nutrient solution composition (Arnon and Hoagland, 1940)

<b>Chemical compound</b>	<b>Concentration</b>
Potassium nitrate, KNO <sub>3</sub>	3.0 mM
Calcium nitrate tetrahydrate, Ca(NO <sub>3</sub> ) <sub>2</sub> ·4H <sub>2</sub> O	2.0 mM
Monopotassium phosphate, KH <sub>2</sub> PO <sub>4</sub>	10.0 mM
Magnesium sulphate heptahydrate, MgSO <sub>4</sub> ·7H <sub>2</sub> O	0.5 mM
Boric acid, H <sub>3</sub> BO <sub>3</sub>	3.0 μM
Manganese(II) chloride, MnCl <sub>2</sub>	2.0 μM
Zinc sulphate hepta hydrate, ZnSO <sub>4</sub> ·7H <sub>2</sub> O	2.0 μM
Copper(II) sulphate pentahydrate, CuSO <sub>4</sub> ·5H <sub>2</sub> O	1.0 μM
Ammonium heptamolybdate tetrahydrate, (NH <sub>4</sub> ) <sub>6</sub> Mo <sub>7</sub> O <sub>24</sub> ·4H <sub>2</sub> O	0.1 μM
Ethylenediaminetetraacetic acid, Fe(Na)EDTA	60.0 μM
MES, 2-(N-morpholino)ethanesulfonic acid, C <sub>6</sub> H <sub>13</sub> NO <sub>4</sub> S (Buffer)	2.0 mM

A total Se concentration of 25 μM was chosen which is below the reported toxicity value threshold for wheat in hydroponic system (Guerrero et al., 2014; Li et al., 2008). The treatments and the nutrient solution were renewed weekly together until the plants reached senescence. The plants were grown in a controlled growth environment with relative humidity of ~70%, light intensity of 320 μE·m<sup>-2</sup>·s<sup>-1</sup> and different photoperiod based on the plant growth stage.

Matured wheat plants were harvested and divided into roots, shoots and grains. Samples were oven dried at 65 °C, ground into fine powder using an automatic agate mortar and pestle grinder, and stored in airtight tubes until further processing.

Table 3.2: Hg and Se treatments

<b>Treatment</b>	<b>Treatment description</b>
Control	No Hg and No Se
Hg	0.5 $\mu\text{M}$ of Hg (mercury(II) chloride, $\text{HgCl}_2$ )
Hg+Se <sup>4+</sup>	0.5 $\mu\text{M}$ of Hg + 25 $\mu\text{M}$ Se <sup>4+</sup> (sodium selenite, $\text{Na}_2\text{SeO}_3$ )
Hg+Se <sup>6+</sup>	0.5 $\mu\text{M}$ of Hg + 25 $\mu\text{M}$ Se <sup>6+</sup> (sodium selenate, $\text{Na}_2\text{SeO}_4$ )
Hg+Semix	0.5 $\mu\text{M}$ of Hg + 12.5 $\mu\text{M}$ Se <sup>4+</sup> + 12.5 $\mu\text{M}$ Se <sup>6+</sup>

### 3.2.2 Sample preparation and analysis

For shoots and grains, the Hg concentration was determined using a direct mercury analyzer, DMA-80 (Milestone) based on based on thermal decomposition, gold amalgamation, and atomic absorption spectroscopy (AAS). For the analysis, 2 mg of lyophilized powdered sample were used. The reported error bars correspond to the measurements' uncertainty.

On the other hand, since the Hg level in roots was too high to be measured by the direct mercury analyzer, the Hg concentration was calculated considering the integrated counts of the Hg  $L\alpha_1$  emission line (9988.8 eV) collected by the X-ray fluorescence detector during the XAS measurements. The XRF spectra collected at 12500 eV, far from the Hg  $L_3$  absorption edge, was used. The background counts were determined from the XRF spectra collected in the absence of Hg fluorescence (i.e. incident energy set at 12165 eV). For determining the Hg concentration from the Hg  $L\alpha_1$  XRF signal, the Zn  $K\alpha$  emission peak (8638.86 eV) was taken as reference and the appropriate calibration of the XRF signal was done taking into account the Zn concentration determined by ICP-MS (Table 3.3). In addition, the different fluorescence yield of Zn K and Hg  $L_3$  edges 0.481 and 0.333, respectively, was taken into consideration.

The uncertainty reported corresponds to the standard deviation of the averaged fluorescence counts of the independent channels of the fluorescence detector.

Table 3.3: Zinc concentration of samples (Analysed using ICP-OES (Perkin Elmer Nexton 350D))

Treatment	Concentration of Zn in $\mu\text{g/g}$ with standard deviation of measurement		
	Root	Shoot	Grain
Hg	307.2(15.3)	130.7(7.9)	189.1(8.6)
Hg+Se <sup>4+</sup>	92.6(5.3)	222.3(4.3)	118.4(0.8)
Hg+Se <sup>6+</sup>	141.1(14.2)	200.9(24.1)	136.4(1.3)
Hg+Semix	182.3(7.9)	220.9(10.2)	106.6(9.4)

Elemental concentration of Se was analyzed in different parts of the plants by ICP-MS. Samples were previously microwave digested (MARS5 digester) with nitric acid and hydrogen peroxide at 180 °C with a holding time of 10 minutes. The concentration was determined by external calibration of high purity Se standard along with the addition of internal standards (<sup>45</sup>Sc, <sup>69</sup>Ga, <sup>115</sup>In, <sup>89</sup>Y) for proper monitoring. The concentration of Se is displayed as mean $\pm$ SD (n=6) with significance between treatments (p<0.05).

XAS at the Hg L<sub>3</sub>-edge was measured at the BL22 CLÆSS beamline of the ALBA CELLS synchrotron, Spain (Simonelli et al., 2016). Powdered samples (~20 mg) were pressed into 5 mm pellets using a hydraulic press. The synchrotron radiation emitted by a wiggler source was monochromatized using a double crystal Si(311) monochromator. The rejection of higher harmonics was done by selecting the appropriate angles and coatings of the collimating and focusing mirrors. Conventional XAS measurements were performed in fluorescence mode at liquid nitrogen temperature using a multi-element silicon drift detector with Xspress3 electronics. High energy resolution Hg L<sub>3</sub>-edge XANES (HERFD) spectra were collected using the CLEAR spectrometer available at the beamline based on Johansson-like dynamical-bent diced-analyzer Si crystals for scanning-free energy dispersive acquisition. The Hg L $\alpha_1$  emission was collected using the Si(444) reflection of the analyzers working in back-scattering geometry. The energy resolution estimated from the FWHM of the quasi-elastic line was around 1.4 eV. The X-ray absorption

spectra were processed using Athena software of the Demeter package (Ravel and Newville, 2005) following standard procedures.

### 3.3 Results and discussion

#### 3.3.1 Concentration of element of interest

The Se concentration found in grains, 132-223  $\mu\text{g/g}$ , indicates that the Se-biofortification of the wheat grains was achieved (Subirana, 2018). The elemental concentration of Hg in the different parts of the plant is displayed in Figure 3.1. For shoots and grains the Hg concentration drops around two orders of magnitude respect from the amount of Hg found in roots.

Regarding roots, the higher concentration of Hg is found for Hg+Semix, 3080  $\mu\text{g/g DW}$ , whereas the other treatments had a slightly lower concentration. For grains, the highest Hg concentration is found for Hg+Se<sup>6+</sup>, and a significantly lower amount of at least a factor 2 was found for the treatments those including Se<sup>4+</sup>, i.e., Hg+Se<sup>4+</sup> and Hg+Semix treatments.

Table 3.4: Translocation factors of Hg along the plants

	<b>Hg</b>	<b>Hg+Se<sup>4+</sup></b>	<b>Hg+Se<sup>6+</sup></b>	<b>Hg+Semix</b>
Roots to shoots	0.0075 (+/- 0.0003)	0.0146 (+/- 0.0004)	0.0066 (+/- 0.0008)	0.0062 (+/- 0.0001)
Shoots to grains	0.58 (+/-0.02)	0.77 (+/-0.03)	2.46 (+/-0.10)	0.37 (+/-0.02)
Roots to grains	0.0043 (+/- 0.0003)	0.0113 (+/- 0.0004)	0.0162 (+/- 0.0008)	0.0023 (+/- 0.0001)

The Hg translocation factor based on concentration along the plants is reported in Table 3.4. It was calculated from the ratio of the Hg concentration obtained for different parts of the plants. The results show that Hg is highly accumulated in roots, and very little is translocated to shoots and grains. Plants treated with Hg+Se<sup>4+</sup> show higher translocation from roots to shoots (a factor 2 respect the other treatments) whereas plants grown with Hg+Se<sup>6+</sup> have higher translocation of Hg from shoots to grains (a factor 5 more than the other treatments). The translocation from

roots to grains for all the treatments is rather small. Interestingly it is minimized by the mixture of Se species in the feeding, Semix.

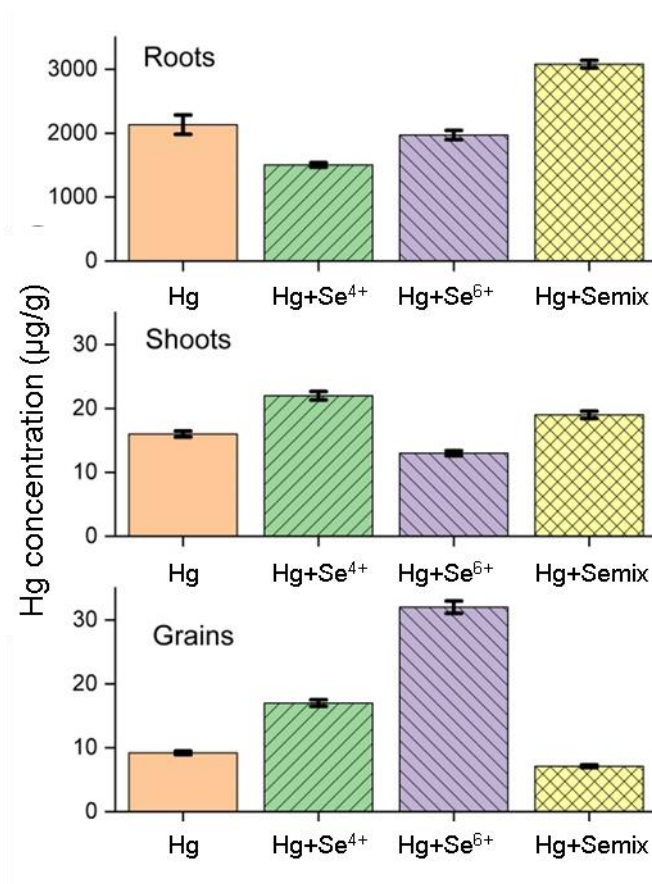


Figure 3.1: Concentration of Hg ( $\mu\text{g/g}$  DW) in different parts of the wheat plant grown under different Se bio-fortification and Hg exposure treatments. See text for details.

The high Hg uptake in roots can be ascribed to phytostabilization (complexation mechanisms related with root exudates) reducing Hg bioavailability (Chang et al., 2020; Dang et al., 2019; Tangahu et al., 2011). The Hg distribution found in our wheat plants resembles the trend reported in previous studies on Hg accumulation in Se-biofortified rice grains (Li et al., 2015). The increased Hg concentration in the shoots from roots, showing less accumulation in the grains for the Semix sample could indicate the role of different species of Hg in the plant life cycle (Fortmann L.C. et al., 1978; Siegel et al., 1974). However, this trend is opposite in case of selenate treatment, interesting considering that the uptake efficiency of selenate (Ellis and Salt, 2003) correlates with



Hg transformation. However, considering the shoots as an intermediate stage, the overall translocation from roots to grains for the individual Se species acts in similar way.

Moreover, Semix enhances the accumulation of Hg primarily in roots compared to the Se-biofortification by individual Se species,  $\text{Se}^{4+}$  or  $\text{Se}^{6+}$ , and the control treatment with only Hg. This suggests that the interaction of the different Se species with Hg is not simply additive, but that separated accumulative processes might be behind this enhanced Hg uptake. It is possible that the interaction of Hg with the mixture of the two Se species results in an enhanced transport through root cell transporters. Despite of the higher concentration found in roots for Hg+Semix, this treatment results in the lowest mercury accumulation in grains and thus the least harmful for animal or human consumption.

### 3.3.2 Hg speciation and component analysis along the plant

To get a better insight about the translocation of Hg species in wheat plants and the interaction between Hg and Se, Hg  $L_3$ -edge XAS measurements were performed to investigate the chemical state of Hg. Figure 3.2 shows the comparison of the Hg  $L_3$ -edge XAS spectra collected on roots, shoots and grains with the most representative Hg references for our study among all references measured: mercury selenide ( $\text{HgSe}$ ), methylmercury hydrochloride ( $\text{HgCH}_3\text{Cl}$ ) and mercury sulfide ( $\text{HgS}$ ). The spectra of roots, shoots and grains of wheat plants reveal spectral differences that can be ascribed to changes in the speciation depending on the Se-biofortification treatment used and the tissue studied. The spectral profile of each Hg species contained in the sample contributes additively to the total spectrum of the sample, hence, fingerprint comparison and linear combination fitting analysis using the reference spectra can allow the determination of the species present in the plant samples. The XANES spectra of the samples are shown in the Figure 3.2(a). The most characteristic spectral features in the references have been labelled from A to F. Regarding the Hg references,  $\text{HgCH}_3\text{Cl}$  shows enhanced spectral weight around A, B, and F at 12288.5, 12297.4 and 12330.7 eV;  $\text{HgSe}$  is characterized by features C and E at 12308.6 and 12324.4 eV, and  $\text{HgS}$  by D and slightly shifted from F at 12312.9 and 12332.5 eV.

The XANES spectra of grains samples have better defined the features A and B than the spectra of shoots and roots. This suggests that a larger amount of  $\text{HgCH}_3$  species are present in grains. Complementary information can be obtained from the extended X-ray absorption fine

structure (EXAFS) region, see Figure 3.2(b). EXAFS oscillations characteristic of the HgSe species are visible in the roots treated with  $\text{Se}^{4+}$  and Semix, while the spectra for Hg control and  $\text{Se}^{6+}$  suggest the presence of other species such as  $\text{HgCH}_3$  or  $\text{HgS}$ . In the case of shoots and grains, the EXAFS oscillations are similar irrespective of the Se treatment and confirm the presence of  $\text{HgCH}_3$  species. A complementary comparison of the spectra along the plants and respect to the different treatments is shown in Figure 3.3.

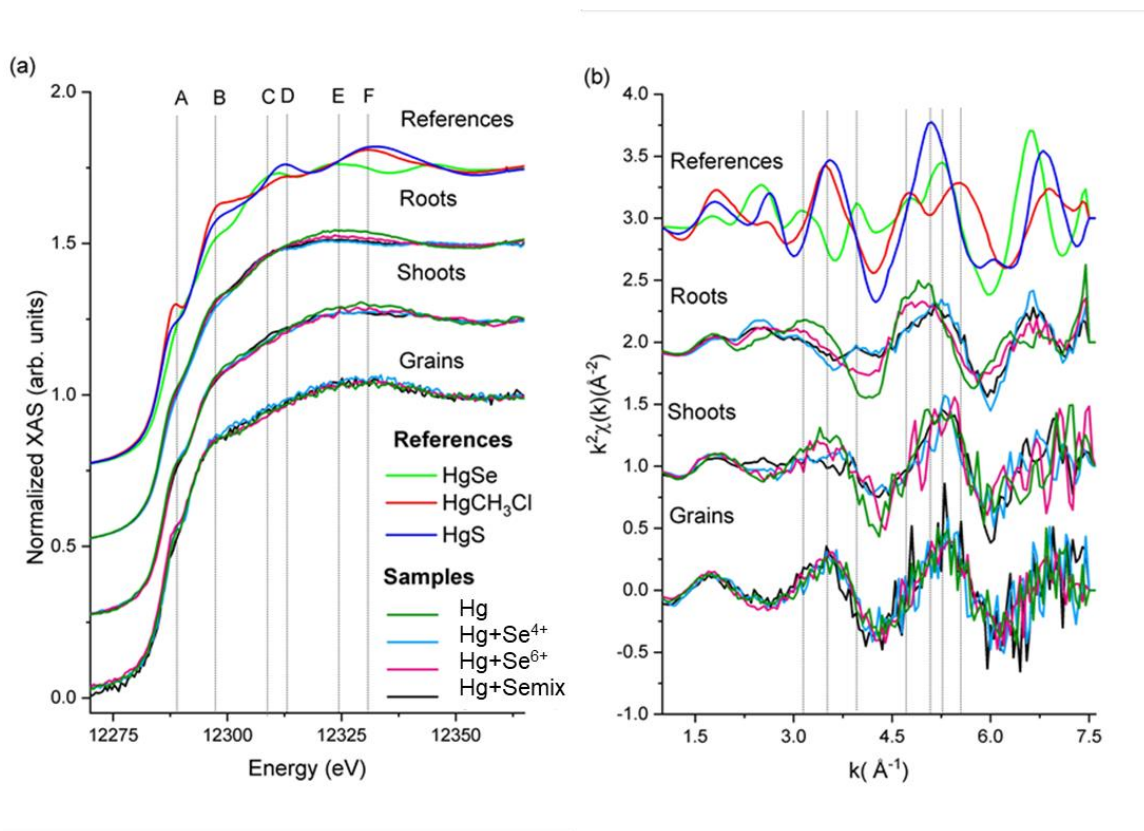


Figure 3.2: Hg L<sub>3</sub>-edge spectra XANES region (a), and k<sup>2</sup>-weighted EXAFS signal (b) acquired over different part of the plants grown with different Se and Hg treatments.

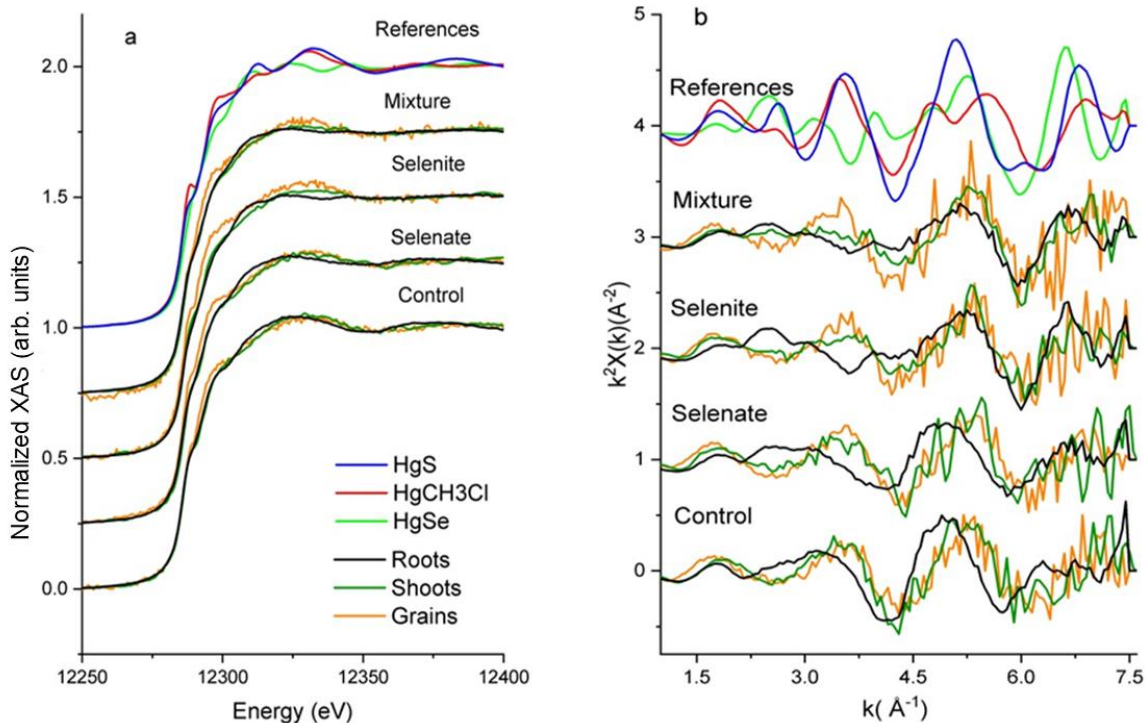


Figure 3.3: XANES (a) and EXAFS (b) comparison respect to different treatments at various parts of the plant.

In order to confirm the observations obtained from the fingerprint analysis, HERFD-XANES spectra were collected at the Hg  $L\alpha_1$  emission line ( $3d_{5/2}-2p_{3/2}$  transition) on roots samples and Hg references. This technique allows overcoming the intrinsically large core-hole lifetime broadening of the Hg( $2p_{3/2}$ ) level of the Hg  $L_3$ -edge (5.5 eV) (Krause, 1979) by monitoring the  $3d_{5/2}$  final state (2.28 eV) (Proux et al., 2017). The spectral enhancement achieved allows to clearly identifying the energy position of the shoulder features of HgS, HgCH<sub>3</sub>Cl and HgSe references. The comparison of the samples and references spectra suggests that the presence of HgS in roots might be negligible since the energy position of the pronounced shoulder at the rising absorption edge in the samples appears at higher energy, ~12288 eV, than feature A in HgS reference, ~12286 eV (Figure 3.4).

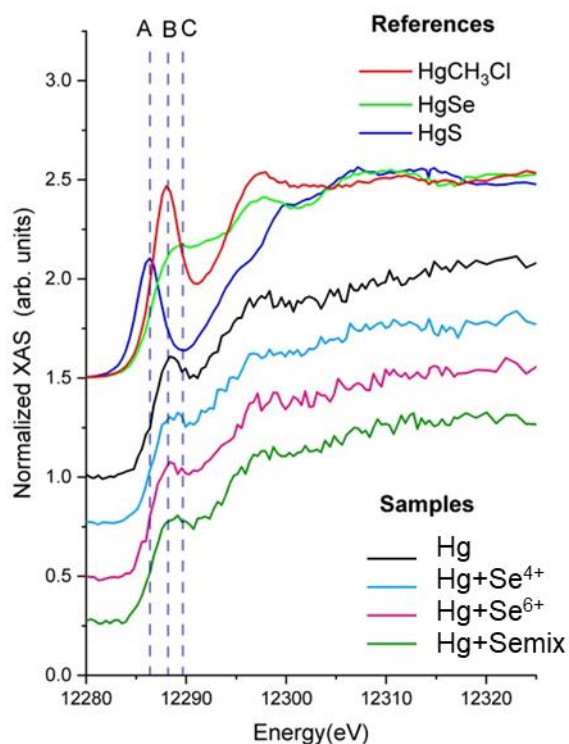


Figure 3.4: HERFD-XANES spectra collected at the Hg L<sub>3</sub>-edge in the root samples grown with different treatments.

In order to confirm the previous qualitative analysis and to better assess the ratio of Hg species present in roots, a linear combination fitting (LCF) analysis of the HERFD-XANES was done. The results for LCF analysis of HERFD-XANES are reported in Table 3.5 and it confirms that the main specie present in roots is HgSe, while HgS is probably not present.

Table 3.5: Results from the LCF analysis of HERFD-XANES measurements in roots.

<b>3</b>	<b>Hg+Se<sup>4+</sup></b>	<b>Hg+Se<sup>6+</sup></b>	<b>Hg+Semix</b>
<b>HgCH<sub>3</sub>Cl</b>	0.073	0.148	0.101
<b>HgSe</b>	0.886	0.795	0.840
<b><i>R-factor</i></b>	<i>0.010</i>	<i>0.012</i>	<i>0.012</i>

The LCF of the standard XANES was performed over all the samples considering the three Hg references (HgSe, HgS, and HgCH<sub>3</sub>Cl). The results systematically showed that, in agreement with the HERFD-XANES analysis and the observations reported above, the HgS contribution is absent or negligible in the full set of data. Hence, HgS reference was excluded in the final LCF analysis shown in Figure 3.5 and Table 3.6.

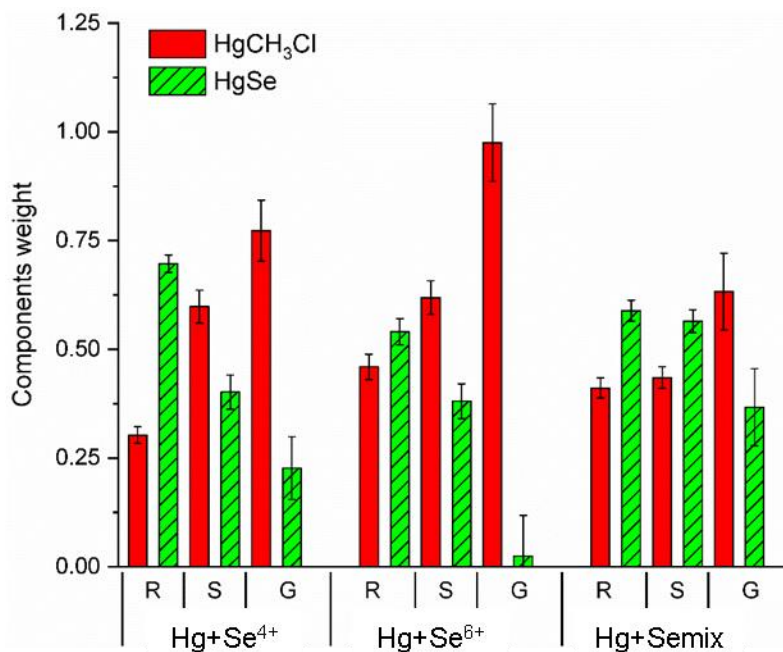


Figure 3.5: Results from the LCF analysis of the XANES spectra of different parts of the plants (R: roots, S: shoots, G: grain) under different treatments.

Table 3.6: Results from the LCF analysis of XANES region of the spectra. R, S and G stand for root, shoot and grain, respectively.

	<b>Hg+Se<sup>4+</sup></b>			<b>Hg+Se<sup>6+</sup></b>			<b>Hg+Semix</b>		
	<b>R</b>	<b>S</b>	<b>G</b>	<b>R</b>	<b>S</b>	<b>G</b>	<b>R</b>	<b>S</b>	<b>G</b>
<b>HgCH<sub>3</sub>Cl</b>	0.303	0.598	0.773	0.460	0.619	0.975	0.411	0.435	0.633
<b>HgSe</b>	0.697	0.402	0.227	0.540	0.381	0.025	0.589	0.565	0.367
<b><i>R-factor</i></b>	<i>0.001</i>	<i>0.002</i>	<i>0.006</i>	<i>0.001</i>	<i>0.002</i>	<i>0.010</i>	<i>0.001</i>	<i>0.001</i>	<i>0.008</i>

The LCF of the EXAFS signal is reported in Figure 3.6 and Table 3.7 confirms these trends as well.

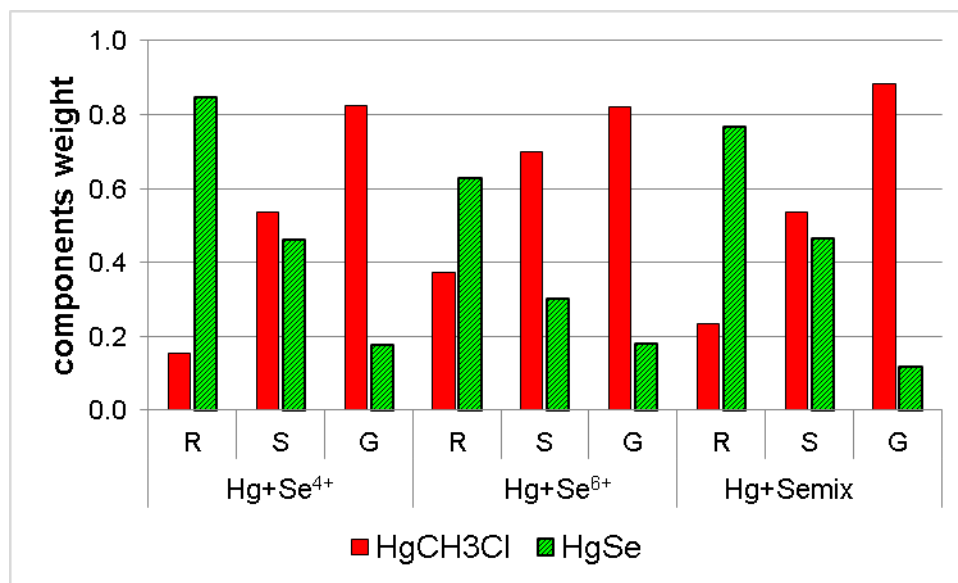


Figure 3. 6: Results from the LCF analysis of the EXAFS region of the spectra.

Table 3.7: Results from the LCF analysis of the EXAFS region of the spectra. R, S and G stand for root, shoot and grain, respectively.

	<b>Hg+Se<sup>4+</sup></b>			<b>Hg+Se<sup>6+</sup></b>			<b>Hg+Semix</b>		
	<b>R</b>	<b>S</b>	<b>G</b>	<b>R</b>	<b>S</b>	<b>G</b>	<b>R</b>	<b>S</b>	<b>G</b>
<b>HgCH<sub>3</sub>Cl</b>	0.152	0.538	0.823	0.371	0.698	0.819	0.233	0.535	0.884
<b>HgSe</b>	0.848	0.462	0.177	0.629	0.302	0.181	0.767	0.465	0.116
<b>R-factor</b>	0.090	0.403	0.574	0.528	0.668	0.349	0.118	0.350	0.509

These results should be taken as semi-quantitative since the chemical state of Hg in the plant will be slightly different to the one of the references selected. In fact, the complexation of Hg-Se in plants will not be as crystalline as the references used, and the methylmercury group in

plants will bound preferentially to thiol groups and amino acids instead to a chlorine atom as in the reference used (Wang et al., 2011, 2014). In addition, it is important to bear in mind that the set of Hg references chosen might be incomplete, i.e. there might be some Hg coordination environment in the plant that it is not represented by the Hg reference compounds chosen. For example, it is expected that the Hg control sample does not contain a significant amount of HgSe since no Se was included in the treatment. Instead, the control roots spectra are not fully represented by HgCH<sub>3</sub> alone, which looks to be anyway an important component from the analysis of EXAFS signals (Figure 3.3(b)). Thus, if we assume that, in agreement with the HERFD-XANES results, there is a small or negligible amount of HgS in the roots of the Hg-control sample, we can conclude that most likely we are missing a reference. Moreover, it has been reported that Hg L<sub>3</sub>-edge absorption spectrum of HgS and Hg-Cysteine, Hg-gluthaionine and Hg-phytochelatins are very similar and difficult to differentiate, (Li et al., 2015; Wang et al., 2012) making the speciation analysis very challenging in the present case.

Despite of the limitations of the LCF analysis to quantify the different species, the fitting results shown in Figure 3.5 and 3.6 highlight the presence of HgSe in the roots and its progressive reduction in shoots and grains. Complementarily, the highest concentration of HgCH<sub>3</sub> is found in grains whereas it is lower in shoots and roots. This methylated Hg looks to be present all along the plant irrespective of the addition of Se to the treatment. This concentration increase of the methylated groups from roots to grains which was characteristically observed during grain development stages is also expressed in other rice plant species (Dang et al., 2019; Li et al., 2019; Meng et al., 2011; Pickering et al., 1999; Wang et al., 2014).

Our study was conducted in hydroponic culture. Unlike soil, where the presence of different organisms helps in the conversion of Hg species to organic forms (Dang et al., 2019). In our case, it is reasonable to assume that the methylated Hg found in the wheat plant has been originated by the processes occurring within the plant itself.

Bioavailable Hg species, especially methylmercury, can be easily transported from shoots to grains, being the methylated Hg groups in soluble fraction mobile in the nutrient transport of the plants (Arif et al., 2016; Li et al., 2015; Meng et al., 2011). Hg+Se<sup>4+</sup> and Hg+Semix treatments have higher Hg translocation from roots to shoots with less bioavailable species in the system and lower translocation from shoots to grains. Also, the presence of heavier metal in the nutrient phloem pathway may affect the photosynthetic activity or accumulate in the cell vacuoles of shoots

which is typical to phytoaccumulation of heavy metal in plants (Álvarez-Fernández et al., 2014; Arif et al., 2016; Singh et al., 2016; Tangahu et al., 2011) leading to less accumulation. The differences between selenium treatments may arise from the interaction of the different species with the root exudates and complex formation assisting either in breakdown or accumulation of heavy metal species. Selenite is more water soluble than selenate, and selenite has the potential to form root complexes easier than selenate leading to better protective effects against Hg. Indeed, there is a noticeable decrease in both the treatments including selenite of the Hg accumulation in grains and its translocation percentage from roots to grains (0.0113 and 0.0023 for Hg+Se<sup>4+</sup> and Hg+Semix treatments, respectively). However, this supports the role of roots being a major inhibitor of heavy metal translocation (Chang et al., 2020; Dang et al., 2019; Q. Q. Huang et al., 2017; Li et al., 2015). Nevertheless, the mobility depends on the Hg species. Methylmercury is expected to have higher mobility compared with Hg-Se complexes in the plant system (Dang et al., 2019; Li et al., 2019; Zhou et al., 2015). The formation of a complex between Hg and Se would reduce the fast ligand exchange mechanism of the system due to their stronger bonding. In the same manner, the preference of Hg to form complexes with Se over thiol and sulfhydryl groups would reduce its bioavailability and mobility through the plant metabolism (Li et al., 2019).



### 3.4 Conclusions

In summary, our Hg speciation study along Se biofortified wheat plants grown hydroponically in Hg contaminated environment allows accessing the pathway and mechanism of accumulation of organic and inorganic Hg species. The results show that methylated species are formed both with and without Se-biofortification conditions and that they are accumulated in the grains. The formation of Hg-Se complexes, present in higher amount in the roots, is believed to reduce the translocation of Hg. The 1:1 mixture of  $\text{Se}^{4+}$  and  $\text{Se}^{6+}$  species in the feeding yields the lowest translocation factor of Hg to the grains. This Se-biofortification treatment inhibits the accumulation of methylmercury in grains offering protection against the Hg-induced plant toxicity to a certain extent. These findings can be applied to reduce the presence of Hg in wheat-based food.

**Soil culture**

**Chapter 4**

**Soils and Selenium**

## 4.1 Introduction

For horticulturist and farmers, soil is the fundamental foundation of plant life since it is an essential reservoir of nutrients and provide water supply to the plants. However, soil is not an essential element for plant growth, since, as it has been seen, plants can be grown as well hydroponically, by providing to the plants all the necessary nutrients directly in solution.

Soil can be broadly defined as a naturally occurring system mainly consisting of minerals (rocks and sediments), organic matter, water, and gases trapped in the pores (“Soils - Randall J. Schaetzl, Michael L. Thompson - Google Books,” n.d.). All these parameters make soil a complex system, fact to be considered when designing biofortification practices.

The different elements present in soils are categorized as major or trace elements depending if their concentration is above or below 100  $\mu\text{g/g}$ , respectively. There are around 17 major elements. Among them carbon (C), nitrogen (N), sulphur (S) and phosphorous (P) are major macronutrients, which helps in thriving lifecycle of the living organisms (“The Chemistry of Soils - Garrison Sposito - Google Books,” n.d.).

Se biofortification helps to incorporate Se in food crops in Se deficient regions. The different inorganic and organic Se species in their respective oxidation states (VI, IV, 0 and –II) interact differently with the soil depending on the soil organic matter content, solubility, and redox potential. These factors affect the overall availability of Se to the plants. For instance, Se(VI) and Se(IV) species are generally present in aerobic soils, due to the high presence of oxygen which contributes to the Se oxidation. Se(IV) presents the highest water solubility, but considering the high Se(IV) affinity for soil particles, like metal oxides and organic matter, it readily forms complexes reducing its mobility in soils. Instead, Se(VI) has higher mobility in soils than Se(IV) which helps in an easy plant uptake. Elemental Se, Se(0), is not soluble in water and it is poorly available. Hence, the reduction of Se(VI) and Se(IV) to Se(0) can reduce the mobility of Se in the food chain. The organic Se species (SeMet, SeMeCys, SeCyst, SeCys),  $\text{Se}^{-2}$  are naturally formed by biotic factors (organic matter, microorganisms) in soil and are available to the living organisms (Qin et al., 2017) .

Se in soil can be then divided into different subgroups based on the Se binding strength as water soluble Se, exchangeable Se, iron/manganese oxide bound Se, organic matter (OM) bound Se and residual Se. The different Se fractions in soil present variable mobility and bioavailability. Water soluble fraction is easily available for both plant uptake and soil microorganisms. The OM-bound fraction defines all Se species bound to organic matter, they are not readily available to plants however, they can slowly become available after the break down of the OM bonds through the soil stabilization process. Se Fe/Mn-bound fraction and residual elemental Se are strongly fixed by soil components and are poorly or not available (Z. Li et al., 2017). Generally, Se is strongly immobilized in acidic and reductive soils, leading to reduced species that are less mobile (Dinh et al., 2017; Z. Li et al., 2017). More in particular, the Se availability to plants has been found indirectly proportional to the soil organic acid content. Indeed, some studies propose that the organic matter improves the Se mobilization in the soil, having the ability to immobilize or release Se (binding to OM, kinetic rate of oxidation process, microbial reduction) (Z. Li et al., 2017). Also, the organo-mineral complexes and their adsorption behaviour towards Se plays a role in the Se mobility and availability (Tolu et al., 2014) .

In acidic soils, Se availability normally ranges from 19-53%, whereas in alkaline soils availability decrease from 5.9 to 40%. In acidic soils they decrease steadily compared to sudden drop in alkaline soils (Wang et al., 2017). In general Se of 5-100 g/ha in both species and all soil types were visualized as good fertilization conditions (Curtin et al., 2006; Lyons et al., 2003). Also, some reports conclude the higher the soluble fraction on the Se applied better the uptake irrespective of the total concentration applied.

Here we address the Se-biofortification process on wheat plants grown in soil. Even if only one soil example have been considered (gardening soil), the soil properties (with higher organic matter content (98%) at average pH 5.5) and interaction with the different Se species provided to the plants in the biofortification process have been analysed. The fortification process was carried out by direct soil application (SA) and as well by foliar application (FA) on wheat plants in soil culture. The results between their comparison, and further details of FA is given in section 5.2 (experimental design and methodology) and results respect to plants will be discussed in the next chapter (5).

## 4.2 Experimental methodology

### 4.2.1 Soil pre-culturing and initial analysis

Commercial gardening soil of universal substrate (Compo Sana) were used for the cultivation. 3L cylindrical pots (WT\*WB\*H: 16x12.5x22) were used for the study. The pots were filled leaving 5-8 cm from the top free of soil (soil capacity ca. 1.1 kg/pot).

Initial studies to determine the water retention capacity of the soil were carried out by placing the pots inside a controlled chamber with a photoperiod of 10h day and 14h night. The light intensity was kept the same as for the hydroponic experiments described in previous chapters,  $320 \mu\text{Em}^{-2}\text{s}^{-1}$ . Different volume of water (5, 10, 25, 50, 75, 100, 200 ml) and time intervals (1, 3 and 7 days) were tested. The results of this preliminary study indicated that a volume of 50 ml of water per pot every week was the best amount to preserve the required humidity in the soil. This irrigation volume was used in the whole cultivation study using soil pots.

The pH of the soil was measured as follow: a 1:1 (w/w) soil to water suspension was prepared and stirred for 1h for the pH to stabilize, afterwards the pH was measured in the supernatant using a pH meter. The average pH found was  $5.2 \pm 1.5$ . Alternatively, the soil pH was also determined by direct soil measurements using a soil pH meter (Groline, Hanna instruments) obtaining pH  $5.5 \pm 3$ .

The stabilization of Se species in preconditioned soils was studied by performing solid-phase extraction experiments with columns filled with soil. Glass columns were filled with 120 g of soils up to 2/3 of its height (45 cm) and divided into four groups (Control, Selenite, Selenate and Mixture). The withholding water capacity of the soils in the columns was 100 ml. The concentration of Se used for this experiment was set to 50  $\mu\text{M}$ . This is 5 times higher than the concentration that will be used for the soil experiments in the soil application methodology, 10  $\mu\text{M}$ , but it was designed like this to have a concentration similar to the one that will be reached in the soil after the wheat cultivation experiment. Soil from the first day and after a week was collected for speciation studies to study the evolution. To perform the solid-phase extraction, different fractions were collected, first water was used to remove the soluble and available Se fraction, and afterwards hydrochloric acid, (HCl) was used to remove the rest of the species.

## 4.2.2 Soil sample preparation and characterization

Soils from soil and foliar application (as described in section 5.2. experimental methodology) at the time of harvest were collected from middle of the pot height and stored at  $-80^{\circ}\text{C}$  for further characterization. Elemental analysis was carried out to measure the total Se and other nutrients in soil from microwave digested samples. From the total 9 pots, average of two pots with replicates were analysed, the error bar reported was the standard deviation between two pools of pots from same group. XAS measurements were carried out at liquid nitrogen temperature in lyophilized and homogenised soil samples collected from three pots per group. The soil was powdered and made into 5 mm pellets. The results are discussed in the next section.

## 4.3 Results and discussion

### 4.3.1 Soil elemental concentration

The concentration of Se in soils obtained by ICP-MS is reported in Figure 4.1. Besides the SA and FA groups mentioned above in the Introduction, an additional set of pots was considered as control for the soil application (CSA). This consists on pots filled with soil in which the treatments were applied as for SA but no wheat was grown. Generally, SA has lower concentration of Se than CSA. This difference can be attributed to the plants' uptake in the case of SA. Moreover, the Se concentration in CSA reduces progressively from  $0.9\pm 0.02\ \mu\text{g/g}$  for  $\text{Se}^{4+}$  to  $0.4\pm 0.07\ \mu\text{g/g}$  for  $\text{Se}^{6+}$  case when increasing the  $\text{Se}^{6+}$  fraction. This might be probably due to the volatility of Se intermediate species generated when  $\text{Se}^{6+}$  reduces to  $\text{Se}^{4+}$  (Ellis and Salt, 2003; Sors et al., 2005; Tolu et al., 2014). As expected, the Se concentration found for FA was very small,  $0.01\pm 0.003\ \mu\text{g/g}$ , which results negligible in comparison with the CSA sample, therefore, we can neglect any biofortification influence of the Se reaching the soil in the case of FA. It is worth mentioning that the control soils (no Se was applied) of the three different application methodologies (CSA, SA, FA) showed that the soil used for the experiments have a Se level below  $0.005\pm 0.002\ \mu\text{g/g}$  (detection limit) and can be consider completely negligible. Also, the detection limit is given based on the calibration range (0 -100  $\mu\text{g/g}$ ).

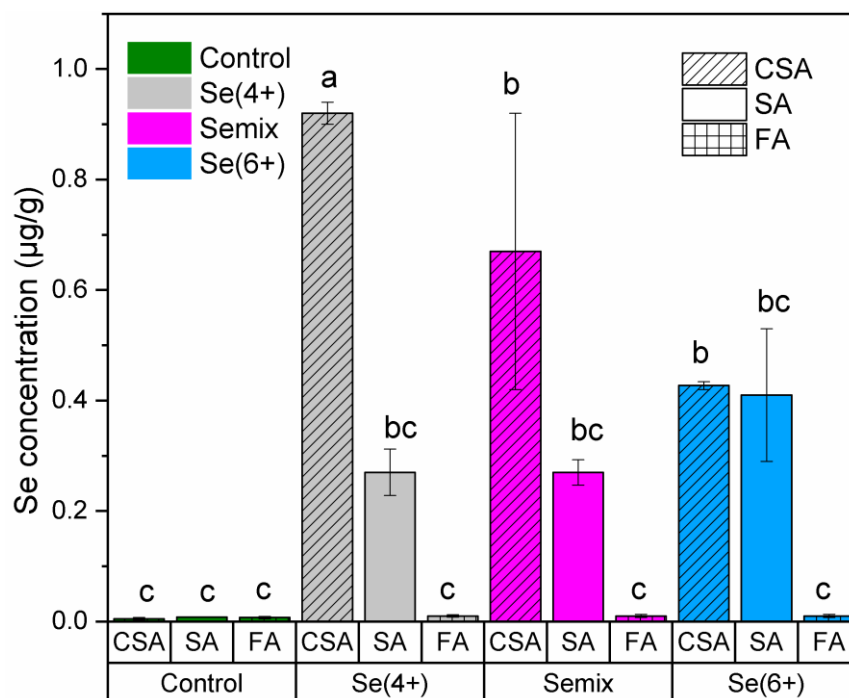


Figure 4.1: Selenium concentration in soils ( $\mu\text{g/g DW}$ ) as a function of the Se treatment provided. The treatments groups are represented as Control (dark green),  $\text{Se}^{4+}$  (grey), Semix 1:1 (pink), and  $\text{Se}^{6+}$  (blue) and application methods CSA—diagonal pattern (control group no plants), SA- no pattern (soil application) and FA- squared pattern (foliar application). The error bar shows the standard deviation of measurements from two set ( $n=3$ ). The statistical significance between different treatments based on means comparison of technical replicates was shown by student t-test with significance  $\alpha=0.05$ . Different letters define the level of significance.

Figure 4.2 reports the concentration of different micro (B, Fe, Zn, Cu, Mn) and macro (Mg, P, K,) nutrients present in the soils, with the objective of comparing the Se biofortification with the elemental uptake.

Except for the Mn concentration, CSA group has slightly lower concentrations of the investigated elements compared to SA and FA. These can be due to the water retention capacity of the roots and their interaction with the soil. The ability of the soil to retain the applied solution without leaching away and how the elements present affected the diffusion or competition in

uptake between plant and soil. For the rest, the average values are comparable in between treatments. Despite the error bar, it can be seen higher amounts of micronutrients in the soils by increasing  $\text{Se}^{4+}$  fraction in the FA treatment. FA may affect the plant metabolism respect to the Se species applied. FA can stimulate transpiration in plant leaves and increase the photosynthetic activity leading to more exchange of elements in plants and soil. Moreover, the concentration of nutrients found in the soil for SA are overall slightly lower than respect to FA.

Figure 4.3 shows the Se K-edge absorption spectra measured on soil samples obtained by different Se application methods and Se treatments. The Se K-edge reference spectra of the inorganic ( $\text{Se(IV)}$ ,  $\text{Se(VI)}$ ) and organic ( $\text{SeMet}$ ,  $\text{SeCyst}$  and  $\text{MeSecys}$ ) Se species are displayed on the top of the figure. CSA and SA groups show a similar spectral profile for the same Se treatment applied. In both cases the  $\text{Se}^{4+}$  feeding is mainly transformed to organic species, while the  $\text{Se}^{6+}$  feeding remains in its original form. In the case of FA, the low concentration Se found in the soil seems to be in organic form, independently of the Se treatment applied. The level of Se in the control sample (no Se applied) was below the detection limit and therefore the native species of Se in the soil could not be determined.



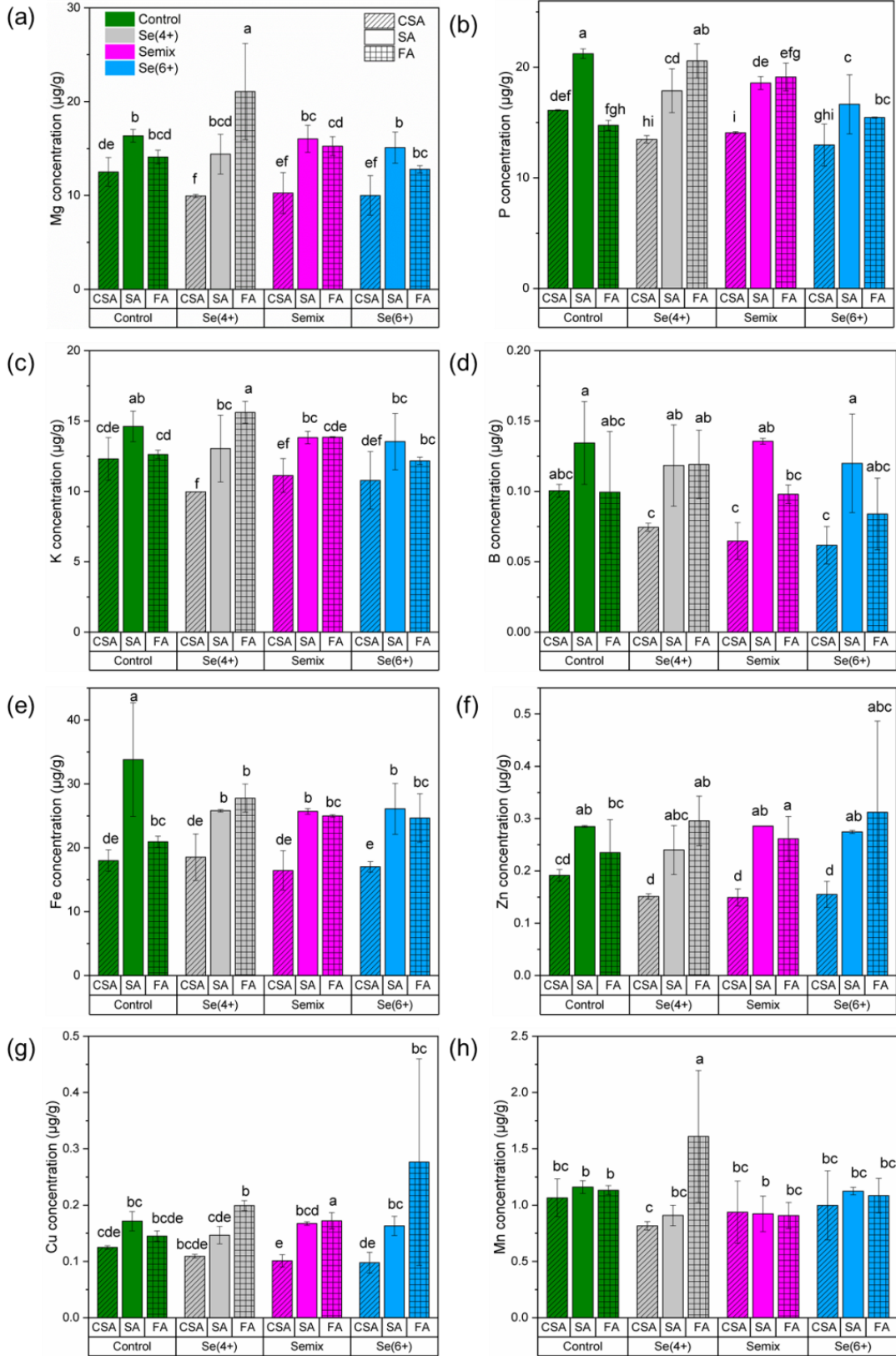


Figure 4.2: Concentration of macro (Mg, P, K) and micro (B, Fe, Zn, Cu, Mn) nutrients, in soils as a function of the Se treatment provided. The treatments groups are represented as Control (dark green),  $\text{Se}^{4+}$  (grey), Semix 1:1 (pink), and  $\text{Se}^{6+}$  (blue) and application methods CSA—diagonal pattern (control group no plants), SA- no pattern (soil application) and FA- squared pattern (foliar application). The error bar shows the standard deviation of measurements from two set (n=3). The statistical significance between different treatments based on means comparison of technical replicates was shown by student t-test with significance  $\alpha=0.05$ . Different letters define the level of significance.

### 4.3.2 Speciation in soils

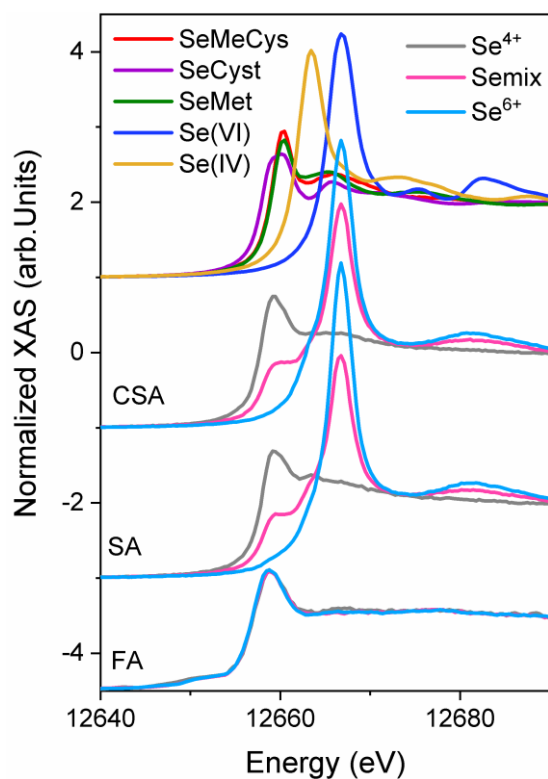


Figure 4.3: Se K-edge XANES spectra collected on soils treated with different Se applications. From top to bottom, the spectra of selected references, CSA (control no plants), SA (soil application) and FA (foliar application) is shown.

To have a better understanding of the evolution of the different Se species in the soil, a experiment was performed in glass columns in which the Se speciation in soils was monitored as a function of time from application and the Se treatment selected. The corresponding XAS results are reported in Figure 4.4.

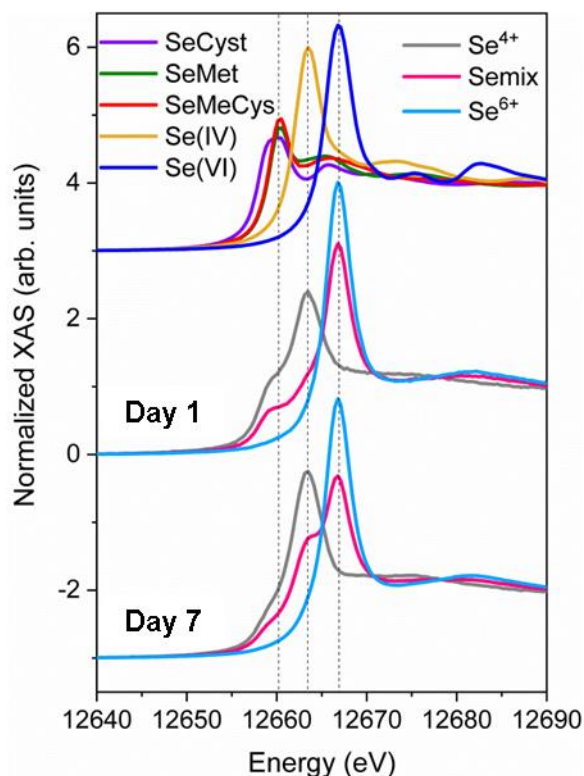


Figure 4.4: Se K-edge spectra collect over CSA, i.e. from columns respect to time of collection and treatment. Spectra represented from top to bottom indicate, references, samples from day1 followed by day 7.

The samples collected after 1<sup>st</sup> and 7<sup>th</sup> day from application show similar spectral profile in the case of Se<sup>6+</sup> treatment which corresponds to Se(VI) inorganic compound. Regarding Se<sup>4+</sup>, the first day samples show a Se(IV) contribution and a small organic contribution and this organic contribution gets reduced in 7<sup>th</sup> day where the Se(IV) increases. Semix spectra lie in between Se<sup>6+</sup> and Se<sup>4+</sup> treatments.

## 4.4 Conclusions

The characterization of the soils corresponding to the Se bio-fortification process investigated was reported.  $\text{Se}^{4+}$  species in the soil are progressively transformed into organic species which are less available for the plant uptake. Instead,  $\text{Se}^{6+}$  is more slowly transformed to  $\text{Se}^{4+}$ , forming intermediate Se species, thus it is more immediately available for the plant uptake.

The Se amount provided to soils is reduced by the wheat plant uptake, in higher extent for the  $\text{Se}^{4+}$  feeding, because of the volatility of the Se intermediate phases. Similarly, the strong decrease of the Se concentration by increasing the  $\text{Se}^{6+}$  fraction in the control soil suggests a possible partial loss of Se through volatile species.

Regarding the foliar application, a negligible amount of Se is detected in the soil and only in organic forms. FA seems to affect the plant metabolism respect to the Se species applied.

## **Chapter 5**

### **Se biofortification by soil and foliar application**

## 5.1 Introduction

For practical applications of the Se biofortification processes many parameters should be considered. First of all, Se inorganic species have better solubility and are more bioavailable for the plant's uptake (Dinh et al., 2017; Lara et al., 2019; Qin et al., 2017; Ros et al., 2016). Moreover, they are more cost-effective and hence can be effectively used for large scale agronomic practices. Taking into consideration that the uptake capacity of plants in soils can be less than 5% from the total Se applied, hence, it is crucial to optimize the Se biofortification process considering all the parameters that may affect it. This includes, the Se species provided to the plants and the application method, time, frequency and concentration of the applications, and the intrinsic soil properties (e.g. organic matter content, minerals and pH). These parameters can strongly influence the outcome from the biofortification process since the plant uptake efficiency can vary from 1 to 50% (Ros et al., 2016).

Among different application methods, soil application (hereafter denoted as SA), in which Se fertilization is applied directly in the soils, and foliar application (hereafter denoted as FA), in which Se is sprayed over the surface of the leaves in the cultivation area, are widely practiced. In terms of species,  $\text{Se}^{6+}$  has high bioavailability in soils as it is more mobile and available for plant uptake. Comparatively,  $\text{Se}^{4+}$  is less available for plants as it bounds to clay components and organic matter present in the soils, which decrease its mobility. On the other hand, studies on rice (Lidon et al., 2019) and carrot (de Oliveira et al., 2018) showed better Se uptake when  $\text{Se}^{4+}$  is applied by FA, as this species can be easily accumulated on the leaf surface and taken up by the vacuolar cells of the aerial parts of the plants (Ros et al., 2016). It was reported that  $\text{Se}^{4+}$  applied by foliar increases the Se concentration in rice grains 10 times fold compared to  $\text{Se}^{6+}$  application (Lidon et al., 2019). In terms of quantity, the FA of 10 g  $\text{Se}^{4+}$ /ha in rice corresponded to an increase of Se concentration in the grain 1.54  $\mu\text{g/g}$  (Lidon et al., 2019). In case of wheat, the SA of  $\text{Se}^{6+}$  at 10 g/ha is equivalent to the FA of  $\text{Se}^{6+}$  at 50 g/ha to obtain the equivalent Se grain concentration or similar fortification benefits (Curtin et al., 2006; Lyons et al., 2003). Generally, FA, are always carried out with the help of adjuvants, which acts as a surfactant, helping the absorption of the applied droplets by reducing their surface tension. Studies also reported that the use of adjuvants increased the Se uptake two folds in wheat plants (Lyons et al., 2003).

The time of application respect to the growth stage of the plant is also an important factor influencing the Se uptake (Boldrin et al., 2016; Lara et al., 2019; Lidon et al., 2019; Ros et al., 2016). Overall, both SA and FA during the heading stage and grain filling improves the yield and Se concentration in crops (Ros et al., 2016). On the other hand, FA at vegetative stage results to accumulate Se less than 30% due to the reduced dimensions of the leaves., (Ros et al., 2016).

The amount of Se needed for biofortification differs based on species and application method. Depending upon soil properties, SA of at least 10 g/ha in the form of  $\text{Se}^{6+}$  is needed to obtain up to a maximum of 0.5  $\mu\text{g/g}$  of Se in grains (Curtin et al., 2006; Lyons et al., 2003). It has been reported that for an application of 20 g/ha  $\text{Se}^{6+}$  in soils there is an increase in grain yield (Lara et al., 2019). In general, for SA 5-30g/ha of  $\text{Se}^{6+}$  applied in the fluorescence stage is effective for fortification process (Curtin et al., 2008, 2006; Lara et al., 2019; Lyons et al., 2003).

The soil properties like pH and type (clay or more OM based) changes the Se accumulation pattern (Lyons et al., 2003). However, irrespective of species and application conditions, Se biofortification of 5-100 g/ha is considered good for fortification purposes (Dinh et al., 2017; Lyons et al., 2003).

Several studies have reported how wheat Se enrichment can affect the plant metabolism and the final wheat production, however, a systematic study on the effect of different application methods and of the effect induced by different Se species treatments is missing.

Here we study the effects of the Se biofortification process on wheat plants, where different Se species ( $\text{Se}^{4+}$ ,  $\text{Se}^{6+}$ ) are provided both by SA and FA methods. Following the results obtained by hydroponic culture as reported in the previous chapters and previous works (Subirana, 2018; Xiao et al., 2021, 2020), here it is included the treatment with the mixture of both Se species in a 1:1 ratio, which, to our knowledge, has not been addressed at all in the literature. The Se concentration for the study was defined from the literature 21 g/ha of Se for SA (Curtin et al., 2006; Lyons et al., 2003) and five times the concentration in case of FA to achieve the desired results (Lyons et al., 2003). The idea is to exploit the different Se species uptake characteristics to optimize the Se biofortification process for applications, with a particular focusing on the Se species finally present in the wheat grains.

## 5.2 Experiments and methodology

### 5.2.1 Cultivation of plants in soils by different Se application methods

The soil used and its initial characterization is described in 4.2. The pots were filled with the same weight of soil (1.1 kg) and compacted to remove air pockets. The germinated wheat seedlings (method as described in 1.2.1 section) were placed in the soils of about 3 cm in depth with one plant per pot to better control the treatment and growth. The plants were grown in similar conditions as hydroponics culture, with the same photoperiod. 50 ml of water were added every 7 days. In the cultivation, 18 plants per treatment group which are sub-divided into two application method (soil application-SA and foliar application -FA), in total 72 plants were grown. Along with these pots with plants, control group of soil only pots (CSA) without plants was included in the study. The Se treatment was applied only after the plants reached the flag leaf stage accordingly to the previous studies, i.e. to optimize the Se biofortification by reducing the toxicity effects.  $\text{Se}^{4+}$ ,  $\text{Se}^{6+}$  and their mixture in the 1:1 ratio was applied to the plants, as listed on table 5.1.

Table 5.1: treatment groups under SA and FA

Control
Selenite ( $\text{Se}^{4+}$ )
Mixture 1:1 ratio ( $\text{Se}^{4+}$ : $\text{Se}^{6+}$ )
Selenate ( $\text{Se}^{6+}$ )

In SA, Se 10  $\mu\text{M}$  in 50ml (were added to every pot. The CSA group were treated in the same way as SA group.

In case of FA, the plants were grouped together in an area of 0.18  $\text{m}^2$  to optimize the application, i.e. to minimize the fraction of Se biofortified solution following to the soil. The Se concentration was increased to account the less Se availability to plants. Se 50  $\mu\text{M}$  (7 g/ha of Se) in approximately 40 ml from the stock solution along with adjuvant (Tween 20-surfactant) were



sprayed on the leaves surface. In FA control group only, water with adjuvant was added. Moreover, the soil was irrigated with 50ml of water to keep the correct plant feeding.

In both SA and FA, the soil pH was checked at regular intervals. It has been found around pH 5-6 for all treatments. The plants of all the groups were harvested together after they have completely matured. The soils from the pots were collected for further characterization as discussed in section 4.2. The plants were divided into roots, stems, leaves and spikes. The roots, stems and leaves were lyophilized and stored for further studies as described in section 1.2.1. The grains were stored after collecting from the spikes.

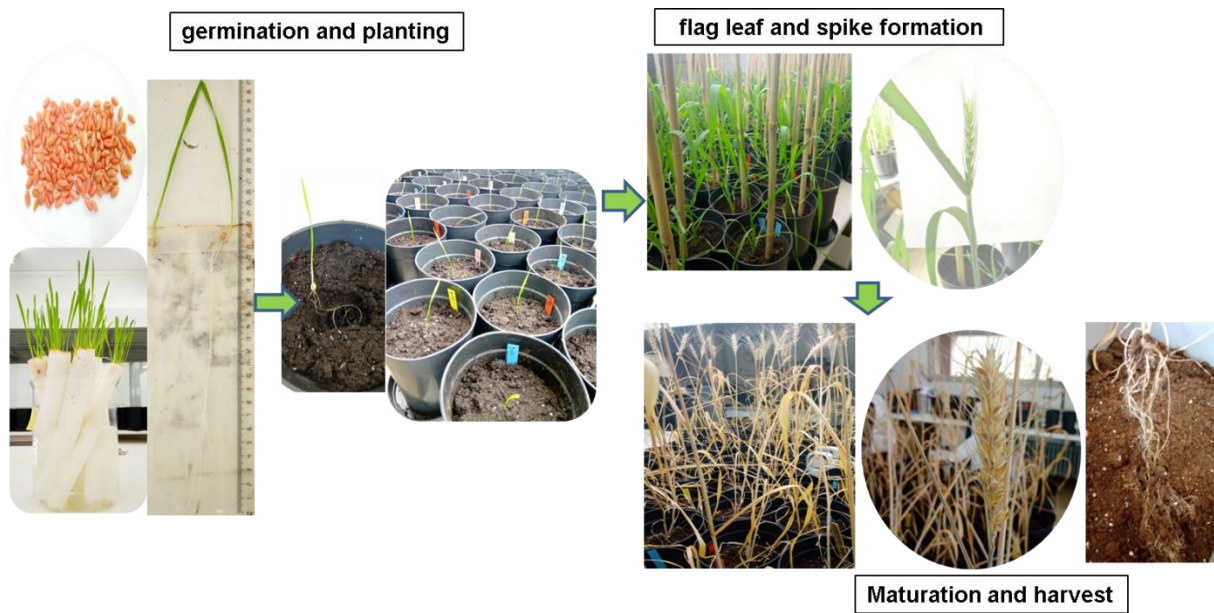


Figure 5.1: wheat plant cultivation in soils from germination to harvest

## **5.3 Results and discussion**

### **5.3.1 Plant growth parameters**

Similar to the previous chapters, the biomass of the plants, represented as the average dry weight (DW) of their different parts, has been investigated and it is reported for both SA and FA methods in Figure 5.2.

The biomass of roots and leaves are not significantly affected by the different Se treatments, neither by the application method. Instead, while the stems and grains DW looks not significantly affected by the different Se treatments, they are slightly reduced by FA respect SA method, including the FA control sample. This can be ascribed to the adjuvant application, wich seems to reduce both the stems and grains development.

Interestingly, the FA control produced an enhanced amount of grains, respect the control and all the SA and FA Se treated plants, whit the FA showing a slightly smaller grain production.

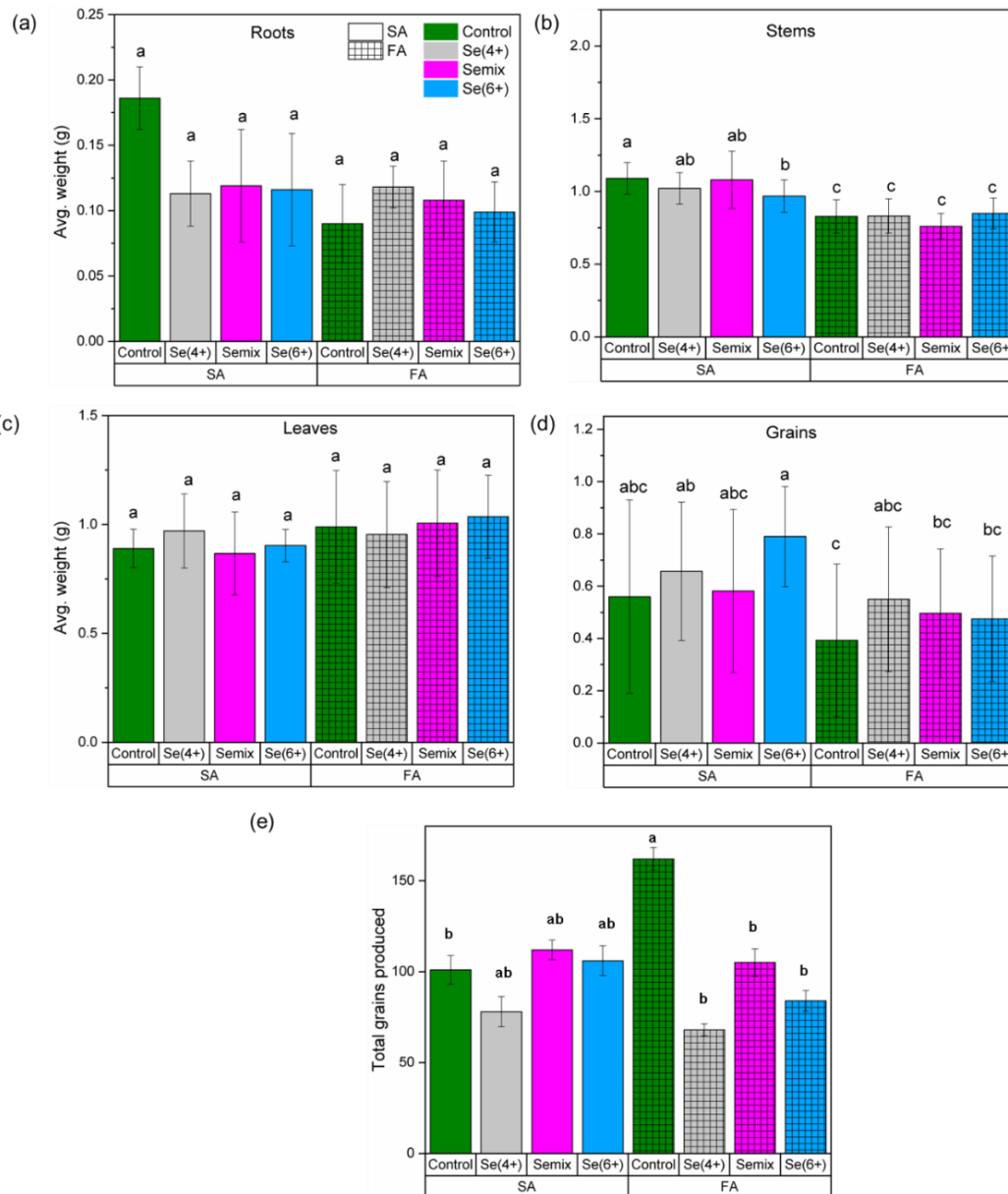


Figure 5.2: Average dry weight of different parts of the plants roots (a), stems (b), leaves (c) and grains (d) and total grains produced (e). The different treatments are represented as Control (dark green), Se<sup>4+</sup> (grey), Semix (pink), Se<sup>6+</sup> (blue) and application methods SA (no pattern) and FA (squared pattern). The statistical significance between different treatments based on means comparison of technical replicates was shown by student t-test with significance  $\alpha=0.05$ . Different letters define the level of significance.

### 5.3.2 Concentration of elements in the plants

The Se concentration at different parts of the plants is reported in Fig 5.3. It is helpful to address the influence of the treatment and application method applied on the Se uptake and transfer along the plant tissues.

The Se concentration along the plants is of an order of magnitude higher in SA respect FA method, and it is higher at the application place. In SA roots, stems, leaves, and grains the Se concentration has been found around or below 150, 60, 50, 75  $\mu\text{g/g}$ , respectively. Instead, in FA roots, stems, leaves, and grains the Se concentration has been found around 2, 3, 10, 3  $\mu\text{g/g}$ , respectively. While in SA the Se concentration in the different plant parts decreases by increasing  $\text{Se}^{4+}$  in the treatment, in FA it is not showing a Se treatment dependence.

The reduced Se concentration in SA roots with  $\text{Se}^{4+}$  treatment is in agreement with the expected Se(IV) immobilization in the soil and the Se(VI) high mobility in xylem transport (Cubadda et al., 2010; Curtin et al., 2006, Xiao et al 2021).

Instead, in FA samples, the increased Se concentration in leaves most likely corresponds to the leaves ability of accumulating metals as a defence mechanism, i.e. to reduce the plant stress and undesired metal translocation (Angulo-Bejarano et al., 2021).

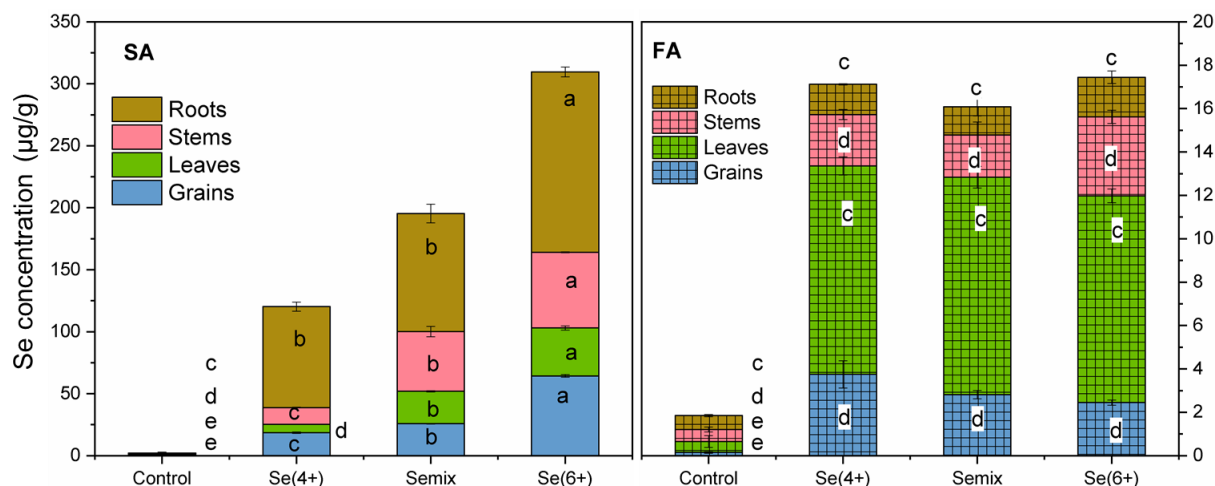


Figure 5.3: Se concentration along the different parts of the plant (grains, leaves, roots and stems). The error bar is given by SD between different measurements (n=3). The different parts of the plant are represented as roots (brown), stems (pink), leaves (green) and grains (blue). and based on applications SA-no pattern and FA-squared pattern. The statistical significance between different treatments based on means comparison of technical replicates was shown by student t-test with significance  $\alpha$ -0.05. Different letters define the level of significance.

In general, the Se applied is expected to be translocated and transformed along the different parts of the plants, affecting the Se mobility and accumulation. The translocation factor (TF), as defined in the previous chapter 1.3, identifies how much an element is transported along the plant. TF of Se from different parts of the plant to grains is reported in Figure 5.4. Being in SA and FA the Se uptaken by the roots and diffused by the leaf epidermis cell vacuoles, respectively, it is of particular interest the roots-to-grains (R to G) and leaf-to-grains (L to G) TF in SA and FA, respectively. It is worth to recall that the TF should be higher than one to denote metal translocation along two different parts of the plant (Usman et al., 2019). Nevertheless, the high TF from R to G in FA depends only by the very small Se amount in roots, because of the application method. The R to G Se translocation in SA increases with the  $\text{Se}^{6+}$  treatment, probably because of the high  $\text{Se(VI)}$  mobility in the xylem transport (Cubadda et al., 2010; Curtin et al., 2006, Xiao et al 2021), while this trend is opposite in FA for the L to G TF. In both cases the TF is below 1, characterizing a relatively poor Se translocation from the application site to grains. The stems to grains TF is

instead close or above 1 for both treatments, with a minimum for Semix and  $\text{Se}^{6+}$  for SA and FA, respectively.

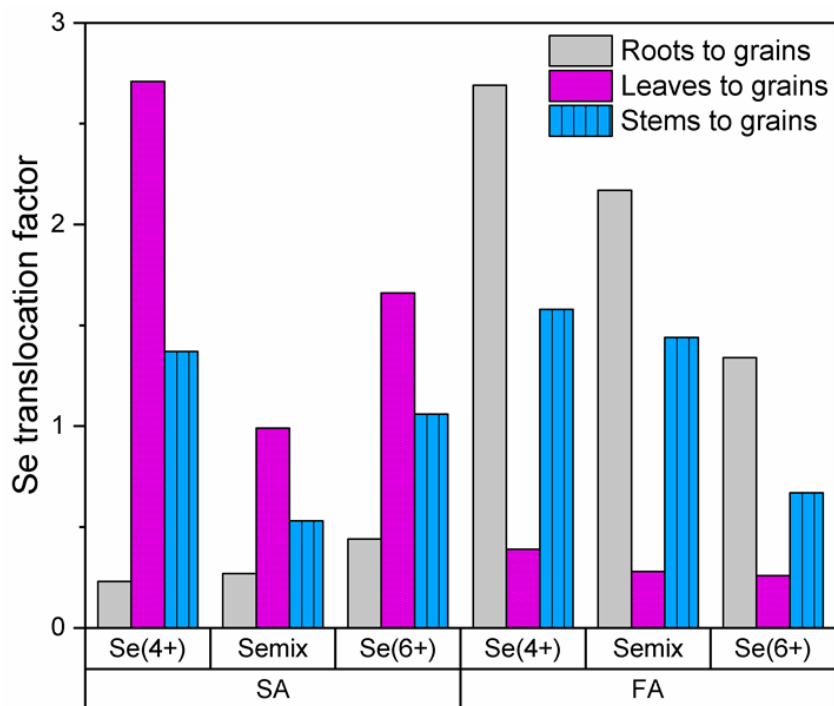


Figure 5.4: Translocation of Se from different parts of the plant to grains. The treatment groups are given by  $\text{Se}^{4+}$  (grey), Semix (pink) and  $\text{Se}^{6+}$  (blue) representing roots-to-grains (dashes) leaves-to-grains (no pattern) and stems-to-grains (lines).

The concentration of other important micronutrients like Cu, Mn, Fe and Zn along the different parts of the plants is shown in the Figure 5.5. Panel (a) focus on the Cu distribution.

Roots have higher concentration of Cu, followed by grains compared to the aerial parts. The Cu concentration in roots and stems are not significantly different among treatments. The level of Cu in leaves control group is significantly lower than in all the Se treated plants. In the case of SA grains,  $\text{Se}^{4+}$  and Semix slightly decrease the Cu level, while Se treatments slightly decrease the Cu content respect to control. Under FA,  $\text{Se}^{4+}$  increases significantly the amount of Cu in the grains.

Mn concentration is seen in Figure. 5.5(b). The leaves sample of the control plant was lost during the elemental analysis. The accumulation of Mn is the highest in leaves, where it does not show clear trends as a function of the Se treatment or application method. Mn level in roots are not different, while in stems is lower in SA with respect to FA. In FA stems lower Mn level is seen for  $\text{Se}^{4+}$  treatment. In grains, FA causes higher Mn accumulation than SA. Grains treated under SA, show a significant reduction of the Mn level in  $\text{Se}^{4+}$  and Semix.

Fe accumulation is shown in Fig 5.5(c). In the case of the leaves sample of the control plant have less Fe content compared to other treatments. In stems, Fe is found in higher amount in FA, while in grains for SA.

Zn concentration is reported in Fig 5.5(d). In the stems and leaves Zn accumulates more for FA than SA. Zn accumulation in grains is significantly reduced independently of the application in Semix treatment and enhanced in  $\text{Se}^{4+}$  for FA method.

Mn, Zn and Cu participate in major enzymatic activities. Differently from the here reported results, in the work by Xiao et al. (2020) the Zn and Cu accumulations in wheat roots grown hydroponically under a bio-stimulant and  $\text{Se}^{4+}$  application were significantly increased respect to the control. This suggests that bigger data sets are necessary to address statistically the effect of the Se treatments on the other micronutrients accumulation and their eventual correlations.

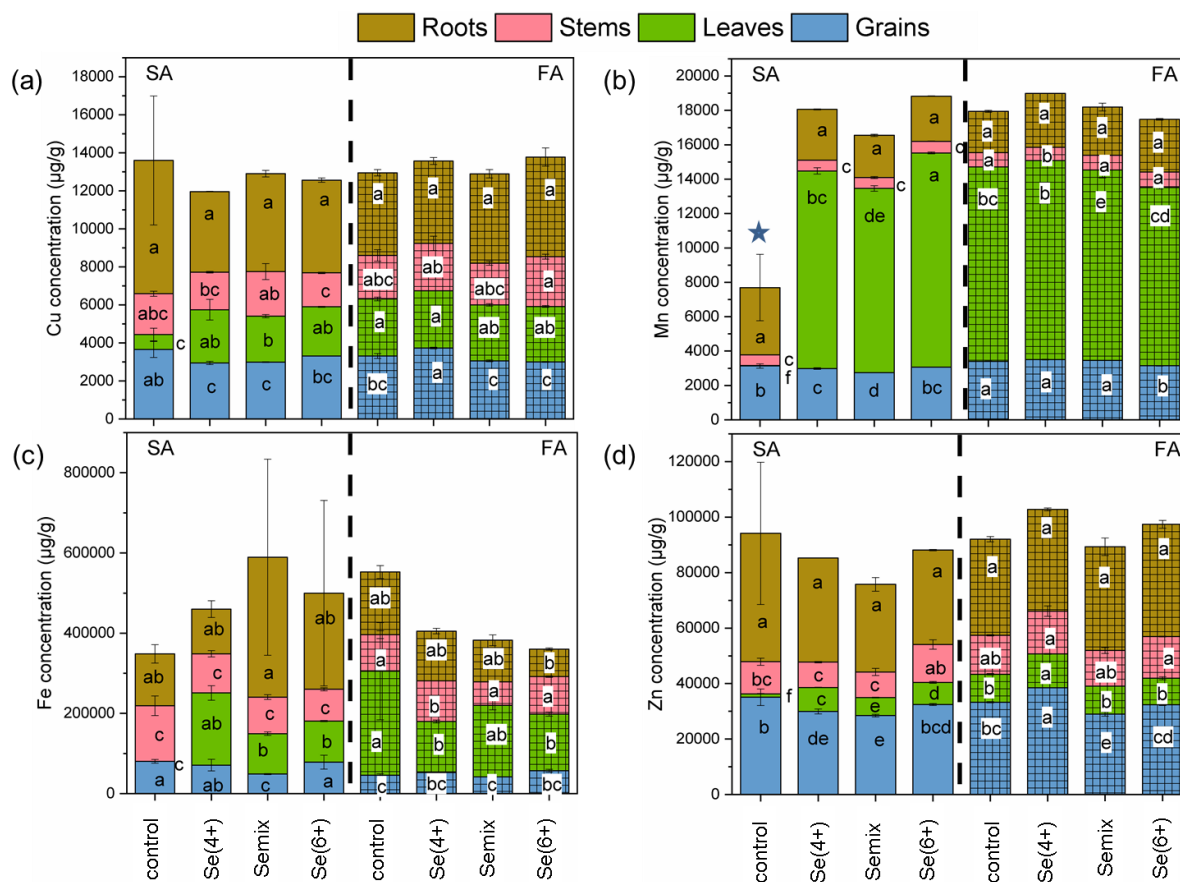


Figure 5.5: Concentration of other essential elements along the plant from top left Cu (a), Mn (b), Fe (c) and Zn (d). The error bar is given by SD of between two different measurements ( $n=3$ ). The different parts of the plant are represented as roots (brown), stems (pink), leaves (green), grains (blue), and applications methods SA- no pattern and FA- squared pattern. The statistical significance between different treatments based on means comparison of technical replicates was shown by student t-test with significance  $\alpha=0.05$ . Different letters define the level of significance. The star mark in the control sample of Mn indicates experimental error.



### 5.3.3 Se speciation and distribution in the grain: XANES and $\mu$ XRF

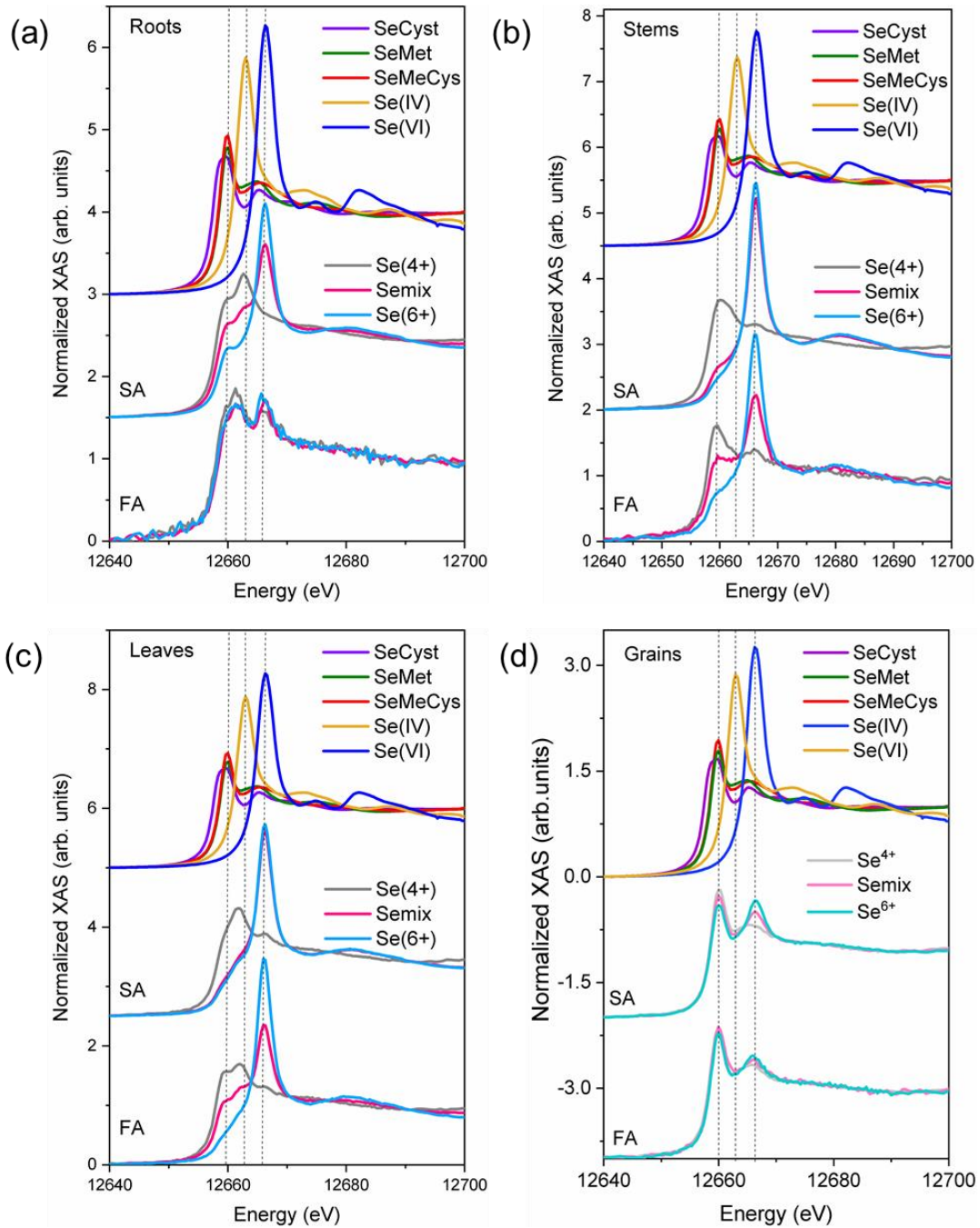


Figure 5.6: Se K-edge spectra collected over different parts of the plants: (a) roots (b) stems (c) leaves and (d) grains. The spectra corresponding to different Se treatments were given by grey ( $\text{Se}^{4+}$ ), pink (Semix), blue ( $\text{Se}^{6+}$ ). The vertical lines are marked as a guide to the reader. The spectra are shown in the order of references, SA and FA (from top to bottom) in the panels.

In order to better understand the plant metabolism and to correlate the translocation and the accumulation of Se with the Se species present in the plant, especially in grains, Se direct speciation was performed by XAS at the Se K-edge. The evolution of the Se species along the different parts of the plants can be visualized in Figure 5.6. The spectral signal has been systematically optimized during the measurements, and higher signal to noise ratio generally corresponds to higher Se concentration (see Fig 5.3). Dashed vertical lines are a guide for the eyes and indicate the position of the white-line corresponding to C-Se-C organic, Se(IV), and Se(VI) species, appearing at 12660, 12663, and 12667 eV, respectively. In some cases, a spectral feature appears at energy lying between the organic and Se(IV) white-line energies, around 12661.5 eV. As it was mentioned in previous chapters, when describing the speciation results from the hydroponic culture, it is likely that this contribution corresponds to selenide intermediate species (Ellis and Salt, 2003).

Overall, large spectral differences are found at the different part of the plants as function of the Se species used for the treatment. However, for the grains, a similar spectral profile, resembling the one of the Se organic species, was observed for both SA and FA and for all the treatments. A minor Se(VI) component appeared being more pronounced for SA and for the treatments containing  $\text{Se}^{6+}$ . In all the other part of the plants and for both applications methods the Se(VI) species dominate the spectral profile as soon as  $\text{Se}^{6+}$  is included in the treatment.

The SA roots spectra and their evolution as a function of the Se treatment, resembles the one found for FA leaves spectra, with coexisting organic, intermediate and Se(VI) phases. In both cases, the intermediate selenide component become evident only by including  $\text{Se}^{4+}$  in the treatments. Moreover, by increasing the  $\text{Se}^{4+}$  feeding fraction the contribution of the organic species increases at the expenses of the inorganic Se(VI). The results clearly show that the ratio of the Se species at the parts of the plants where the Se is applied is similar, independently of the application method.

In both, SA and FA stems, the contribution from the selenide species is reduced respect to the amount found in roots and leaves, respectively. The Se(VI) dominates the spectral profile for  $\text{Se}^{6+}$  treated plants whereas the Se organic species are more prominent when feeding the plants with  $\text{Se}^{4+}$ . Most likely it is the result of the plants natural defence systems, which, to avoid Se toxicity, oxidize selenide to selenate species (Xiao et al., 2021).

To address the weight of the different Se species contributing to the different spectra, a linear combination fitting analysis was performed on the XANES region (as described in the method section), considering the Se(VI), Se(IV), SeMeCys, SeMet, and SeCyst references. The semi-quantitative results are reported in Figure 5.7. The R-factor, representing the quality of the fit (as described in section 1.3), is reported in Table 5.1.

The results confirm the qualitative description reported in the previous paragraph, while finer details can be now appreciated, including the discrimination in between the different organic species contribution.

Regarding the parts of the plants where the Se was applied, roots for SA and leaves for FA, there are similarities in the detected organic species (SeMet and SeCyst) and their evolution as a function of the Se treatment, with SeMet increasing and SeCyst decreases by increasing the Se<sup>6+</sup> fraction in the treatment. Moreover, as expected, the Se(IV) (or, more properly, the intermediates selenide species) and Se(VI) contributions are inversely related and their ratio correlate with to the Se treatments applied. Instead, in stems, the SeMet fraction stay approximately constant respect the application methods, while SeCyst looks clearly suppressed in favour of the Se(VI) component, with a stronger effect for SA. It highlights the competition of this two Se species in the Se assimilation process from roots (SA) or leaves (FA) to stems. Moving further toward leaves (SA) or roots (FA), SeMet looks to not significantly change in both cases, while Se(VI) transforms in SeMeCys for SA and the among of both SeCyst and Se(VI) diminishes in favour of Se(IV), i.e. intermediated phases, for FA. Regarding grains, SeMeCys is the main component for both applications methods, mainly at the expenses of Se(VI) and SeCyst. Interestingly, in SA SeMet decreases, while SeMeCys increases by increasing the fraction of Se<sup>6+</sup> in the treatment. In the case of FA while SeMeCys increases by increasing the fraction of Se<sup>6+</sup> in treatment, SeMet stay constant. Differently from FA, SeCyst is not present in SA.

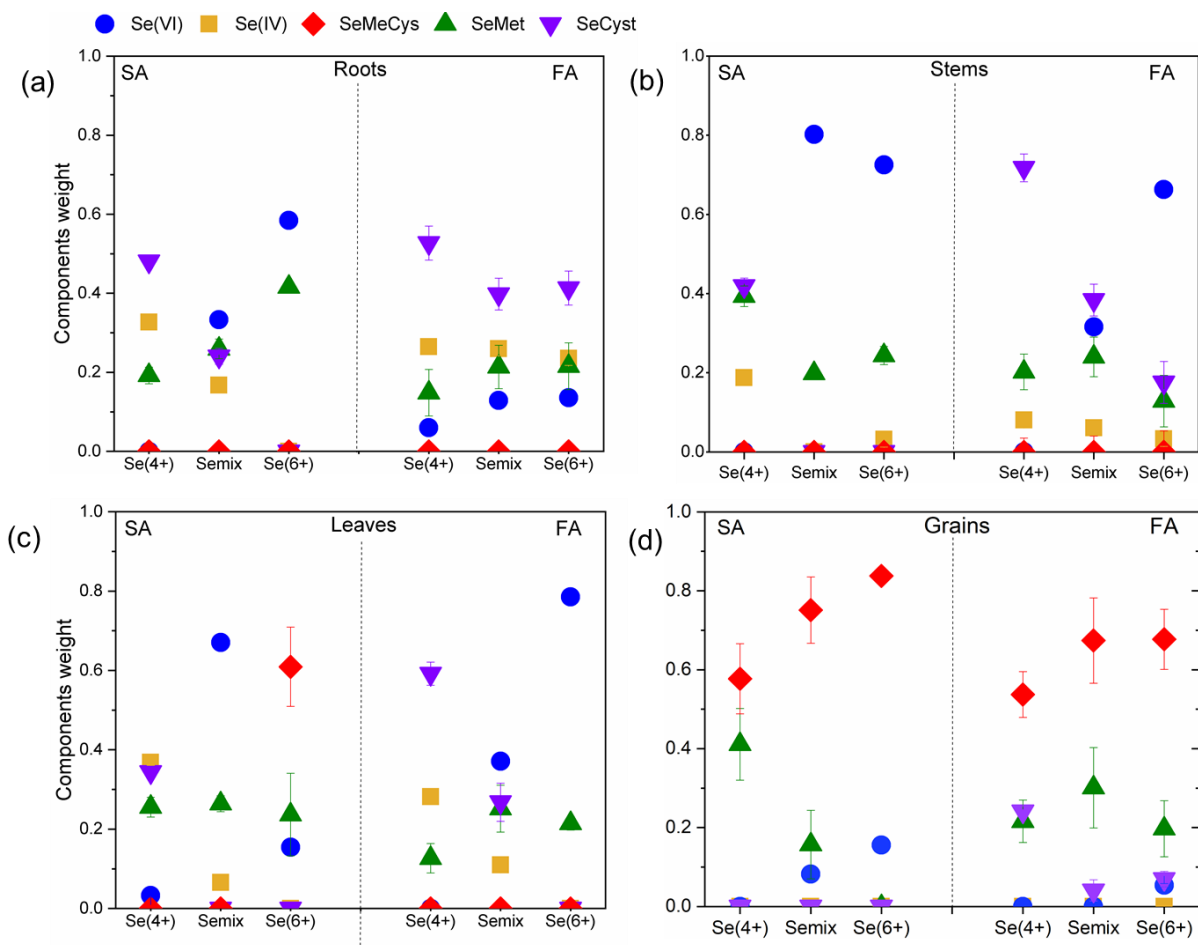


Figure 5.7: LCF of Se K-edge XANES spectra along different parts of the plant: roots (a), stems (b), leaves (c) and grains (d) from top left. The E0 (rising edge position) of Se(IV) have been left free to fit the selenide intermediate phase. The average shift in the E0 of Se(IV) in the LCF fit is -0.5 eV for roots for all treatments, while for stems of leaves -1 eV and 0.2 eV for Se<sup>4+</sup> and Se<sup>6+</sup> treatment, respectively.

We can conclude that within SA the grains contain only C–Se–C species (e.g. SeMet or SeMeCys, and SeCys), while in the case of FA a minor fraction (around 10%) of C–Se–Se–C species (e.g. SeCyst) is present. Characterizing the ratio of the Se species contained in the wheat grains, including the ratio of the seleno-amino acids formed, it is not only important to understand Se mechanism in plant, but it is also essential to determine the benefits of Se-enriched food for human health. Indeed, the different seleno-amino acids are differently assimilated by the human

body and they fulfill distinguished functions related with specific health benefits. C-Se-C bonds can be readily incorporated in the humans in serum albumin of the blood. Also, they could be further converted into dimethylselenide or dimethyl-diselenide to be further reduced and incorporation of methyl Se species by leaving the Selenide and the intermediate volatile compounds with the help of methyltransferase and cysteine based enzymes.

Table 5.1: R-factor of the linear combination fits along different parts of the plant

		Roots	Stems	Leaves	Grains
Soil	Se <sup>4+</sup>	0.002	0.002	0.002	0.004
	Semix	0.002	0.005	0.007	0.004
	Se <sup>6+</sup>	0.005	0.008	0.030	0.004
Foliar	Se <sup>4+</sup>	0.009	0.008	0.004	0.001
	Semix	0.008	0.008	0.008	0.004
	Se <sup>6+</sup>	0.009	0.006	0.008	0.002

The SeCyst found in the FA grain could reflect the original level of SeCys, since it has been pointed out that SeCyst found in the plant are usually due to the oxidation of SeCys (Chan et al., 2010). Anyway, being the C–Se–C species having less harmful effects, since the incorporation of SeCyst into the protein could interfere with the formation of disulfide bridge affecting tertiary structure of S-proteins (Terry et al., 2000), our results show that eventual Se toxicity is less severe in SA than in FA. Also, on the other hand as reported under the Zn distribution by the assimilation of heavy metals, in the leaves vacuoles Se can be less mobile in the plants, this is true in case of Se(IV) as they can easily converted into aminoacids in plants without the need to reduce for plant metabolism compared to Se(VI). In conclusion, being as well the Se accumulation process more efficient in the SA, it looks finally the best application method ones compare with FA.

In the next part, we address the spatial distribution of Se and the different Se species along selected grains (300 μm thick sections, spatial resolution of 50 μm). The grain sections have been obtained from the centre of the grain along its longitudinal direction. It was impossible to obtain perfectly identical grain sections, anyhow the main regions of interest (bran, eye, filament, and endosperm) are easy to identify in all the sections. Se Kα emission μ X-ray fluorescence (μXRF)

maps collected over grains obtained by different Se treatments and application methods are shown in Figure 5.8. The Se distribution along the different regions of grains can be easily visualized. For SA, Se is clearly accumulated along the outer bran region, in the eye, and in the filament region. Instead, for FA, Se seems more diffuse, being more present also in the endosperm region.

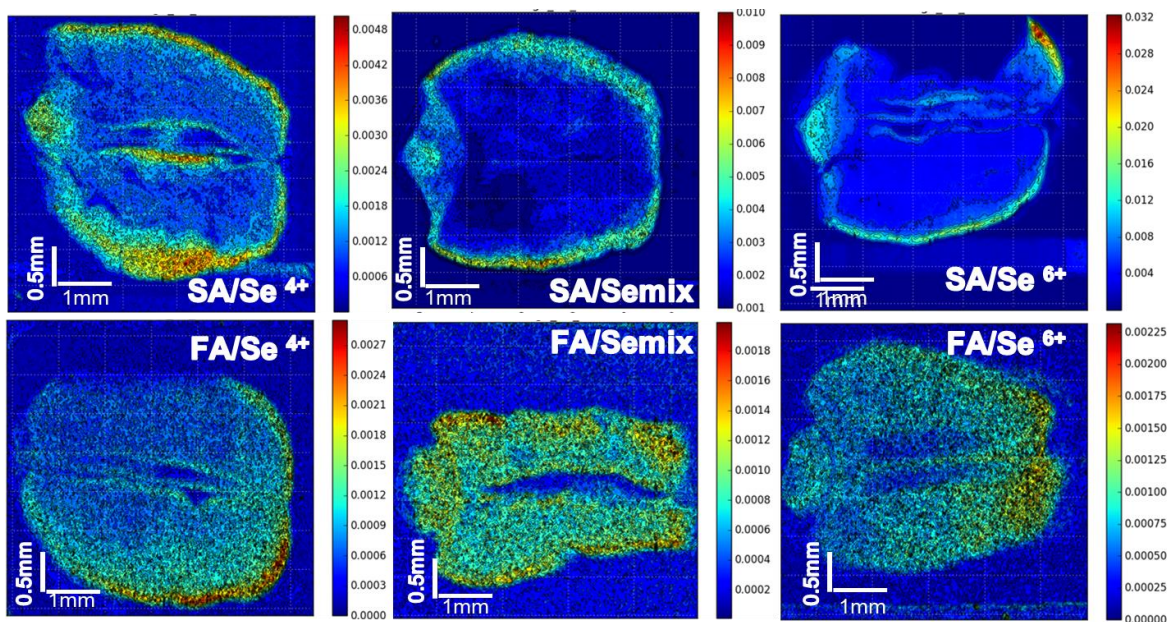


Figure 5.8: Spatial distribution of Se along the grains respect to treatment and application methods. Top row shows the SA and bottom row shows the FA.

Se K-edge  $\mu$ XANES were collected at different points over the regions of interest. Figure 5.9(a) and 5.9(b) report the Se K-edge  $\mu$ XANES spectra collected on the eye bran endosperm and filament of SA and FA grains. The merge of all the  $\mu$ XANES spectra collected over a grain agrees with the measurement obtained from the ground grains that have been previously reported in Fig. 5.6(d). Minor spectral changes among grain regions can be seen. The spectral features are varying slightly, with Se(VI) contribution appearing for increasing Se<sup>6+</sup> in the treatment.

The linear combination fitting analysis was possible only in the SA case. The  $\mu$ XANES spectra from FA were too noisy in accordance with the very little Se concentration present. The R-factor of the fitting results SA is reported in the Table 5.2. LCF of FA was not reported due to

as the signal to noise ratio of the spectra were high. SeMeCys is the major component in all the regions, except the eye, where a similar amount of SeMet is found (50%). In the endosperm, SeMet is present only for the Se<sup>4+</sup> treatment (20%). In the bran SeMet is around the 10% and looks suppressed with Se<sup>6+</sup> treatment. Finally, in the filament SeMet is around the 20% irrespectively of the Se treatment applied. Se(VI) is present everywhere in small amount (below the 10%) as Se<sup>6+</sup> is included in the treatment.

The spatial distribution of the Se Species in soil samples are shown in Figure 5.10. In accordance with the above results, the SeMet is mainly seen in filament and eye region and SeMeCys can be present along the full grain, as Se(VI). Thus, we can conclude that the desired Se bioavailable species are produced in the regions which generally are not eliminated in wheat grain processing for human consumption.

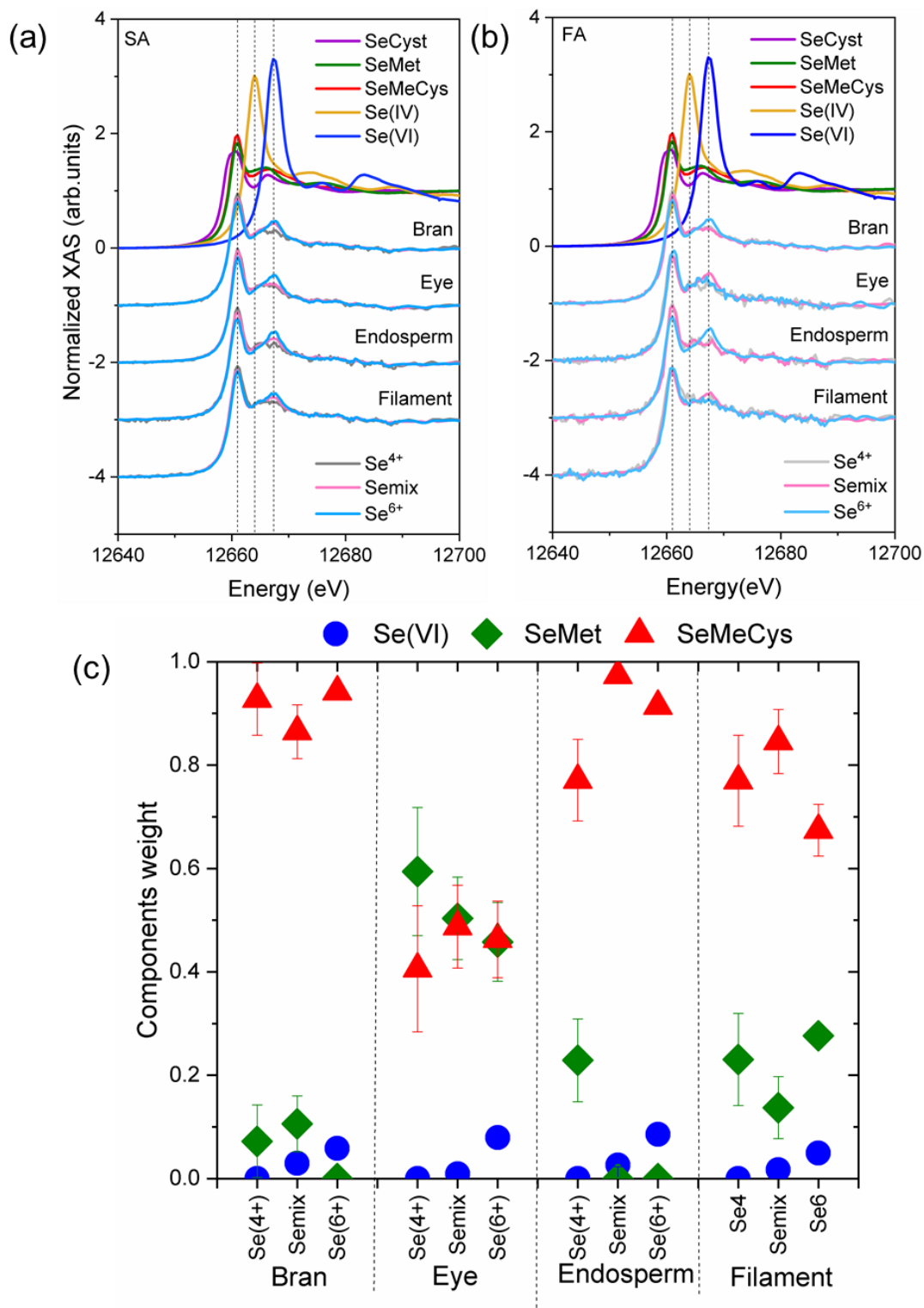


Figure 5.9: Se K-edge spectra of  $\mu$ XANES of soil (a) and foliar (b) application. The LCF of the average spectra respect to regions in grains of SA. (c)



Table 5.2: R-factor of the linear combination fits along grain regions

	<b>SA</b>
<b>Bran</b>	
Se(4+)	0.004
Semix	0
Se(6+)	0.004
<b>Eye</b>	
Se(4+)	0.004
Semix	0.076
Se(6+)	0.074
<b>Endosperm</b>	
Se(4+)	0.004
Semix	0
Se(6+)	0.005
<b>Filament</b>	
Se(4+)	0.008
Semix	0.0058
Se(6+)	0.054

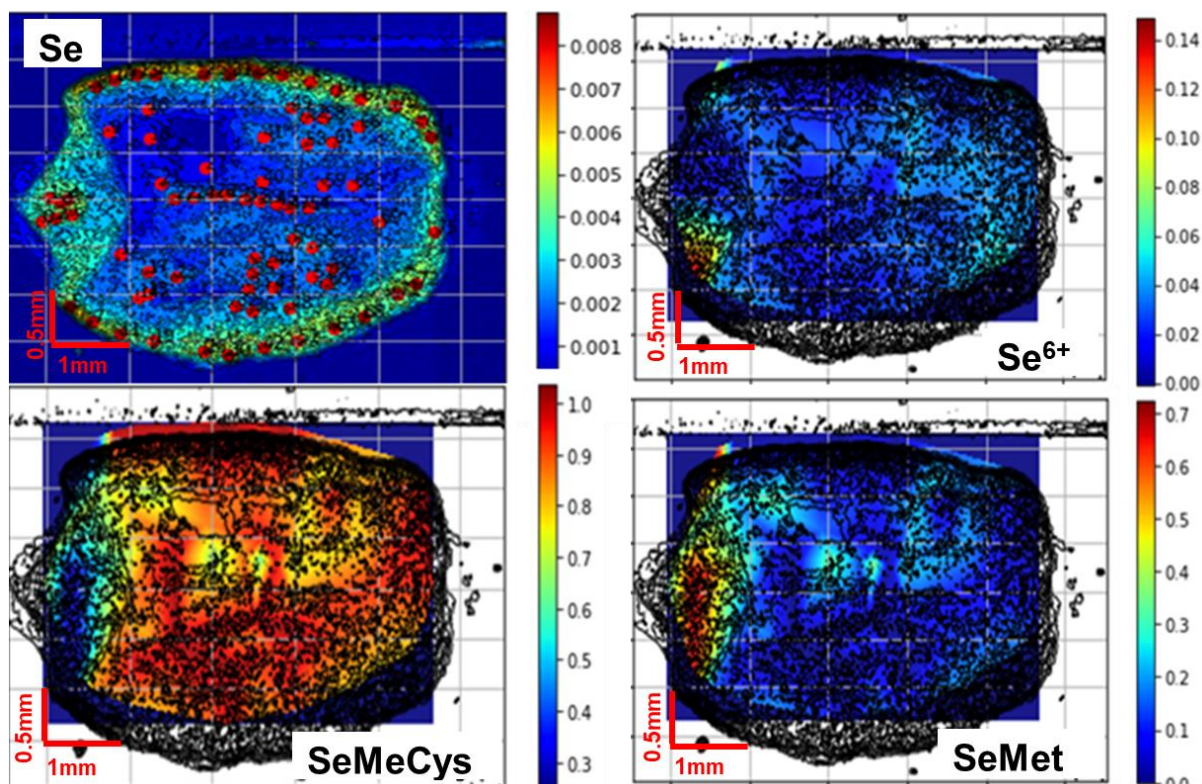


Figure 5.10: Spatial distribution of Semix treatment representative of SA treatments, and LCF of different species distribution SeMeCys, Se(VI) and SeMet

The distribution of other micronutrients is reported in Figure 5.11 (Zn) and 5.12 (K). Zn is mainly accumulated in the filament strand and, in minor amount, in the eye and bran. Instead K is mainly accumulated in the bran, and in minor amount in the filament and eye. On the other hand, previous studies on wheat grains biofortified with Zn, shows localization of Zn in filament and eye in the grain. The localization of Zn in the reported regions could be due to the bonding with the wheat proteins natural distribution (Singh et al., 2018; Xiao et al., 2021). Whereas, K are found along the outer bran region, where protein distribution is less (Xiao et al., 2021).

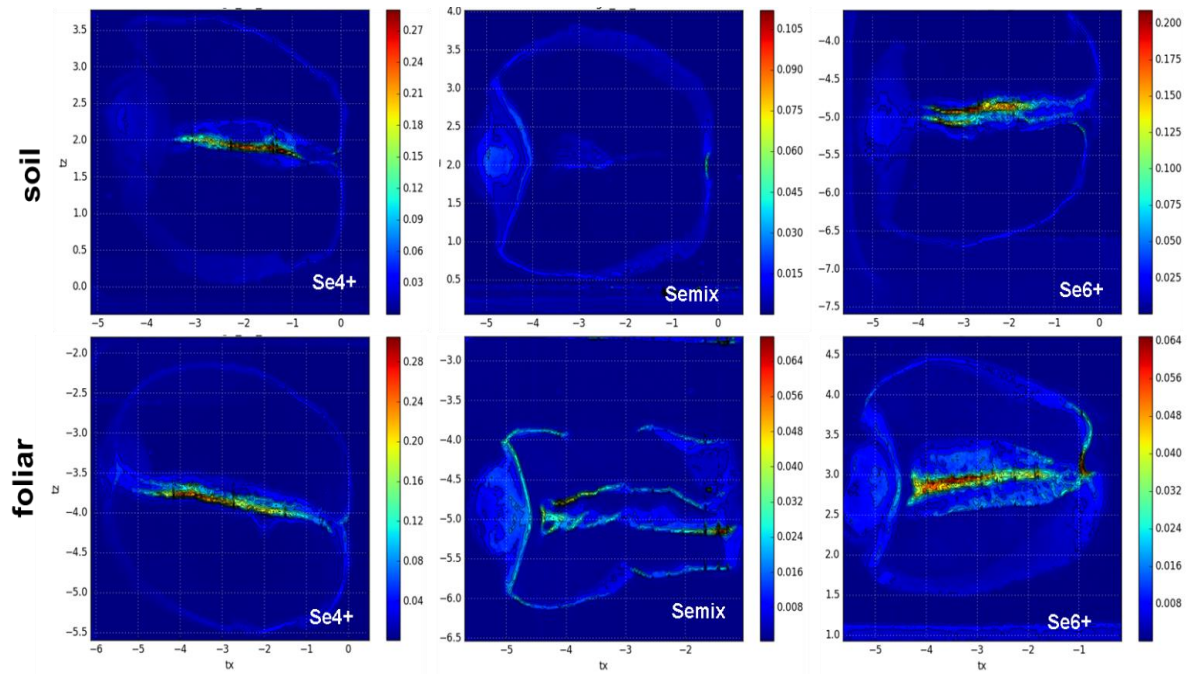


Figure 5.11 Zn distribution along the grain grown under different treatments and Se application methods. Top row shows the SA and bottom row shows the FA.

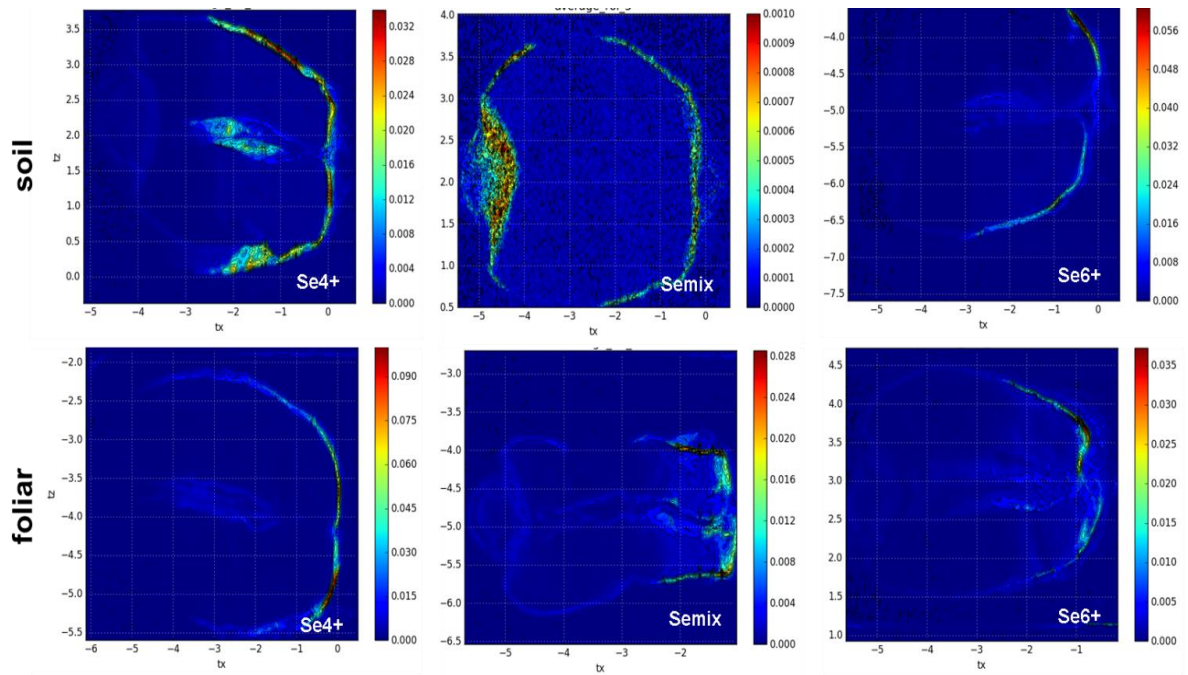


Figure 5.12: K distribution along the grains grown under different Se treatments and application methods. Top row shows the SA and bottom row shows the FA.

To access finer details  $\mu$ XRF maps and Se K-edge  $\mu$ XANES spectra were collected at I18 beamline at Diamond light source, using a beam size of  $4 \times 2 \mu\text{m}^2$  and a reduced beam flux ( $2 \times 10^{12}$  photons/s). Elemental maps and spectra have been acquired at low temperature (80K) to avoid radiation damage. Figure 5.13, shows the Se spatial distribution along the grains for different Se treatments of both application methods. Like the above reported results, obtained at CLÆSS beamline with a lower spatial resolution, Se accumulates in the bran, filament, and eye, and it is found in minor amount on the endosperm regions. Simultaneous acquisition of different elemental maps permitted the co-localization of such elements along with Se. The tricolour maps of Se (green), Zn (red), and K (blue) of all grains is given in Fig. 5.14. In some samples like  $\text{Se}^{6+}$  treatments a higher ratio of Zn and K in eye respect to Se can be appreciated, while Se is clearly more distributed in the endosperm. The elemental coexistence is expected in regions were proteins are more localized like the endosperm, filament and eye, identifying as well similar accumulation mechanisms for the different elements.

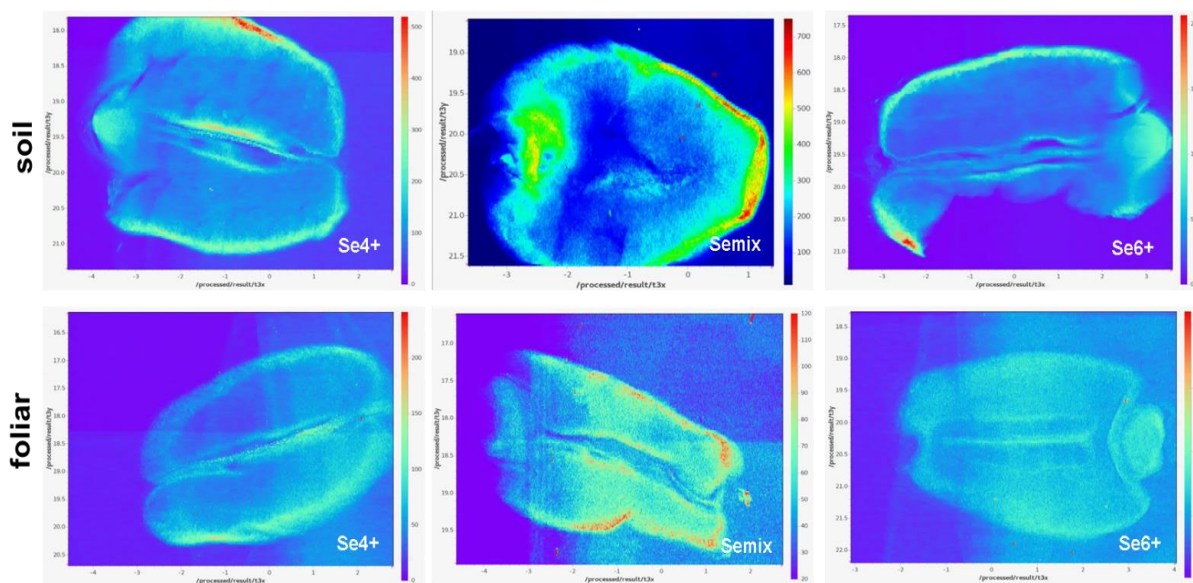


Figure 5.13: Spatial distribution of Se collected with a  $4 \times 2 \mu\text{m}^2$  beam size on grains. Top row showing SA and bottom row FA, as a function of Se treatment: from left to right  $\text{Se}^{4+}$ , Semix and  $\text{Se}^{6+}$ .

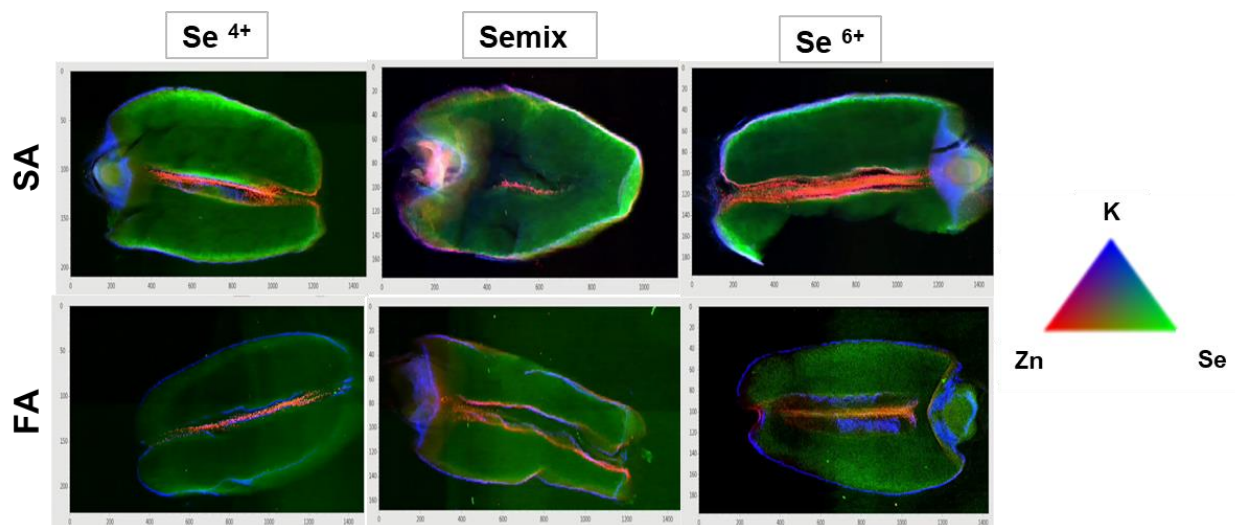


Figure 5.14 : Tricolor maps of coexisting elements along the grain (Se (green), Zn (red), and K(blue)) collected with a  $4 \times 2 \mu\text{m}^2$  beam size on grains. Top row showing SA and bottom row FA, as a function of Se treatment: from left to right  $\text{Se}^{4+}$ , Semix and  $\text{Se}^{6+}$ .

The production of the grains clearly reflects the influence of the different Se treatment and application methods have in the biofortification process. In the case of SA samples, both the production and the concentration are higher in the  $\text{Se}^{6+}$  treatment than the  $\text{Se}^{4+}$ , followed by the Semix treatment. This agrees with the results previously reported in the literature. As suggested in those works, it could be due to the complex formation of  $\text{Se}^{4+}$  with soil organic matter and therefore being less available to plants, while,  $\text{Se}^{6+}$  being easily available for plant uptake and transformation (Dinh et al., 2017; Lidon et al., 2019; Ros et al., 2016). On the other hand, FA shows higher total grain weight for  $\text{Se}^{4+}$ , whereas the total number of grains is larger for Semix. Regarding Se concentration, although we found that the values for FA are much lower than those for SA, their translocation, especially that of  $\text{Se}^{4+}$ , is higher in plants as reported in literature from leaves to grains (Lidon et al., 2019; Lyons et al., 2003). We found that the Semix provide an intermediate behaviour in both the applications, leaning towards the fraction of soluble fraction in the application adaptable to application technique. As Se(IV) can be easily bounded to organic content and Se(VI) is more mobile and not readily converted in the plants, the combination of both helps in the immediate access and the slow release of Se available to plants (as discusses in 4.1).

Regarding the Se species in grains, the presence of SeMeCys, SeMet and Se(VI) in SA samples and the additional presence of SeCyst only in the FA ones could be assessed based on the metabolism of the plant. In the plants, SeCyst can be further broken-down to form methylated Se complex species by leaving some residual compounds (selenide and dimethylselenide). Presence of Se fertilization on the surface of the leaves could be the cause of the SeCyst presence in FA which does not occur on SA. In the latter, the Se-soil interaction could also directly form complexes which immobilize the Se species making them not available to the plants. Likewise, the SeCys could be oxidized and less bioavailable to plants (Xiao et al, 2021). Also, in the studies regarding the speciation and concentration of Se in SA, Se<sup>6+</sup> treated group have higher Se present in the soil after cultivation respect to SCA treated samples.

The spatial studies helps us to visualize the major bioavailable species in the protein rich regions of eye and filament (SeMet) and in endopserm, both protein and carbohydrate rich region (SeMeCys), the antioxidant pathway affected by the Se stress can induce more biomass in terms of carbohydrates in the crops (Ros et al., 2016). From our results we can conclude that, in terms of biofortification, Semix is a good candidate for foliar application and Se<sup>6+</sup> in case of soil application.

SeMeCys and SeMet with C-Se-C bonds are more bioavailable in human, as they can be converted into dimethylselenide, dimethyldiselenide complexes with help if methyltransferase reactions and easily incorporated into proteins. However, the SeCyst C-Se-Se-C is not bioavailable as it was more energy efficient to break the bond of the Se to be incorporated into amino acids. In terms of species, as reported SA produced more bioavailable species than FA and also at higher concentrations.

### 5.3.4 Speciation and distribution of S in grains

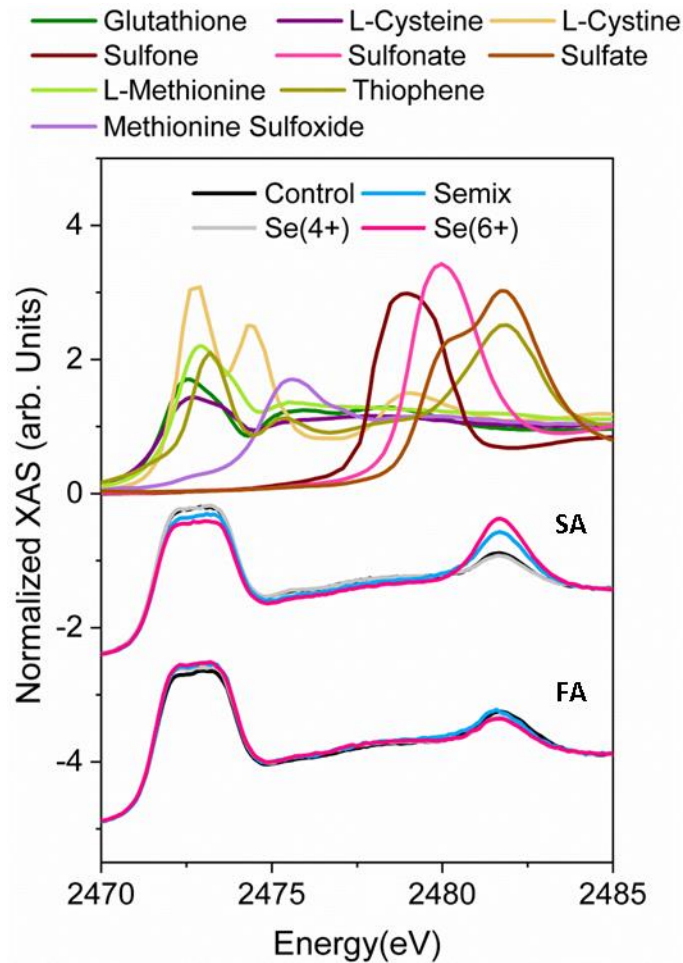


Figure 5.15: S K-edge spectra collected on grains grown under different Se treatments and application methods. The figure represents the reference, SA and FA spectra (from top to bottom).

Sulphur speciations have been studied in the grains of both application methods and treatments. The corresponding S K-edge spectra are shown in the Figure 5.15. Similarly, to the hydroponic application method, discussed in section 1.3, (Figure 1.1), the spectra report organic high S oxidation state contributions. In this case the spectra are more similar and very few changes are found as a function of the Se treatments or application method. Only for SA sample, S(VI) contribution is clearly enhanced by the  $\text{Se}^{6+}$  treatment.

The S(VI) species is expected due to the detoxification of sulfite with its transformation in sulphate by plants as a protective mechanism (Yarmolinsky et al., 2013). It is seen higher in Se<sup>6+</sup> treatments, where Se(VI) is also present due to the detoxification processes.

Sulphur species spatial distribution in the SA and FA grains have been obtained as explained in hydroponic corresponding section 1.3. The SA and FA sulphur species distribution for the Semix treatment is compared with the control in Figure 5.16. Also, the sulphur species distribution for the FA selenium treatments Se<sup>4+</sup> and Se<sup>6+</sup> are reported in Figure 5.17. Similar to the hydroponic case, the maps focus on the organic (maps collected at 2472.6 eV of incoming energy) and highly oxidized S species distribution (maps collected at 2481.5 eV of incoming energy). While the organic species resulted mainly concentrated in bran region and in the filament, the highly oxidized S species appeared to be predominant in the endosperm, irrespectively of the Se treatment or application method.



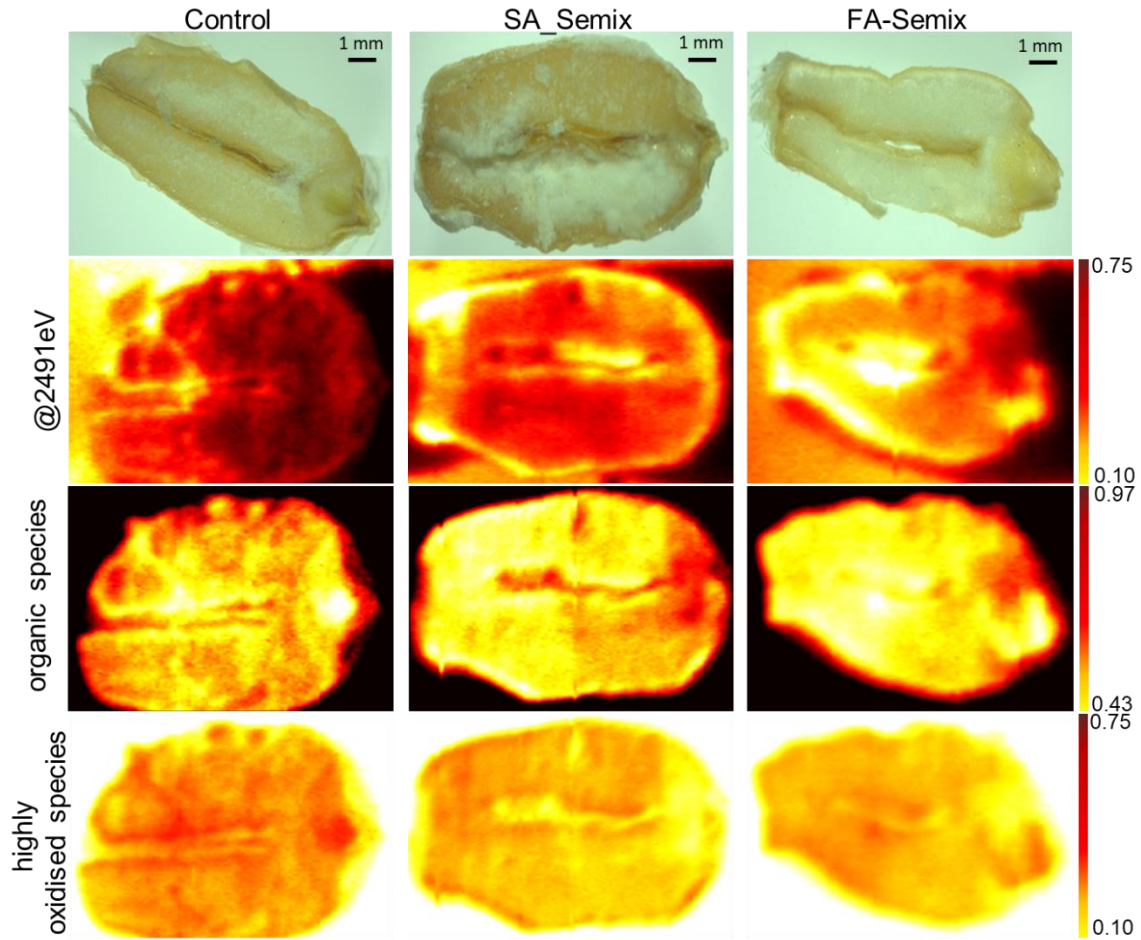


Figure 5.16: Sulfur elemental and organic and highly oxidized S species distribution in grains corresponding to control and SA and FA of Semix treatments. The different organic (third row) and highly oxidized S species (fourth row) are shown respect to the sulfur distribution (second row). On the top the image of the investigated grains.

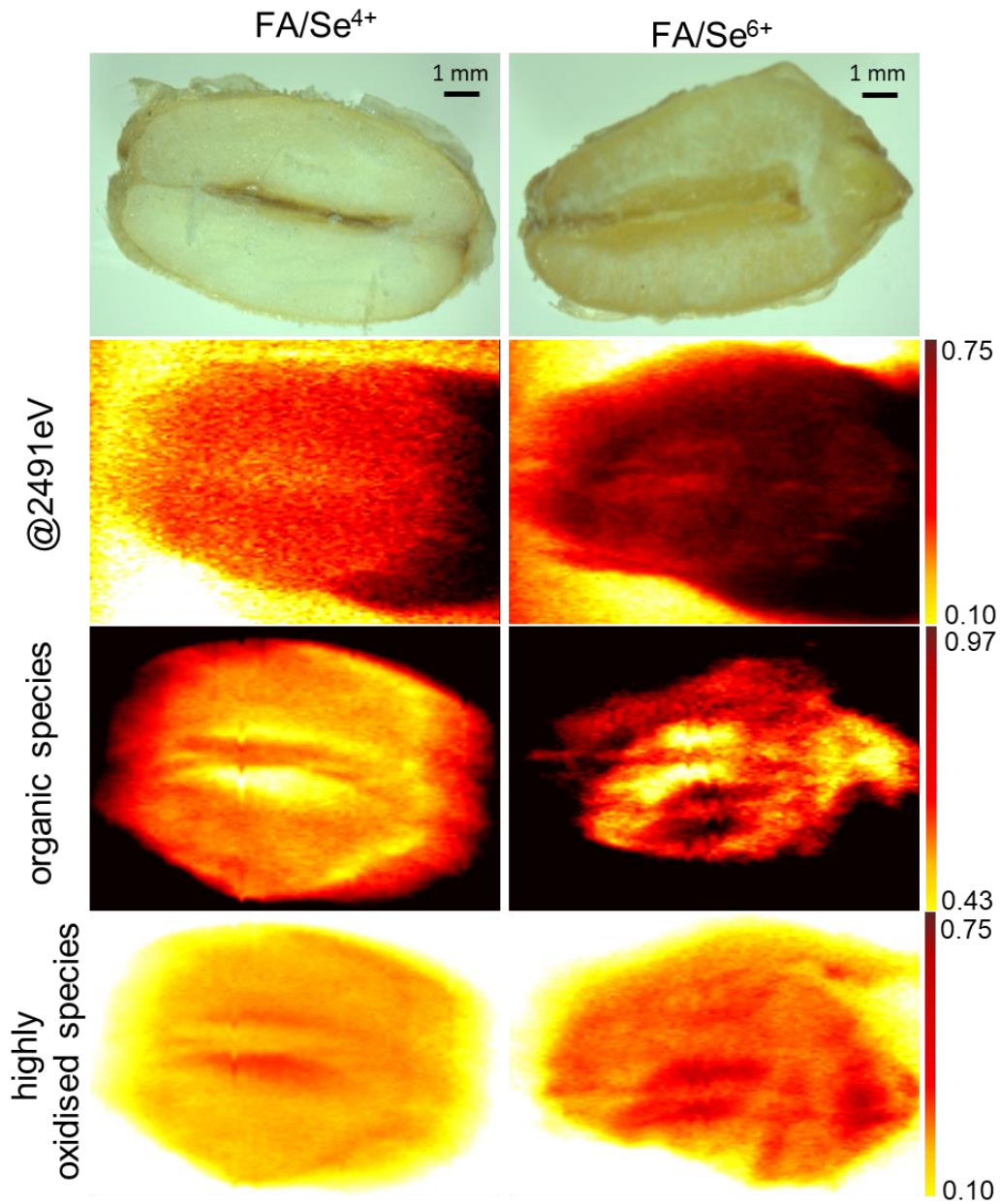


Figure 5.17: Sulfur elemental and organic and highly oxidized S species distribution in grains grown under  $\text{Se}^{4+}$  and  $\text{Se}^{6+}$  treatments with FA. The different organic (third row) and highly oxidized S species (forth row) are shown respect to the sulfur distribution (second row). On the top the image of the investigated grains.

### 5.3.5 FTIR in grain sections

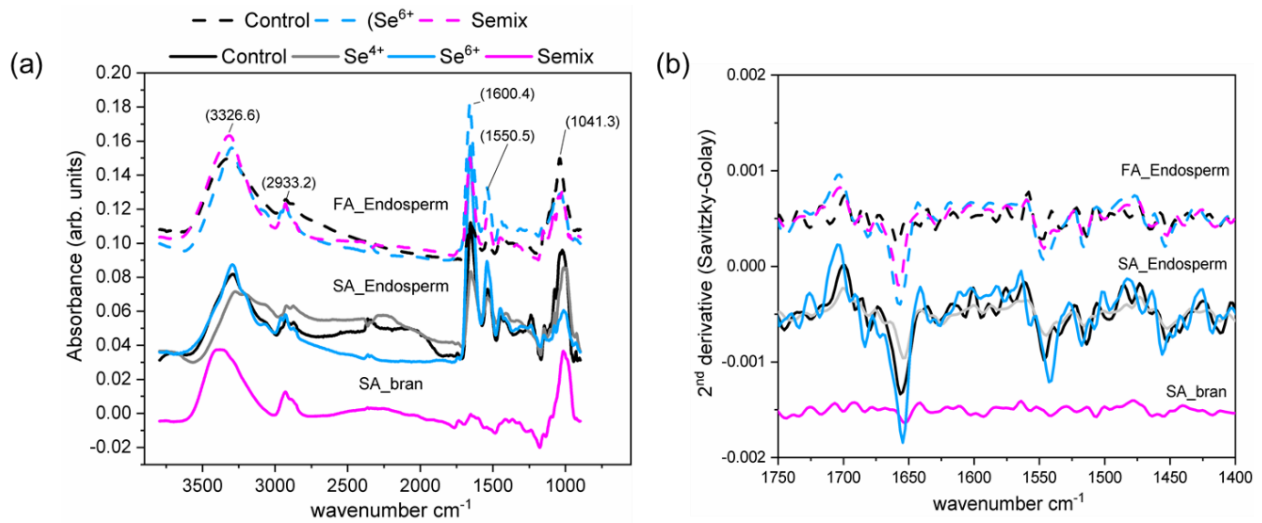


Figure 5.18: FTIR spectrum collected on grain sections (a), second derivative of peaks respect to protein functional groups (b).

To understand the effect of Selenium treatments in the functional groups of the wheat proteins due to incorporation of Se in plant tissues was the aim to study FTIR spectroscopy using synchrotron is studied. The wheat section of 40micron thickness treated with 1% amylase solution for 8 hours after removing the excess starch content was used for the study. The removal of starch was not very successful hence it was difficult to study in transmission in the samples. However, some regions in the sections could be accessed and those data in different treatments were presented in Figure 5.18.

The major functional groups respect to wheat proteins amide I at  $1600\text{-}1700\text{ cm}^{-1}$  and amide II at  $15000\text{-}1500\text{ cm}^{-1}$  is of high interest as amide I peak can help to see secondary protein structures in the samples. Also, the contribution at higher wavelength could be attributed to C-N stretching of amine complexes or from alcohol compounds. The detailed functional groups and corresponding wavelengths are described in section 1.3, under Table 1.4. In SA samples difference between the bran of Semix treatment and endosperm of other treatments shows the absence of proteins in the outer barn region and their presence mainly in the inner regions of the grain, where

also wheat proteins are expected. Also, in SA over all spectral differences among the treatments can be visualized. The second derivative also shows the amide peak at  $1660\text{ cm}^{-1}$  in all the samples. The data quality does not permit direct comparison. Further studies are necessary to get more information.

## 5.4 Conclusions

In the present chapter, the soil and foliar application for Se biofortification has been addressed.

No major changes on the biomass of roots and leaves has been detected as a function of the different Se treatments applied or by the application method used. Although no differences have been detected for SA, Se reduced the number of grains produced in the FA respect to the control. Even though, the number of grains and weight was similar in all the Se treatments independently of the application method.

In comparison with the hydroponic results previously reported, although the number of grains is similar, their average weight is almost doubled, probably because the lower Se toxicity. Indeed, in hydroponics, the absence of organic matter in the culture media permits the Se dosed to the media to be fully available for the plant and, therefore, the total Se accumulation strongly increases.

The Se concentration and translocation factor (TF) gives information about the overall biofortification achieved. Plants accumulate substantially more Se by SA respect to FA. In SA, along the full plant, the Se accumulation is reduced by the Se<sup>4+</sup> treatment. This is due to the fact that Se(IV) is rapidly assimilated into organic forms which are retained in soils, while Se(VI) is highly mobile. The Se TF from roots-to-grains in SA is enhanced, while from leaves-to-grains in FA it is reduced for Se<sup>6+</sup> treatment. In both cases, the TF is below 1, indicating a poor Se translocation. The reported trends express the different Se pathways respect to plant metabolism.

Micronutrients like Cu, Mn, Fe and Zn are involved in major enzymatic activity. In the present work, their concentrations in the different parts of plants do not show drastic changes as a function of the Se treatment applied or the application method.

Se and S speciation has been addressed by XAS. For the Se K-edge XAS, large spectral differences are found at the different part of the plants as function of the Se species used for the treatment. However, for the grains, a similar spectral profile, resembling the one of the Se organic species, was observed for both SA and FA and for all the treatments. Within SA group the grains

contain only C–Se–C species (e.g. SeMet or SeMeCys, and SeCys), while in the case of FA a minor fraction (around 10%) of C–Se–Se–C species (e.g. SeCyst) is present. Since the C–Se–C species are more bioavailable for humans, the above reported results show that the Se biofortification via SA is more efficient than in FA in terms of the produced health benefits.

A minor Se(VI) component appeared in grains for the treatments containing  $\text{Se}^{6+}$  and it is more pronounced for SA. In all the other part of the plants and for both application methods, the Se(VI) species is dominating the spectral profile as soon as  $\text{Se}^{6+}$  is present in the treatment. The tendency of an increased Se(VI) presence in shoots is probably due to the plant detoxification mechanism, which tends to oxidize Se to reduce its potential toxicity.

The S K-edge XAS spectra has been collected only for the grains. In a similar way to the Se K-edge spectra, they do not significantly change when varying the Se treatment or the application method, and show the coexistence of organic and highly oxidised S species.

The Se species distribution in the grain has been characterized only for SA method. SeMeCys is the major component in all the regions, except the eye, where a similar amount of SeMet is found (50%). In the endosperm, SeMet is present only for the  $\text{Se}^{4+}$  treatment (20%). In the bran SeMet is around the 10% and looks suppressed with  $\text{Se}^{6+}$  treatment. Finally, in the filament SeMet is around the 20% irrespectively of the Se treatment applied. Se(VI) is present everywhere in small amount (below the 10%) as  $\text{Se}^{6+}$  is included in the treatment.

From the previously reported results, it is possible to expect a different Se species formation in the grains as soon as the total Se accumulation increases. Indeed, in the hydroponic case, six times more Se accumulation in the grains was corresponding to the formation of 73% of SeMet and 37% of SeCyst distributed mainly in the eye and in the bran, respectively. Since the SeCyst is less desirable in terms of Se health benefits respect to SeMet and SeMeCys, attention should be paid to tune the formation of the most desirable Se organic species.

The S species spatial distribution has been obtained for both SA and FA grains. While the S organic species resulted mainly concentrated in bran region and in the filament, the higher S oxidation species appeared to be predominant in the endosperm, irrespectively of the Se treatment or application method.

Instead, similar to the hydroponic case, the grain FTIR results show that the presence of amide protein, which could be linked to seleno aminoacid, varies little in the endosperm depending upon the treatments and the application method. The difference obtained by comparing the endosperm and bran spectra reflects differences in the proteins present in these two regions. In any case, the results do not permit to easily correlate to Se proteins, subject of the present study.

Our results support the idea that the Se accumulation process is more efficient in the case of SA than the FA, being Se better up taken by the plant from the soil in the form of  $\text{Se}^{6+}$ , and considering that only a minor fraction of Se(VI) can be expected to co-exist in the grains together with the desired organic species.

## 6 Thesis Conclusions

The reported results and related discussions lead to the following conclusions

Se biofortification in wheat plants with different Se treatments ( $\text{Se}^{4+}$  and/or  $\text{Se}^{6+}$ ) and culture conditions was performed to study the influence of the presence of pollution (Cd, Hg) in the cultivation media and the application methods (soil and foliar application) in fortification process. The major conclusions are summarized as follows:

In hydroponic cultivation, the biomass and grain yield were reduced by the Se biofortification process, as well as by the Cd application. The total number of grains produced under Cd treatments were not significantly different from the Control, but it got reduced in the presence of Se. The Se uptake and translocation was reduced by 50% under Cd pollution, with a maximum of Se accumulation in grains for the 50/50 treatment. Instead, the Cd translocation from roots to grains increased in the presence of Se, with a maximum for the 50/50+Cd treatment. It is observed due to the combined toxicity effect from Cd and Se applications. Also, the influence of stress can be seen from gene expression of stress indicators in plants (APS and PCS) especially in shoots in our study. Se and Cd treatments affect the uptake and storage of the essential micronutrients as Mo, Zn, Cu and Mn because of the competing uptake mechanisms.

SeMet and SeCyst are the major Se species found in Se biofortified grains, approximately 73% and 37%, respectively. In the presence of Cd, SeMeCys is forming while the amount of SeMet species gets reduced. The effect of Cd on the Se speciation does not affect the Se biofortification process as SeMet and SeMeCys are both directly bioavailable for human body, while SeCyst is less desired.

S speciation showed both organic and highly oxidized S species coexist along the plant and in the grains. SeMet and highly S oxidised species are mainly located in the eye and filament regions, while the SeCyst and S organic species are present in the endosperm. Instead, SeMet, SeCyst, and highly S oxidated species are present in the bran region of the grains. This is in accordance with the known natural distribution of wheat proteins. The FTIR results show that the presence of Amide protein, which could be linked to seleno aminoacid, varies slightly depending upon the treatments.



Considering the Se speciation and total Se accumulation reported, the 50/50 treatment is better in terms of Se-biofortification of wheat plants grown in hydroponic media.

Gene expression studies in young plants showed that the sulphate transporter genes, which are expected to affect the Se and Cd mobility, are more active in the aerial parts of the plants for SULTR1:3 and SULTR4:1, while they are suppressed in the roots. However, the major root transporter SULTR1:1 is seen active in roots. Se<sup>6+</sup> treatments are the most upregulated as Se(VI) inhibits S uptake in the roots, whereas Se<sup>4+</sup> treatments show downregulation. The stress responsive gene expressions in roots are suppressed by the presence of Se and Cd respect to the control sample, suggesting a reduced stress response in the Se biofortified wheat roots.

In shoots, the expression level of the sulphate transporter genes is not strongly altered by any of the Se treatments, but they are increased for the Cd treatment respect to the control and even more by the combination of Se treatments with Cd. In addition, OASTL (catalyse the synthesis of cysteine) in shoots, is upregulated in the presence of Se<sup>4+</sup>, in agreement with the higher detected SeCyst content when increasing the Se<sup>4+</sup> fraction in the treatment. Moreover, the presence of Cd increases significantly the stress responsive gene expression for both APX and PCS in shoots, suggesting a relative tolerance to such element at low concentration.

The presence of Cd and of different Se species influences the plant metabolism and affects the Se biofortification process, with the different chemical species competing in the sulphate pathways and transformation.

Hg speciation study along Se biofortified wheat plants grown hydroponically in Hg contaminated environment show that methylated species are formed both with and without Se-biofortification conditions and that they are accumulated in the grains.

The formation of Hg-Se complexes, present in higher amount in the roots, is believed to reduce the translocation of Hg. The 1:1 mixture of Se<sup>4+</sup> and Se<sup>6+</sup> species in the feeding yields the lowest translocation factor of Hg to the grains.

Se-biofortification treatment inhibits the accumulation of methylmercury in grains offering protection against the Hg-induced plant toxicity to a certain extent. These findings can be applied to reduce the presence of Hg in wheat-based food.

Soils studies corresponding to the Se bio-fortification process shows Se<sup>4+</sup> species in the soil are progressively transformed into organic species which are less available for the plant

uptake. Instead,  $\text{Se}^{6+}$  is more slowly transformed to  $\text{Se}^{4+}$ , forming intermediate Se species, thus it is more immediately available for the plant uptake.

The Se amount provided to soils is reduced by the wheat plant uptake, in higher extent for the  $\text{Se}^{4+}$  feeding, because of the volatility of the Se intermediate phases. Similarly, the strong decrease of the Se concentration by increasing the  $\text{Se}^{6+}$  fraction in the control soil suggests a possible partial loss of Se through volatile species. In foliar application, a negligible amount of Se is detected in the soil and only in organic forms.

Se biofortification in soils based on soil and foliar application methods does not show any major changes on the biomass of roots and leaves has been detected as a function of the different Se treatments applied or by the application method used. Although no differences have been detected for SA, Se reduced the number of grains produced in the FA respect to the control. Even though, the number of grains and weight was similar in all the Se treatments independently of the application method.

In comparison with the hydroponic (HP) results previously reported, although the number of grains is similar, their average weight is almost doubled. This is probably related with the toxicity induced by Se since, in hydroponics, even though the same concentration of Se is used, the absence of organic matter in the culture media permits the Se dosed to the media to be fully available for the plant and, therefore, the total Se accumulation strongly increases. Moreover, leaching of elements and transpiration of some volatile species is reduced in hydroponic system.

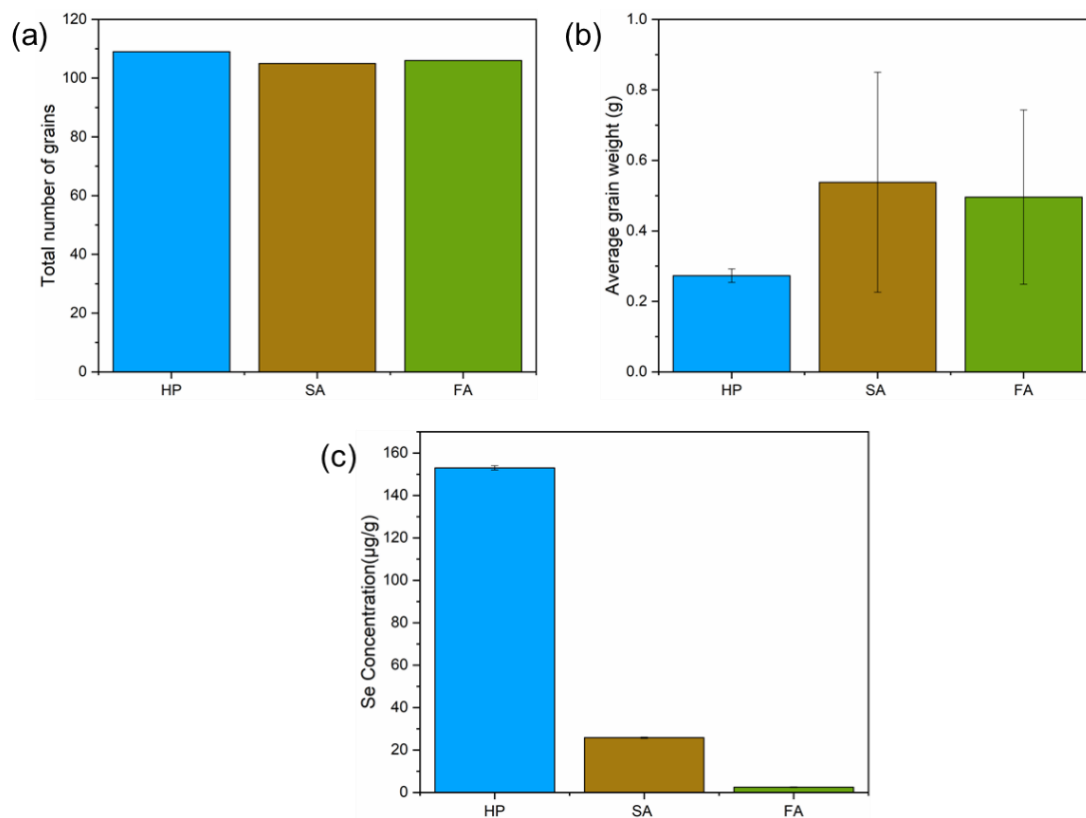


Figure 1: Grain production and Se concentration in grains obtained for the Semix treatment for the different cultivation methodologies used in this work: hydroponic (HP)-blue, Soil application (SA)-brown and Foliar application (FA)-green.

Plants accumulate substantially more Se by SA respect to FA. In SA, along the full plant, the Se accumulation is reduced by the  $\text{Se}^{4+}$  treatment. This is due to the fact that  $\text{Se}(\text{IV})$  is rapidly assimilated into organic forms which are retained in soils, while  $\text{Se}(\text{VI})$  is highly mobile. The Se TF from roots-to-grains in SA is enhanced, while from leaves-to-grains in FA it is reduced for  $\text{Se}^{6+}$  treatment. In both cases, the TF is below 1, indicating a poor Se translocation. The reported trends express the different Se pathways respect to plant metabolism. Micronutrients like Cu, Mn, Fe and Zn are involved in major enzymatic activity and their concentrations in the different parts of plants do not show drastic changes as a function of the Se treatment applied or the application method suggesting minor influences.

Se and S speciation has been addressed by XAS show large spectral differences at the different part of the plants as function of the Se species used for the treatment. However, for the grains, a similar spectral profile, resembling the one of the Se organic species, was observed for both SA and FA and for all the treatments.

Within SA group the grains contain only C–Se–C species (e.g. SeMet or SeMeCys, and SeCys), while in the case of FA a minor fraction (around 10%) of C–Se–Se–C species (e.g. SeCyst) is present. Since the C–Se–C species are more bioavailable for humans, the above reported results show that the Se biofortification via SA is more efficient than in FA in terms of the produced health benefits.

A minor Se(VI) component appeared in grains for the treatments containing  $\text{Se}^{6+}$  and it is more pronounced for SA. In all the other part of the plants and for both application methods, the Se(VI) species is dominating the spectral profile as soon as  $\text{Se}^{6+}$  is present in the treatment. The tendency of and increased Se(VI) presence in shoots is probably due to the plant detoxification mechanism, which tend to oxidize Se to reduce its potential toxicity. The S species do not significantly change when varying the Se treatment or the application method, and show the coexistence of organic and highly oxidised S species.

The Se species distribution in the grain has been characterized only for SA method shows SeMeCys is the major component in all the regions, except the eye, where a similar amount of SeMet is found (50%). In the endosperm, SeMet is present only for the  $\text{Se}^{4+}$  treatment (20%). In the bran SeMet is around the 10% and looks suppressed with  $\text{Se}^{6+}$  treatment. Finally, in the filament SeMet is around the 20% irrespectively of the Se treatment applied. Se(VI) is present everywhere in small amount (below the 10%) as  $\text{Se}^{6+}$  is included in the treatment.

From the previously reported results, it is possible to expect a different Se species formation in the grains as soon as the total Se accumulation increases. Indeed, in the hydroponic (HP) case, six times more Se accumulation in the grains was corresponding to the formation of 73% of SeMet and 37% of SeCyst distributed mainly in the eye and in the bran, respectively. Since the SeCyst is less desirable in terms of Se health benefits respect to SeMet and SeMeCys, attention should be paid to tune the formation of the most desirable Se organic species.

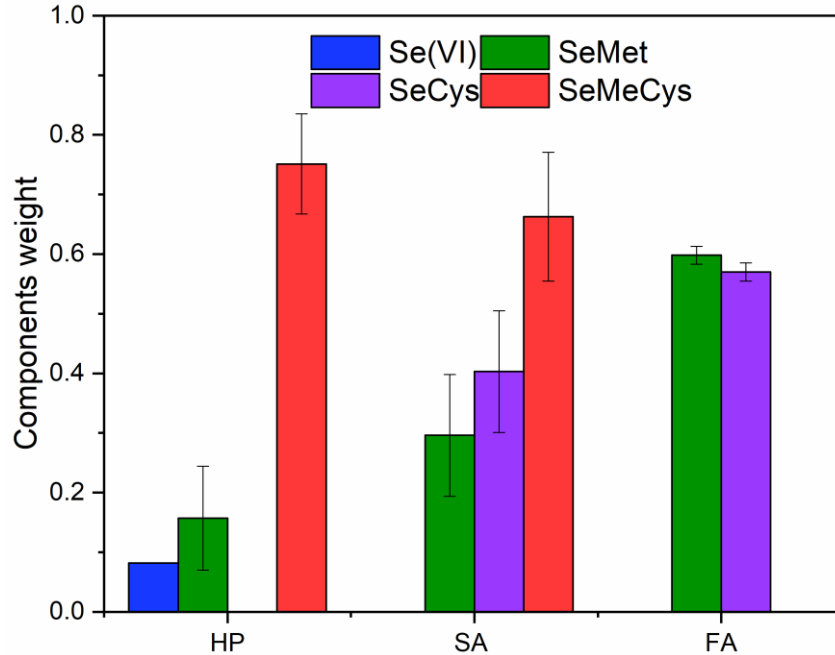


Figure 2: Se species in grains for Semix treatment for different cultivation methodologies used in this work: hydroponic (HP), Soil application (SA) and Foliar application (FA). Se species Se(VI)-blue; SeMet- green; SeCys-violet; SeMeCys-red.

The S species spatial distribution has been obtained for both SA and FA grains. While the S organic species resulted mainly concentrated in bran region and in the filament, the higher S oxidation species appeared to be predominant in the endosperm, irrespectively of the Se treatment or application method. Instead, similar to the hydroponic case, the grain FTIR results show that the presence of amide protein, which could be linked to seleno aminoacid, varies little in the endosperm depending upon the treatments and the application method. The difference obtained by comparing the endosperm and bran spectra reflects differences in the proteins present in these two regions. In any case, the results do not permit to easily correlate to Se proteins, subject of the present study.

Our results shows that the Se accumulation process is more efficient in the case of SA than the FA, being Se better up taken by the plant from the soil in the form of  $\text{Se}^{6+}$ , and considering that only a minor fraction of Se(VI) can be expected to co-exist in the grains together with the desired organic species.

## References

2020(EU), E., n.d. Annual Crop Statistics Handbook (2020).

Adamczyk-Szabela, D., Lisowska, K., Romanowska-Duda, Z., Wolf, W.M., 2020. Combined cadmium-zinc interactions alter manganese, lead, copper uptake by *Melissa officinalis*. *Sci. Reports* 2020 101 10, 1–10. <https://doi.org/10.1038/s41598-020-58491-9>

Affholder, M.-C., Flöhr, A., Kirchmann, H., 2019. Can Cd content in crops be controlled by Se fertilization? A meta-analysis and outline of Cd sequestration mechanisms. *Plant Soil* 2019 4401 440, 369–380. <https://doi.org/10.1007/S11104-019-04078-X>

Álvarez-Fernández, A., Díaz-Benito, P., Abadía, A., López Millán, A.F., Abadía, J., 2014. Metal species involved in long distance metal transport in plants. *Front. Plant Sci.* 5, 1–20. <https://doi.org/10.3389/fpls.2014.00105>

Andrews, J.C., 2006. Mercury Speciation in the Environment Using X-ray Absorption Spectroscopy. In: Atwood D.A. (eds) *Recent Developments in Mercury Science*, in: *Structure and Bonding*. pp. 1–35. [https://doi.org/10.1007/430\\_011](https://doi.org/10.1007/430_011)

Angulo-Bejarano, P.I., Puente-Rivera, J., Cruz-Ortega, R., 2021. Metal and Metalloid Toxicity in Plants: An Overview on Molecular Aspects. *Plants* 10, 635. <https://doi.org/10.3390/PLANTS10040635>

Appels, R., Eversole, K., Feuillet, C., Keller, B., Rogers, J., Stein, N., Pozniak, C.J., Choulet, F., Distelfeld, A., Poland, J., Ronen, G., Barad, O., Baruch, K., Keeble-Gagnère, G., Mascher, M., Ben-Zvi, G., Josselin, A.A., Himmelbach, A., Balfourier, F., Gutierrez-Gonzalez, J., Hayden, M., Koh, C.S., Muehlbauer, G., Pasam, R.K., Paux, E., Rigault, P., Tibbits, J., Tiwari, V., Spannagl, M., Lang, D., Gundlach, H., Haberer, G., Mayer, K.F.X., Ormanbekova, D., Prade, V., Wicker, T., Swarbreck, D., Rimbart, H., Felder, M., Guilhot, N., Kaithakottil, G., Keilwagen, J., Leroy, P., Lux, T., Twardziok, S., Venturini, L., Juhasz, A., Abrouk, M., Fischer, I., Uauy, C., Borrill, P., Ramirez-Gonzalez, R.H., Arnaud, D., Chalabi, S., Chalhoub, B., Cory, A., Datla, R., Davey, M.W., Jacobs, J., Robinson, S.J., Steuernagel, B., Van Ex, F., Wulff, B.B.H., Benhamed, M., Bendahmane, A., Concia, L., Latrasse, D., Alaux, M., Bartoš, J., Bellec, A., Berges, H., Doležal, J., Frenkel, Z., Gill, B., Korol, A., Letellier, T., Olsen, O.A., Šimková, H., Singh, K., Valárik, M.,

Van Der Vossen, E., Vautrin, S., Weining, S., Fahima, T., Glikson, V., Raats, D., Toegelová, H., Vrána, J., Sourdille, P., Darrier, B., Barabaschi, D., Cattivelli, L., Hernandez, P., Galvez, S., Budak, H., Jones, J.D.G., Witek, K., Yu, G., Small, I., Melonek, J., Zhou, R., Belova, T., Kanyuka, K., King, R., Nilsen, K., Walkowiak, S., Cuthbert, R., Knox, R., Wiebe, K., Xiang, D., Rohde, A., Golds, T., Čížková, J., Akpınar, B.A., Biyiklioglu, S., Gao, L., N'Daiye, A., Číhalíková, J., Kubaláková, M., Šafář, J., Alfama, F., Adam-Blondon, A.F., Flores, R., Guerche, C., Loaec, M., Quesneville, H., Sharpe, A.G., Condie, J., Ens, J., Maclachlan, R., Tan, Y., Alberti, A., Aury, J.M., Barbe, V., Couloux, A., Cruaud, C., Labadie, K., Mangenot, S., Wincker, P., Kaur, G., Luo, M., Sehgal, S., Chhuneja, P., Gupta, O.P., Jindal, S., Kaur, P., Malik, P., Sharma, P., Yadav, B., Singh, N.K., Khurana, J.P., Chaudhary, C., Khurana, P., Kumar, V., Mahato, A., Mathur, S., Sevanthi, A., Sharma, N., Tomar, R.S., Holušová, K., Plíhal, O., Clark, M.D., Heavens, D., Kettleborough, G., Wright, J., Balcárková, B., Hu, Y., Ravin, N., Skryabin, K., Beletsky, A., Kadnikov, V., Mardanov, A., Nesterov, M., Rakitin, A., Sergeeva, E., Kanamori, H., Katagiri, S., Kobayashi, F., Nasuda, S., Tanaka, T., Wu, J., Cattonaro, F., Jiumeng, M., Kugler, K., Pfeifer, M., Sandve, S., Xun, X., Zhan, B., Batley, J., Bayer, P.E., Edwards, D., Hayashi, S., Tulpová, Z., Visendi, P., Cui, L., Du, X., Feng, K., Nie, X., Tong, W., Wang, L., 2018. Shifting the limits in wheat research and breeding using a fully annotated reference genome. *Science* (80- ). 361. <https://doi.org/10.1126/science.aar7191>

Arif, N., Yadav, V., Singh, Shweta, Singh, Swati, Ahmad, P., Mishra, R.K., Sharma, S., Tripathi, D.K., Dubey, N.K., Chauhan, D.K., 2016. Influence of high and low levels of plant-beneficial heavy metal ions on plant growth and development. *Front. Environ. Sci.* 4. <https://doi.org/10.3389/fenvs.2016.00069>

Arnon, D.I., Hoagland, D.R., 1940. Crop production in artificial culture solutions and in soils with special reference to factors influencing yields and absorption of inorganic nutrients. *Soil Sci.* 50, 463–485.

Boldrin, P.F., de Figueiredo, M.A., Yang, Y., Luo, H., Giri, S., Hart, J.J., Faquin, V., Guilherme, L.R.G., Thannhauser, T.W., Li, L., 2016. Selenium promotes sulfur accumulation and plant growth in wheat (*Triticum aestivum*). *Physiol. Plant.* 158, 80–91. <https://doi.org/10.1111/ppl.12465>

Boyd, R., 2011. Selenium stories, Nature Publishing Group. <https://doi.org/10.1038/nchem.1076>

Brisson, N., Gate, P., Gouache, D., Charmet, G., Oury, F. X., & Huard, F. (2010). Why are wheat yields stagnating in Europe? A comprehensive data analysis for France. *Field Crops Research*, 119(1), 201–212. <https://doi.org/10.1016/j.fcr.2010.07.012>

Brown, K.M., Arthur, J.R., 2021. Selenium, selenoproteins and human health: a review. <https://doi.org/10.1079/PHN2001143>

Brown, T.A., Shrift, A., 1982. SELENIUM: TOXICITY AND TOLERANCE IN HIGHER PLANTS. *Biol. Rev.* 57, 59–84. <https://doi.org/10.1111/j.1469-185X.1982.tb00364.x> Buchner, P., Takahashi, H., Hawkesford, M.J., 2004. Plant sulphate transporters: co-ordination of uptake, intracellular and long-distance transport. *J. Exp. Bot.* 55, 1765–1773. <https://doi.org/10.1093/JXB/ERH206>

Chang, C., Chen, C., Yin, R., Shen, Y., Mao, K., Yang, Z., Feng, X., Zhang, H., 2020. Bioaccumulation of Hg in Rice Leaf Facilitates Selenium Bioaccumulation in Rice (*Oryza sativa* L.) Leaf in the Wanshan Mercury Mine. *Environ. Sci. Technol.* 54, 3228–3236. <https://doi.org/10.1021/acs.est.9b06486>

Chen, L., Yang, F., Xu, J., Hu, Y., Hu, Q., Zhang, Y., Pan, G., 2002. Determination of selenium concentration of rice in China and effect of fertilization of selenite and selenate on selenium content of rice. *J. Agric. Food Chem.* 50, 5128–5130. <https://doi.org/10.1021/jf0201374>

Chen ShanShan, ; Z.C., ; Z.Q., ; F.M., XiaoBi, S., 2009. Study on interaction between selenium and mercury in the seedling stage of winter wheat. [WWW Document]. *Guizhou Agric. Sci.* No.1 ref.9. URL <https://www.cabdirect.org/cabdirect/abstract/20093135070> (accessed 4.11.21).

Ciaffi, M., Paolacci, A.R., Celletti, S., Catarcione, G., Kopriva, S., Astolfi, S., 2013. Transcriptional and physiological changes in the S assimilation pathway due to single or combined S and Fe deprivation in durum wheat (*Triticum durum* L.) seedlings. *J. Exp. Bot.* 64, 1663–1675. <https://doi.org/10.1093/JXB/ERT027>

Commission Regulation (EC) No 1881/2006, n.d. Official Journal of the European Union L 364. ISSN 1725-2555.



Council Directive 86/278/EEC of 12 June 1986, n.d. Official Journal of the European Communities, L 181, 4 July 1986.

Cui, J., Liu, T., Li, Y., Li, F., 2018. Selenium reduces cadmium uptake into rice suspension cells by regulating the expression of lignin synthesis and cadmium-related genes. *Sci. Total Environ.* 644, 602–610. <https://doi.org/10.1016/J.SCITOTENV.2018.07.002>

Curtin, D., Hanson, R., Lindley, T.N., Butler, R.C., 2006. Selenium concentration in wheat (*Triticum aestivum*) grain as influenced by method, rate, and timing of sodium selenate application. *New Zeal. J. Crop Hortic. Sci.* 34, 329–339. <https://doi.org/10.1080/01140671.2006.9514423>

Curtin, D., Hanson, R., Van Der Weerden, T.J., 2008. Effect of selenium fertiliser formulation and rate of application on selenium concentrations in irrigated and dryland wheat (*Triticum Aestivum*). *New Zeal. J. Crop Hortic. Sci.* 36, 1–7. <https://doi.org/10.1080/01140670809510216>

Cuvin-Aralar, M.L.A., Furness, R.W., 1991. Mercury and selenium interaction: A review. *Ecotoxicol. Environ. Saf.* 21, 348–364. [https://doi.org/10.1016/0147-6513\(91\)90074-Y](https://doi.org/10.1016/0147-6513(91)90074-Y)

Dall'acqua, S., Ertani, A., Pilon-Smits, E.A.H., Fabrega-Prats, M., Schiavon, M., 2019. Selenium Biofortification Differentially Affects Sulfur Metabolism and Accumulation of Phytochemicals in Two Rocket Species (*Eruca Sativa* Mill. and *Diplotaxis Tenuifolia*) Grown in Hydroponics. <https://doi.org/10.3390/plants8030068>

Dang, F., Li, Z., Zhong, H., 2019. Methylmercury and selenium interactions: Mechanisms and implications for soil remediation. *Crit. Rev. Environ. Sci. Technol.* 49, 1737–1768. <https://doi.org/10.1080/10643389.2019.1583051>

de Oliveira, V.C., Faquin, V., Guimarães, K.C., Andrade, F.R., Pereira, J., Guilherme, L.R.G., 2018. Agronomic biofortification of carrot with selenium. *Cienc. e Agrotecnologia* 42, 138–147. <https://doi.org/10.1590/1413-70542018422031217>

Dinh, Q.T., Li, Z., Tran, T.A.T., Wang, D., Liang, D., 2017. Role of organic acids on the bioavailability of selenium in soil: A review. *Chemosphere* 184, 618–635. <https://doi.org/10.1016/j.chemosphere.2017.06.034>

- Dong, Q., Hu, S., Fei, L., Liu, L., Wang, Z., 2019. Interaction between Cd and Zn on Metal Accumulation, Translocation and Mineral Nutrition in Tall Fescue (*Festuca arundinacea*). *Int. J. Mol. Sci.* 2019, Vol. 20, Page 3332 20, 3332. <https://doi.org/10.3390/IJMS20133332>
- Dubey, S., Shri, M., Gupta, A., Rani, V., Chakrabarty, D., 2018. Toxicity and detoxification of heavy metals during plant growth and metabolism. *Environ. Chem. Lett.* 16, 1169–1192. <https://doi.org/10.1007/s10311-018-0741-8>
- EFSA Journal 2017;14(3):4442, 2017. Safety and efficacy of selenium compounds (E8) as feed additives for all animal species: Sodium selenite, based on a dossier submitted by Todini and Co SpA. *EFSA J.* 14. <https://doi.org/10.2903/j.efsa.2016.4442>
- Ellis, D.R., Salt, D.E., 2003. Plants, selenium and human health. *Curr. Opin. Plant Biol.* [https://doi.org/10.1016/S1369-5266\(03\)00030-X](https://doi.org/10.1016/S1369-5266(03)00030-X)
- Esdaile, L.J., Chalker, J.M., 2018. The Mercury Problem in Artisanal and Small-Scale Gold Mining. *Chem. - A Eur. J.* 24, 6905–6916. <https://doi.org/10.1002/chem.201704840>
- Eurostat, 2020. Annual Crop Statistics Handbook (2020).
- Faheem Maqbool, Haji, B., Mohammad, A., 2014. Exposure to mercury from dental amalgams: a threat to society. *Mercur. Dent. amalgams* 69, 339–340.
- Fernández-Martínez, A., Charlet, L., 2009. Selenium environmental cycling and bioavailability: A structural chemist point of view. *Rev. Environ. Sci. Biotechnol.* 8, 81–110. <https://doi.org/10.1007/S11157-009-9145-3>
- Fortmann L.C., Gay. D.D, Wirtz K.O, 1978. Ethylmercury: formation in plant tissues and relation to methylmercury formation.
- Fox, T., Van den Heuvel, E., Atherton, C., Dainty, J., Lewis, D., Langford, N., Crews, H., Lutén, J., Lorentzen, M., Sieling, F., van Aken-Schneyder, P., Hoek, M., Kotterman, M., van Dael, P., Fairweather-Tait, S., 2004. ORIGINAL COMMUNICATION Bioavailability of selenium from fish, yeast and selenate: a comparative study in humans using stable isotopes. *Eur. J. Clin. Nutr.* 58, 343–349. <https://doi.org/10.1038/sj.ejcn.1601787>

- Gailer, J., George, G.N., Pickering, I.J., Madden, S., Prince, R.C., Yu, E.Y., Denton, M.B., Younis, H.S., Aposhian, H. V., 2000. Structural basis of the antagonism between inorganic mercury and selenium in mammals. *Chem. Res. Toxicol.* 13, 1135–1142. <https://doi.org/10.1021/tx000050h>
- Gaudet, M., Pietrini, F., Beritognolo, I., Iori, V., Zacchini, M., Massacci, A., Mugnozza, G.S., Sabatti, M., 2011. Intraspecific variation of physiological and molecular response to cadmium stress in *Populus nigra* L. *Tree Physiol.* 31, 1309–1318. <https://doi.org/10.1093/TREEPHYS/TPR088>
- George, G.N., MacDonald, T.C., Korbas, M., Singh, S.P., Myers, G.J., Watson, G.E., O'Donoghue, J.L., Pickering, I.J., 2011. The chemical forms of mercury and selenium in whale skeletal muscle. *Metallomics* 3, 1232–1237. <https://doi.org/10.1039/c1mt00077b>
- Gigolashvili, T., Kopriva, S., 2014. Transporters in plant sulfur metabolism. *Front. Plant Sci.* 5. <https://doi.org/10.3389/FPLS.2014.00442>
- Gissel-Nielsen, G., Gupta, U.C., Lamand, M., Westermarck, T., 1984. Selenium in soils and plants and its importance in livestock and human nutrition. *Adv. Agron.* 397-460.
- Guerrero, B., Llugany, M., Palacios, O., Valiente, M., 2014. Dual effects of different selenium species on wheat. *Plant Physiol. Biochem.* 83, 300–307. <https://doi.org/10.1016/j.plaphy.2014.08.009>
- Gupta, M., Gupta, S., 2017. An Overview of Selenium Uptake, Metabolism, and Toxicity in Plants. *Front. Plant Sci.* 7, 2074. <https://doi.org/10.3389/FPLS.2016.02074>
- Harada, E., Yamaguchi, Y., Koizumi, N., Hiroshi, S., 2002. Cadmium stress induces production of thiol compounds and transcripts for enzymes involved in sulfur assimilation pathways in *Arabidopsis*. *J. Plant Physiol.* 159, 445–448. <https://doi.org/10.1078/0176-1617-00733>
- Hawkesford, M.J., Zhao, F.J., 2007. Strategies for increasing the selenium content of wheat. *J. Cereal Sci.* 46, 282–292. <https://doi.org/10.1016/J.JCS.2007.02.006>
- Hou, W., Chen, X., Song, G., Wang, Q., Chang, C., 2006. Effects of copper and cadmium on heavy metal polluted waterbody restoration by duckweed (*Lemna minor*). <https://doi.org/10.1016/j.plaphy.2006.12.005>

Huang, B., Xin, J., Dai, H., Zhou, W., 2017. Effects of Interaction between Cadmium (Cd) and Selenium (Se) on Grain Yield and Cd and Se Accumulation in a Hybrid Rice (*Oryza sativa*) System. *J. Agric. Food Chem.* 65, 9537–9546. <https://doi.org/10.1021/acs.jafc.7b03316>

Huang, Q.Q., Wang, Q., Wan, Y.N., Yu, Y., Jiang, R.F., Li, H.F., 2017. Application of X-ray absorption near edge spectroscopy to the study of the effect of sulphur on selenium uptake and assimilation in wheat seedlings. *Biol. Plant.* 61, 726–732. <https://doi.org/10.1007/s10535-016-0698-z>

Humaira, K.T., 2016. Sources and Effect of Mercury on Human Health : A Review.

Hylander, L.D., Goodsite, M.E., 2006. Environmental costs of mercury pollution. *Sci. Total Environ.* 368, 352–370. <https://doi.org/10.1016/j.scitotenv.2005.11.029>

I. Saidi, N. Nawel, W. Djebali, 2014. Role of selenium in preventing manganese toxicity in sunflower (*Helianthus annuus*) seedling | Elsevier Enhanced Reader. *south african J. Bot.*

Ibrahim, S.R.M., Abdallah, H.M., El-Halawany, A.M., Mohamed, G.A., 2015. Naturally occurring thiophenes: isolation, purification, structural elucidation, and evaluation of bioactivities. *Phytochem. Rev.* 2015 152 15, 197–220. <https://doi.org/10.1007/S11101-015-9403-7>

Ismael, M.A., Mohamed Elyamine, A., Yuan Zhao, Y., Moussa, M.G., Shoaib Rana, M., Afzal, J., Imran, M., Hu Zhao, X., Xiao Hu, C., n.d. Can Selenium and Molybdenum Restrain Cadmium Toxicity to Pollen Grains in *Brassica napus*? <https://doi.org/10.3390/ijms19082163>

Jacob, C., Giles, G.I., Giles, N.M., Sies, H., 2003. Sulfur and Selenium: The Role of Oxidation State in Protein Structure and Function. *Angew. Chemie Int. Ed.* 42, 4742–4758. <https://doi.org/10.1002/ANIE.200300573>

Johri, N., Jacquillet, G., Unwin, R., 2010. Heavy metal poisoning: the effects of cadmium on the kidney. *BioMetals* 2010 235 23, 783–792. <https://doi.org/10.1007/S10534-010-9328-Y>

Karita, K., Sakamoto, M., Yoshida, M., Tatsuta, N., Nakai, K., Iwai-Shimada, M., Iwata, T., Maeda, E., Yaginuma-Sakurai, K., Satoh, H., Murata, K., 2016. Recent epidemiological studies on methylmercury, mercury and selenium. *Japanese J. Hyg.* 71, 236–251.

Kataoka, T., Watanabe-Takahashi, A., Hayashi, N., Ohnishi, M., Mimura, T., Buchner, P., Hawkesford, M.J., Yamaya, T., Takahashi, H., 2004. Vacuolar Sulfate Transporters Are Essential Determinants Controlling Internal Distribution of Sulfate in Arabidopsis. *Plant Cell* 16, 2693. <https://doi.org/10.1105/TPC.104.023960>

Khan, M.A.K., Wang, F., 2009. Mercury-selenium compounds and their toxicological significance: Toward a molecular understanding of the mercury-selenium antagonism. *Environ. Toxicol. Chem.* 28, 1567–1577. <https://doi.org/10.1897/08-375.1>

Kieliszek, M., 2019. Selenium-Fascinating Microelement, Properties and Sources in Food. *Molecules* 24, 1298. <https://doi.org/10.3390/molecules24071298>

Kleiber Tomasz, Krzesiński Włodzimierz, Przygocka-Cyna Katarzyna, Spizewski Tomasz, 2018. Alleviation Effect of Selenium on Manganese Stress of Plants - ProQuest. *Ecol. Chem. Eng.* 143–152.

Koller, L.D., Exon, J.H., 1986. The two faces of selenium-deficiency and toxicity--are similar in animals and man. *Can. J. Vet. Res.* 50, 297.

Krause, M.O., 1979. Atomic radiative and radiationless yields for K and L shells. *J. Phys. Chem. Ref. Data* 8, 307–327. <https://doi.org/10.1063/1.555594>

Krupp, E.M., Mestrot, A., Wielgus, J., Meharg, A.A., Feldmann, J., 2009. The molecular form of mercury in biota: identification of novel mercury peptide complexes in plantsw. <https://doi.org/10.1039/b823121d>

Kumari, N., Parmar, P., Sharma, V., 2015. Differential gene expression in two contrasting wheat cultivars under cadmium stress. *Biol. Plant.* 2015 594 59, 701–707. <https://doi.org/10.1007/S10535-015-0550-X>

Landberg, T., Greger, M., 1994. Influence of selenium on uptake and toxicity of copper and cadmium in pea (*Pisum sativum*) and wheat (*Triticum aestivum*). *Physiol. Plant.* 90, 637–644. <https://doi.org/10.1111/j.1399-3054.1994.tb02518.x>

Lara, T.S., Lessa, J.H. de L., de Souza, K.R.D., Corguinha, A.P.B., Martins, F.A.D., Lopes, G., Guilherme, L.R.G., 2019. Selenium biofortification of wheat grain via foliar application and its

effect on plant metabolism. *J. Food Compos. Anal.* 81, 10–18. <https://doi.org/10.1016/j.jfca.2019.05.002>

Li, H.-F., McGrath, S.P., Zhao, F.-J., 2008. Selenium uptake, translocation and speciation in wheat supplied with selenate or selenite. *New Phytol.* 178, 92–102. <https://doi.org/10.1111/j.1469-8137.2007.02343.x>

Li, H., Liu, X., Wassie, M., Chen, L., 2020. Selenium supplementation alleviates cadmium-induced damages in tall fescue through modulating antioxidant system, photosynthesis efficiency, and gene expression. *Environ. Sci. Pollut. Res.* 2020 279 27, 9490–9502. <https://doi.org/10.1007/S11356-019-06628-3>

Li, R., Wu, H., Ding, J., Fu, W., Gan, L., Li, Y., 2017. Mercury pollution in vegetables, grains and soils from areas surrounding coal-fired power plants. *Sci. Rep.* 7, 1–9. <https://doi.org/10.1038/srep46545>

Li, Y., Hu, W., Zhao, J., Chen, Q., Wang, W., Li, B., Li, Y.F., 2019. Selenium decreases methylmercury and increases nutritional elements in rice growing in mercury-contaminated farmland. *Ecotoxicol. Environ. Saf.* 182, 109447. <https://doi.org/10.1016/j.ecoenv.2019.109447>

Li, Y.F., Zhao, J., Li, Y.F., Li, H., Zhang, J., Li, B., Gao, Y., Chen, C., Luo, M., Huang, R., Li, J., 2015. The concentration of selenium matters: a field study on mercury accumulation in rice by selenite treatment in qingzhen, Guizhou, China. *Plant Soil* 391, 195–205. <https://doi.org/10.1007/s11104-015-2418-4>

Li, Z., Liang, D., Peng, Q., Cui, Z., Huang, J., Lin, Z., 2017. Interaction between selenium and soil organic matter and its impact on soil selenium bioavailability: A review. *Geoderma* 295, 69–79. <https://doi.org/10.1016/j.geoderma.2017.02.019>

Lidon, F.C., Oliveira, K., Galhano, C., Guerra, M., Ribeiro, M.M., Pelica, J., Pataco, I., Ramalho, J.C., Leitaõ, A.E., Almeida, A.N.A.S., Campos, P.S., Ribeiro-Barros, A.N.A.I., Pais, I.P., Silva, M.M., Carvalho, M.L., Santos, J.P., Pessoa, M.F., Reboredo, F.H., 2019. Selenium biofortification of rice through foliar application with selenite and selenate. *Exp. Agric.* 55, 528–542. <https://doi.org/10.1017/S0014479718000157>

- Liu, D., Wang, X., Chen, Z., Xu, H., Wang, Y., 2010. Influence of mercury on chlorophyll content in winter wheat and mercury bioaccumulation, *Plant, Soil and Environment*. <https://doi.org/10.17221/210/2009-PSE>
- Liu, W.X., Liu, J.W., Wu, M.Z., Li, Y., Zhao, Y., Li, S.R., 2009. Accumulation and translocation of toxic heavy metals in winter wheat (*Triticum aestivum* L.) growing in agricultural soil of Zhengzhou, China. *Bull. Environ. Contam. Toxicol.* 82, 343–347. <https://doi.org/10.1007/s00128-008-9575-6>
- Lyons, G., Stangoulis, J., Graham, R., 2003. High-selenium wheat: biofortification for better health. *Nutr. Res. Rev.* 16, 45. <https://doi.org/10.1079/nrr200255>
- Malagoli, M., Schiavon, M., dall'Acqua, S., Pilon-Smits, E.A.H., 2015. Effects of selenium biofortification on crop nutritional quality. *Front. Plant Sci.* 0, 280. <https://doi.org/10.3389/FPLS.2015.00280>
- Marini, C., Roqué-Rosell, J., Campeny, M., Toutouchiavval, S., Simonelli, L., IUCr, 2021. MAP2XANES: a Jupyter interactive notebook for elemental mapping and XANES speciation. *urn:issn:1600-5775* 28, 1245–1252. <https://doi.org/10.1107/S1600577521003593>
- Mehes-Smith, M., Nkongolo, K., Cholewa, E., 2013. Coping Mechanisms of Plants to Metal Contaminated Soil. *Environ. Chang. Sustain.* <https://doi.org/10.5772/55124>
- Meltzer, H.M., Bibow, K., Paulsen, I.T., Mundal, H.H., Norheim, G., Holm, H., 1993. Different bioavailability in humans of wheat and fish selenium as measured by blood platelet response to increased dietary Se. *Biol. Trace Elem. Res.* 36, 229–241. <https://doi.org/10.1007/BF02783957>
- Mendoza-Cózatl, D., Loza-Tavera, H., Hernández-Navarro, A., Moreno-Sánchez, R., 2005. Sulfur assimilation and glutathione metabolism under cadmium stress in yeast, protists and plants. *FEMS Microbiol. Rev.* <https://doi.org/10.1016/j.femsre.2004.09.004>
- Meng, B., Feng, X., Qiu, G., Liang, P., Li, P., Chen, C., Shang, L., 2011. The process of methylmercury accumulation in rice (*Oryza sativa* L.). *Environ. Sci. Technol.* 45, 2711–2717. <https://doi.org/10.1021/es103384v>

Motuzova, G. V., Minkina, T.M., Karpova, E.A., Barsova, N.U., Mandzhieva, S.S., 2014. Soil contamination with heavy metals as a potential and real risk to the environment. *J. Geochemical Explor.* 144, 241–246. <https://doi.org/10.1016/J.GEXPLO.2014.01.026>

Navarro, A., Biester, H., Mendoza, J.L., Cardellach, E., 2006. Mercury speciation and mobilization in contaminated soils of the Valle del Azogue Hg mine (SE, Spain). *Environ. Geol.* 49, 1089–1101. <https://doi.org/10.1007/s00254-005-0152-6>

Nica, A., Popescu, A., Ibănescu, D.C., 2017. A Current Problem : Mercury Pollution. *Curr. Trends Nat. Sci.* 6, 165–169.

Nocito, F.F., Lancilli, C., Giacomini, B., Sacchi, G.A., 2007. Sulfur Metabolism and Cadmium Stress in Higher Plants . *Plant Stress* 1, 142–156.

Ottesen, R.T., Birke, M., Finne, T.E., Gosar, M., Locutura, J., Reimann, C., Tarvainen, T., Albanese, S., Andersson, M., Arnoldussen, A., Batista, M.J., Bel-lan, A., Cicchella, D., Demetriades, A., Dinelli, E., De Vivo, B., De Vos, W., Duris, M., Dusza, A., Eggen, O.A., Eklund, M., Ernstsén, V., Filzmoser, P., Flight, D., Fuchs, M., Fugedi, U., Gilucis, A., Gregorauskiene, V., Gulán, A., Halamić, J., Haslinger, E., Hayoz, P., Hoffmann, R., Hoogewerff, J., Hrvatovic, H., Husnjak, S., Johnson, C.C., Jordan, G., Kaste, L., Keilert, B., Kivisilla, J., Klos, V., Krone, F., Kwecko, P., Kutí, L., Ladenberger, A., Lima, A., Lucivjansky, D.P., Mackovych, D., Malyuk, B.I., Maquil, R., McDonnell, P., Meuli, R.G., Miosic, N., Mol, G., Négrel, P., O'Connor, P., Pasieczna, A., Petersell, W., Poňavič, M., Pramuka, S., Prazeres, C., Rauch, U., Reitner, H., Sadeghi, M., Salpeteur, I., Samardzic, N., Schedl, A., Scheib, A., Schoeters, I., Sefcik, P., Skopljak, F., Slaninka, I., Šorša, A., Stafilov, T., Sellersjö, E., Trendavilov, V., Valera, P., Verougstraete, V., Vidojević, D., Zomeni, Z., 2013. Mercury in European agricultural and grazing land soils. *Appl. Geochemistry* 33, 1–12. <https://doi.org/10.1016/j.apgeochem.2012.12.013>

Pedrero, Z., Madrid, Y., Hartikainen, H., Cámara, C., 2007. Protective Effect of Selenium in Broccoli ( Brassica oleracea) Plants Subjected to Cadmium Exposure. *J. Agric. Food Chem.* 56, 266–271. <https://doi.org/10.1021/JF072266W>



Pickering, I.J., George, G.N., Van Fleet-Slалder, V., Chasteen, T.G., Prince, R.C., 1999. X-ray absorption spectroscopy of selenium-containing amino acids. *J. Biol. Inorg. Chem.* 4, 791–794. <https://doi.org/10.1007/s007750050352>

Poblaciones M.J, Rodrigo S., Santamaria O., Chen Y., McGrath S.P., n.d. Elsevier Enhanced Reader Agronomic selenium biofortification in *Triticum durum* under Mediterranean conditions: From grain to cooked pasta.

Proux, O., Lahera, E., Del Net, W., Kieffer, I., Rovezzi, M., Testemale, D., Irar, M., Thomas, S., Aguilar-Tapia, A., Bazarkina, E.F., Prat, A., Tella, M., Auffan, M., Rose, J., Hazemann, J.-L., 2017. High-Energy Resolution Fluorescence Detected X-Ray Absorption Spectroscopy: A Powerful New Structural Tool in Environmental Biogeochemistry Sciences. *J. Environ. Qual.* 46, 1146–1157. <https://doi.org/10.2134/jeq2017.01.0023>

Punshon, T., Jackson, B.P., 2018. Essential micronutrient and toxic trace element concentrations in gluten containing and gluten-free foods. *Food Chem.* 252, 258–264. <https://doi.org/10.1016/j.foodchem.2018.01.120>

Qin, H.B., Zhu, J.M., Lin, Z.Q., Xu, W.P., Tan, D.C., Zheng, L.R., Takahashi, Y., 2017. Selenium speciation in seleniferous agricultural soils under different cropping systems using sequential extraction and X-ray absorption spectroscopy. *Environ. Pollut.* 225, 361–369. <https://doi.org/10.1016/j.envpol.2017.02.062>

Ravel, B., Newville, M., 2005. ATHENA, ARTEMIS, HEPHAESTUS: Data analysis for X-ray absorption spectroscopy using IFEFFIT, in: *Journal of Synchrotron Radiation*. International Union of Crystallography, pp. 537–541. <https://doi.org/10.1107/S0909049505012719>

Rayman, M.P., 2000. The importance of selenium to human health. *Lancet.* [https://doi.org/10.1016/S0140-6736\(00\)02490-9](https://doi.org/10.1016/S0140-6736(00)02490-9)

Rey, P., Tarrago, L., 2018. Physiological Roles of Plant Methionine Sulfoxide Reductases in Redox Homeostasis and Signaling. *Antioxidants* 7. <https://doi.org/10.3390/ANTIOX7090114>

Robertsa, T.L., 2014. Cadmium and phosphorous fertilizers: The issues and the science, in: *Procedia Engineering*. Elsevier Ltd, pp. 52–59. <https://doi.org/10.1016/j.proeng.2014.09.012>

Roman, M., Jitaru, P., Barbante, C., 2013. Selenium biochemistry and its role for human health. *Metallomics* 6, 25–54. <https://doi.org/10.1039/C3MT00185G>

Ros, G.H., van Rotterdam, A.M.D., Bussink, D.W., Bindraban, P.S., 2016. Selenium fertilization strategies for bio-fortification of food: an agro-ecosystem approach. *Plant Soil* 404, 99–112. <https://doi.org/10.1007/s11104-016-2830-4>

Rüdiger Hell, Christiane Dahl, David B. Knaff, Thomas Leuste, n.d. Sulfur Metabolism in Phototrophic Organisms [WWW Document]. URL <https://books.google.es/books?id=atZa653rcsEC&pg=PA239&lpg=PA239&dq=OASTL+gene&source=bl&ots=SCac6VHxM-&sig=ACfU3U10jJkE5tEj68PvsbZr7TaYKaxMzA&hl=en&sa=X&ved=2ahUKEwiy0M779-fxAhU0olwKHZhvBKoQ6AEwCHoECAoQAw#v=onepage&q=OASTLgene&f=false> (accessed 7.22.21).

Sahu, G.K., Upadhyay, S., Sahoo, B.B., 2012. Mercury induced phytotoxicity and oxidative stress in wheat (*Triticum aestivum* L.) plants. *Physiol. Mol. Biol. Plants* 18, 21–31. <https://doi.org/10.1007/s12298-011-0090-6>

Samargandi, D., Zhang, X., Liu, F., Tian, S., 2014. Fourier Transform Infrared (FT-IR) Spectroscopy for discrimination of fenugreek seeds from different producing areas. Available online [www.jocpr.com](http://www.jocpr.com) *J. Chem. Pharm. Res.* 6, 19–24.

Sambo, P., Nicoletto, C., Giro, A., Pii, Y., Valentinuzzi, F., Mimmo, T., Lugli, P., Orzes, G., Mazzetto, F., Astolfi, S., Terzano, R., & Cesco, S. (2019). Hydroponic Solutions for Soilless Production Systems: Issues and Opportunities in a Smart Agriculture Perspective. *Frontiers in Plant Science*, 10(July). <https://doi.org/10.3389/fpls.2019.00923>

Sánchez-Báscones, M., Antolín-Rodríguez, J.M., Martín-Ramos, P., González-González, A., Bravo-Sánchez, C.T., Martín-Gil, J., 2017. Evolution of mercury content in agricultural soils due to the application of organic and mineral fertilizers. *J. Soils Sediments* 17, 927–935. <https://doi.org/10.1007/s11368-016-1622-z>

Schiavon, M., Berto, C., Malagoli, M., Trentin, A., Sambo, P., Dall'Acqua, S., Pilon-Smits, E.A.H., 2016. Selenium biofortification in radish enhances nutritional quality via accumulation of

methyl-selenocysteine and promotion of transcripts and metabolites related to glucosinolates, phenolics amino acids. *Front. Plant Sci.* 7. <https://doi.org/10.3389/fpls.2016.01371>

Schiavon, M., Nardi, S., dalla Vecchia, F., Ertani, A., 2020. Selenium biofortification in the 21st century: status and challenges for healthy human nutrition. *Plant Soil.* <https://doi.org/10.1007/s11104-020-04635-9>

Shamberger, R.J., 1983. Environmental Occurrence of Selenium, in: *Biochemistry of Selenium.* Springer US, pp. 167–183. [https://doi.org/10.1007/978-1-4684-4313-4\\_6](https://doi.org/10.1007/978-1-4684-4313-4_6)

Shanker, K., Mishra, S., Srivastava, S., Srivastava, R., Dass, S., Prakash, S., Srivastava, M.M., 1996. Study of mercury-selenium (Hg-Se) interactions and their impact on Hg uptake by the radish (*Raphanus sativus*) plant. *Food Chem. Toxicol.* 34, 883–886. [https://doi.org/10.1016/S0278-6915\(96\)00047-6](https://doi.org/10.1016/S0278-6915(96)00047-6)

Shanker, K., Mishra, S., Srivastava, S., Srivastava, R., Dass, S., Prakash, S., Srivastava, M.M., 1995. Chemical Speciation & Bioavailability Effect of selenite and selenate on plant uptake of cadmium by kidney bean (*Phaseolus mungo*) with reference to Cd-Se interaction Effect of selenite and selenate on plant uptake of cadmium by kidney bean (*Phaseolus mungo*) with reference to Cd-Se interaction. *Chem. Speciat. Bioavailab.* 7. <https://doi.org/10.1080/09542299.1995.11083251>

Sharma, B.M., Sáňka, O., Kalina, J., Scheringer, M., 2019. An overview of worldwide and regional time trends in total mercury levels in human blood and breast milk from 1966 to 2015 and their associations with health effects. *Environ. Int.* <https://doi.org/10.1016/j.envint.2018.12.016>

Sharma, S., Singh, R., 1983. Selenium in Soil, Plant, and Animal Systems. *C R C Crit. Rev. Environ. Control* 13, 23–50. <https://doi.org/10.1080/10643388309381701>

Shewry, W.P.R., 2009. DARWIN REVIEW. *J. Exp. Bot.* 60, 1537–1553. <https://doi.org/10.1093/jxb/erp058>

Shinmachi, F., Buchner, P., Stroud, J.L., Parmar, S., Zhao, F.J., Mcgrath, S.P., Hawkesford, M.J., 2010. Influence of sulfur deficiency on the expression of specific sulfate transporters and the distribution of sulfur, selenium, and molybdenum in wheat. *Plant Physiol.* 153, 327–336. <https://doi.org/10.1104/pp.110.153759>

- Shumaker, K.L., Begonia, G., 2005. Heavy metal uptake, translocation, and bioaccumulation studies of *Triticum aestivum* cultivated in contaminated dredged materials. *Int. J. Environ. Res. Public Health* 2, 293–298. <https://doi.org/10.3390/ijerph2005020013>
- Siegel, S.M., Puerner, N.J., Speitel, T.W., 1974. Release of Volatile Mercury from Vascular Plants. *Physiol. Plant.* 32, 174–176. <https://doi.org/10.1111/j.1399-3054.1974.tb03748.x>
- Simonelli, L., Marini, C., Olszewski, W., Avila Perez, M., Ramanan, N., Guilera, G., Cuartero, V., Klementiev, K., 2016. CLÆSS: The hard X-ray absorption beamline of the ALBA CELLS synchrotron. *Cogent Phys.* 3. <https://doi.org/10.1080/23311940.2016.1231987>
- Singh, B.R., Timsina, Y.N., Lind, O.C., Cagno, S., Janssens, K., 2018. Zinc and Iron Concentration as Affected by Nitrogen Fertilization and Their Localization in Wheat Grain. *Front. Plant Sci.* 0, 307. <https://doi.org/10.3389/FPLS.2018.00307>
- Singh, S., Parihar, P., Singh, R., Singh, V.P., Prasad, S.M., 2016. Heavy metal tolerance in plants: Role of transcriptomics, proteomics, metabolomics, and ionomics. *Front. Plant Sci.* 6, 1–36. <https://doi.org/10.3389/fpls.2015.01143>
- Soils - Randall J. Schaetzl, Michael L. Thompson - Google Books [WWW Document], n.d. URL [https://books.google.es/books?hl=en&lr=&id=u-BwBwAAQBAJ&oi=fnd&pg=PR1&dq=Soils&ots=YkNA8ce73R&sig=RzRJ5E3u0JVxDEQoUhccWaicrCE&redir\\_esc=y#v=onepage&q&f=false](https://books.google.es/books?hl=en&lr=&id=u-BwBwAAQBAJ&oi=fnd&pg=PR1&dq=Soils&ots=YkNA8ce73R&sig=RzRJ5E3u0JVxDEQoUhccWaicrCE&redir_esc=y#v=onepage&q&f=false) (accessed 7.5.21).
- Sors, T.G., Ellis, D.R., Salt, D.E., 2005. Selenium uptake, translocation, assimilation and metabolic fate in plants. *Photosynth. Res.* 86, 373–389. <https://doi.org/10.1007/s11120-005-5222-9>
- Subirana, M.M.A., 2018. Selenium biofortification of wheat: Distribution and spatially resolved selenium speciation by synchrotron-based techniques. Universitat Autònoma de Barcelona.
- Sysalová, J., Kučera, J., Drtinová, B., Červenka, R., Zvěřina, O., Komárek, J., Kameník, J., 2017. Mercury species in formerly contaminated soils and released soil gases. *Sci. Total Environ.* 584–585, 1032–1039. <https://doi.org/10.1016/j.scitotenv.2017.01.157>

Tangahu, B.V., Sheikh Abdullah, S.R., Basri, H., Idris, M., Anuar, N., Mukhlisin, M., 2011. A review on heavy metals (As, Pb, and Hg) uptake by plants through phytoremediation. *Int. J. Chem. Eng.* 2011. <https://doi.org/10.1155/2011/939161>

The Chemistry of Soils - Garrison Sposito - Google Books [WWW Document], n.d. URL [https://books.google.es/books?hl=en&lr=&id=XCJnDAAAQBAJ&oi=fnd&pg=PR9&dq=Soils&ots=iHm7gZBZ0D&sig=HY\\_wcJY8B7RT8Gnx9s6w3-bntmU&redir\\_esc=y#v=onepage&q=Soils&f=false](https://books.google.es/books?hl=en&lr=&id=XCJnDAAAQBAJ&oi=fnd&pg=PR9&dq=Soils&ots=iHm7gZBZ0D&sig=HY_wcJY8B7RT8Gnx9s6w3-bntmU&redir_esc=y#v=onepage&q=Soils&f=false) (accessed 7.5.21).

Tolu, J., Thiry, Y., Bueno, M., Jolivet, C., Potin-Gautier, M., Le Hécho, I., 2014. Distribution and speciation of ambient selenium in contrasted soils, from mineral to organic rich. *Sci. Total Environ.* 479–480, 93–101. <https://doi.org/10.1016/j.scitotenv.2014.01.079>

Tóth, G., Hermann, T., Da Silva, M.R., Montanarella, L., 2016. Heavy metals in agricultural soils of the European Union with implications for food safety. *Environ. Int.* 88, 299–309. <https://doi.org/10.1016/j.envint.2015.12.017>

Ulrich, A.E., 2019. Cadmium governance in Europe's phosphate fertilizers: Not so fast? *Sci. Total Environ.* <https://doi.org/10.1016/j.scitotenv.2018.09.014>

Usman, K., Al-Ghouti, M.A., Abu-Dieyeh, M.H., 2019. The assessment of cadmium, chromium, copper, and nickel tolerance and bioaccumulation by shrub plant *Tetraena qataranse*. *Sci. Rep.* 9. <https://doi.org/10.1038/s41598-019-42029-9>

VanGuilder, H.D., Vrana, K.E., Freeman, W.M., 2008. Twenty-five years of quantitative PCR for gene expression analysis. *Biotechniques* 44, 619–626. <https://doi.org/10.2144/000112776>

Verdoliva, S. G., Gwyn-Jones, D., Detheridge, A., & Robson, P. (2021). Controlled comparisons between soil and hydroponic systems reveal increased water use efficiency and higher lycopene and  $\beta$ -carotene contents in hydroponically grown tomatoes. *Scientia Horticulturae*, 279, 109896. <https://doi.org/10.1016/j.scienta.2021.109896>

Vries, W. de, Hettelingh, J.-P., Posch, M., 2015. Critical loads and dynamic risk assessments : nitrogen, acidity and metals in terrestrial and aquatic ecosystems.

- Wan, Y., Yu, Y., Wang, Q., Qiao, Y., Li, H., 2016. Cadmium uptake dynamics and translocation in rice seedling: Influence of different forms of selenium. *Ecotoxicol. Environ. Saf.* 133, 127–134. <https://doi.org/10.1016/J.ECOENV.2016.07.001>
- Wang, D., Zhou, F., Yang, W., Peng, Q., Man, N., Liang, D., 2017. Selenate redistribution during aging in different Chinese soils and the dominant influential factors. *Chemosphere* 182, 284–292. <https://doi.org/10.1016/j.chemosphere.2017.05.014>
- Wang, F., Lemes, M., Khan, M.A.K.K., 2011. Metallomics of Mercury: Role of Thiol- and Selenol-Containing Biomolecules. *Environ. Chem. Toxicol. Mercur.* 517–544. <https://doi.org/10.1002/9781118146644.ch16>
- Wang, J., Feng, X., Anderson, C.W.N., Wang, H., Zheng, L., Hu, T., 2012. Implications of mercury speciation in thiosulfate treated plants. *Environ. Sci. Technol.* 46, 5361–5368. <https://doi.org/10.1021/es204331a>
- Wang, S., Nan, Z., Prete, D., Ma, J., Liao, Q., Zhang, Q., 2016. Accumulation, transfer, and potential sources of mercury in the soil-wheat system under field conditions over the Loess Plateau, northwest China. *Sci. Total Environ.* 568, 245–252. <https://doi.org/10.1016/j.scitotenv.2016.06.034>
- Wang, X., Tam, N.F.Y., Fu, S., Ametkhan, A., Ouyang, Y., Ye, Z., 2014. Selenium addition alters mercury uptake, bioavailability in the rhizosphere and root anatomy of rice (*Oryza sativa*). *Ann. Bot.* 114, 271–278. <https://doi.org/10.1093/aob/mcu117>
- Wang, Y., Dang, F., Evans, R.D., Zhong, H., Zhao, J., Zhou, D., 2016. Mechanistic understanding of MeHg-Se antagonism in soil-rice systems: the key role of antagonism in soil. *Sci. Rep.* 6, 1–11. <https://doi.org/10.1038/srep19477>
- Wang, Y.D., Wang, X., Wong, Y.S., 2013. Generation of selenium-enriched rice with enhanced grain yield, selenium content and bioavailability through fertilisation with selenite. *Food Chem.* 141, 2385–2393. <https://doi.org/10.1016/j.foodchem.2013.05.095>

- Wu, J., Li, R., Lu, Y., Bai, Z., 2021. Sustainable management of cadmium-contaminated soils as affected by exogenous application of nutrients: A review. *J. Environ. Manage.* 295, 113081. <https://doi.org/10.1016/J.JENVMAN.2021.113081>
- Xiao, T., Boada, R., Llugany, M., Valiente, M., 2021. Co-application of Se and a biostimulant at different wheat growth stages: Influence on grain development. *Plant Physiol. Biochem.* 160, 184–192. <https://doi.org/10.1016/j.plaphy.2021.01.025>
- Xiao, T., Boada, R., Marini, C., Llugany, M., Valiente, M., 2020. Influence of a plant biostimulant on the uptake, distribution and speciation of Se in Se-enriched wheat (*Triticum aestivum* L. cv. Pinzón). *Plant Soil* 2020 455, 409–423. <https://doi.org/10.1007/S11104-020-04686-Y>
- Yarmolinsky, D., Brychkova, G., Fluhr, R., Sagi, M., 2013. Sulfite Reductase Protects Plants against Sulfite Toxicity. *Plant Physiol.* 161, 725. <https://doi.org/10.1104/PP.112.207712>
- Zembala, M., Filek, M., Walas, S., Mrowiec, H., Kornaś, A., Miszalski, Z., Hartikainen, H., 2010. Effect of selenium on macro- and microelement distribution and physiological parameters of rape and wheat seedlings exposed to cadmium stress. *Plant Soil* 329, 457–468. <https://doi.org/10.1007/S11104-009-0171-2>
- Zhao, F.J., Hawkesford, M.J., McGrath, S.P., 1999. Sulphur assimilation and effects on yield and quality of wheat. *J. Cereal Sci.* 30, 1–17. <https://doi.org/10.1006/JCRS.1998.0241>
- Zhou, J., Liu, H., Du, B., Shang, L., Yang, J., Wang, Y., 2015. Influence of soil mercury concentration and fraction on bioaccumulation process of inorganic mercury and methylmercury in rice (*Oryza sativa* L.). *Environ. Sci. Pollut. Res.* 22, 6144–6154. <https://doi.org/10.1007/s11356-014-3823-6>
- Zhou, X., Yang, J., Kronzucker, H.J., Shi, W., 2020. Selenium Biofortification and Interaction With Other Elements in Plants: A Review. *Front. Plant Sci.* <https://doi.org/10.3389/fpls.2020.586421>
- Zhu, J., Zhao, P., Nie, Z., Shi, H., Li, C., Wang, Y., Qin, S., Qin, X., Liu, H., 2020. 1Selenium supply alters the subcellular distribution and chemical forms of cadmium and the expression of

transporter genes involved in cadmium uptake and translocation in winter wheat (*Triticum aestivum*). *BMC Plant Biol.* 20, 1–12. <https://doi.org/10.1186/s12870-020-02763-z>



## ANNEX

### Characterization

#### Elemental concentration

The elemental analysis of the samples was performed using inductively coupled plasma mass spectroscopy (ICP-MS), Perkin Elmer Optima 8300. This technique allows analysing the liquid samples in organic and aqueous matrix. The argon plasma is used to ionize the atoms and uses mass per charge ratio to discriminate the desired analytes. This technique is very sensitive and can analyse down to few ppbs.

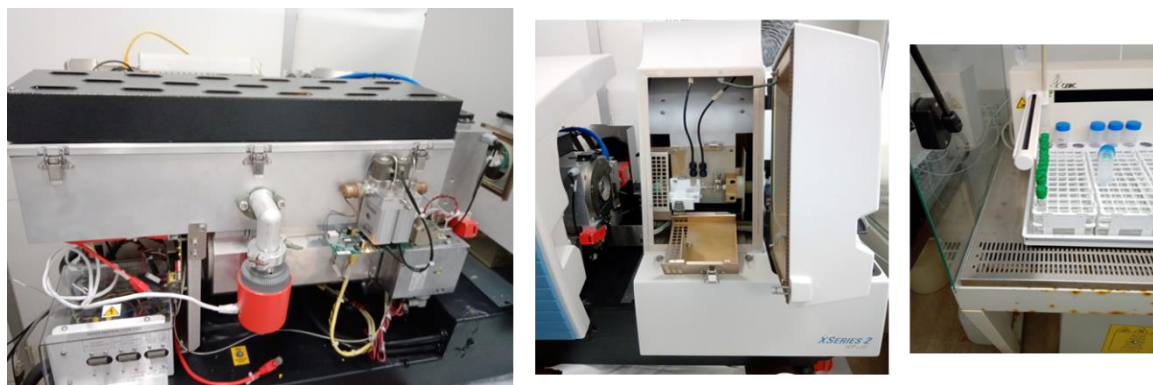


Figure 1: Elemental concentration identification ICP-MS

For these measurements, the plant samples were powdered and 100 mg of each sample was digested in the  $\text{HNO}_3:\text{H}_2\text{O}_2$  (7:3 v/v), the samples were diluted as suitable for ICP-MS measurements. The measurements were categorized based on their concentration in the plants and appropriate calibration for each element of interest was carried out before measuring with high sensitivity and coefficient of the elements. The calibration of each experiment was obtained from isotopes showing highest contribution and less error with good sensitivity. The steps followed in each experiment are explained in the respective chapters. The instrumentation and autosampler setup shown in the Figure 1.

## **X-ray absorption spectroscopy and X-ray fluorescence mapping**

XAS is an element specific technique which provides information about the chemical state and the short-range order structure of the element probed. Synchrotron-based XAS benefits from the high photon flux and the energy tuning capability over a large energy range of the synchrotron source. In the hard x-ray region, the X-ray photon primarily interacts with the core electron rather than the valence electron. The energy required for excitation of the core electrons depends on the electron binding energies and it is representative for each element. Based, on the excited state different edges can be measured, however K-edge (excitation from the 1s orbital) is the most commonly studied in the hard x-ray regime. Broadly, the XAS spectra can be divided in two different regions: XANES (X-ray absorption near edge structure) which is the regions around the absorption edge, and EXAFS (extended X-ray absorption fine structure), which comprises the spectral features present at higher energies, typically over 100eV from the absorption edge.

At the CLÆSS beamline in ALBA synchrotron, the synchrotron radiation is emitted by a wiggler source and monochromatized using a double crystal monochromator, Si(111) or Si(311). The rejection of higher harmonics was done by choosing proper angles and coatings of the collimating and focusing mirrors. The XAS spectra of the samples were collected in fluorescence mode using a multi-element silicon drift detector with Xspress3 electronics due to the lower elemental concentration (Se, Cd, Hg), while the reference spectra were measured in transmission mode using ionization chambers. High energy resolution XANES (HERFD-XANES) spectra were collected using the CLEAR emission spectrometer available at the beamline based on Johansson-like dynamical-bent diced-analyzer Si crystals for scanning-free energy dispersive acquisition. For the measurements, plant samples were made into 5 mm pellets, without adding any binding material. For the references, the appropriate amount for each compound to obtain the desired absorption jump was homogenized with cellulose and made into 5 mm pellets to study in transmission. Further details, regarding individual experiments were described in the experimental section of the chapters. The sample holder representative of pellets and grain sections are given in Figure 2.

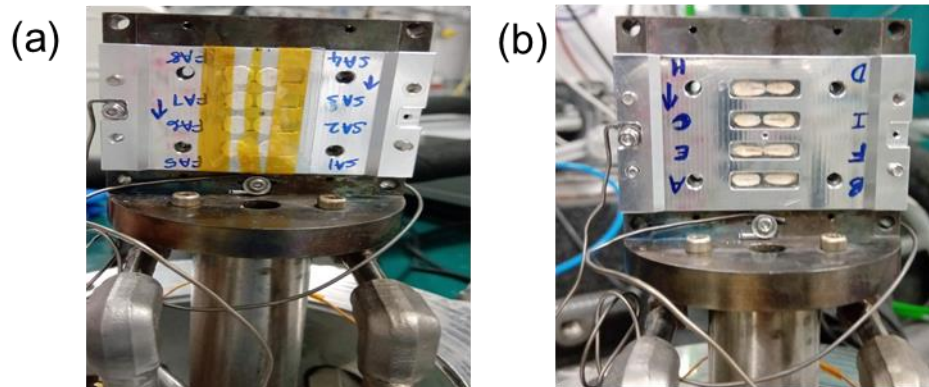


Figure 2: Sample holder mounted in liquid nitrogen cryostat setup grain pellets (a) and sections (b)

$\mu$ XRF (micro-focused beam X-ray fluorescence) maps of wheat grains sections were collected at CLAES using a pinhole of 50  $\mu\text{m}$  diameter and at the I18 microXRF beamline of the Diamond Light Source (undulator source and a Si(111) monochromator) using a  $4 \times 2 \mu\text{m}$  beam focused by a set of Kirkpatrick–Baez mirrors. Grains sections of 300  $\mu\text{m}$  thickness were obtained using LeicaVT1000S vibratome (settings: speed 3 and continuous mode). The sample grains were attached to the plate using super glue and immersed in a 30% glycerol bath. Sections were performed in a way that the different regions of the grain (eye, endosperm, filament and bran) were included in each section.

### Fourier infrared spectroscopy

FTIR can be used to identify both inorganic and organic elements in different states. It is a powerful tool for identifying various types of chemical bonds in an element by producing an infrared absorption spectrum that is like a molecular "fingerprint". Molecular bonds generally vibrate at various frequencies; thus, the absorption peaks correspond to the frequencies of vibrations between the bonds of the atoms making up the material. The functional groups present in the different parts of the plant were characterized by FTIR using a globular source. The samples were prepared by homogenizing 1 mg of plant samples in 99 mg of potassium bromide (KBr), from Sigma Aldrich IR grade and made into 13 mm thin pellets. The background was subtracted

using pure KBr pellet during the analysis. The measurements were carried out in transmission mode, at 36X with 30\*30  $\mu\text{m}$  aperture. Totally, 3 points per sample at different locations in the pellet, with three replicates where collected, with a total of 256 scans per point in the range of 400-4000  $\text{cm}^{-1}$ .

For the  $\mu\text{FTIR}$  measurements, 40  $\mu\text{m}$  thick sections were made with speed 1 in continuous mode. The sections were washed of surface glycerol and treated with 1% amylase solution at room temperature for 8 h for removing the starch (The instrumentation of the wheat sectioning in shown in Figure 3). The dried and treated sections were placed on CaF slides of 0.5 mm for the synchrotron-based IR analysis.



Figure 3: Vibratome (leica) used for wheat grain sectioning (right), sample mounted in glycerol bath (left).

### **Gene expression studies**

Quantitative PCR (qPCR) is a precise method used in molecular biology to quantify the expression of targeted genes. It is effective where the whole genome is not required, and either the gene or the pathway of interest is already known. Nowadays, strong efforts are invested in sequencing the plant genome and wide information is available covering different plant species

and their metabolism from databases like it occurs for Arabidopsis (VanGuilder et al., 2008). For wheat, the availability of the specific draft assembly of the wheat genome by the International Wheat Genome Sequencing Consortium (IWGSC) and release of several RNA-seq datasets played an important role in the study of gene functions (Appels et al., 2018).

The quantification of a gene expression is normally based on its relative expression respect to the expression of a reference gene, which is used as control. The reference genes are normally called housekeeping genes, as they are typically chosen in between the genes related to basic cell functions, which are expressed at constant rates. In the present case, the housekeeping genes have been chosen considering that their expression should be independent by the particular treatment applied (Se or Se+Cd), being the main objective to analyse targeted genes expression related to the applied treatments. Maxwell for plants was used for RNA extraction and cDNA was converted using thermofisher kit. Lightcycler was the instrument used for running the qPCR analysis. The conditions used for the studies and the genes for designed primers are explained in detail in the section 2.2. The steps and instrumentation of qPCR were shown in Figure 4.

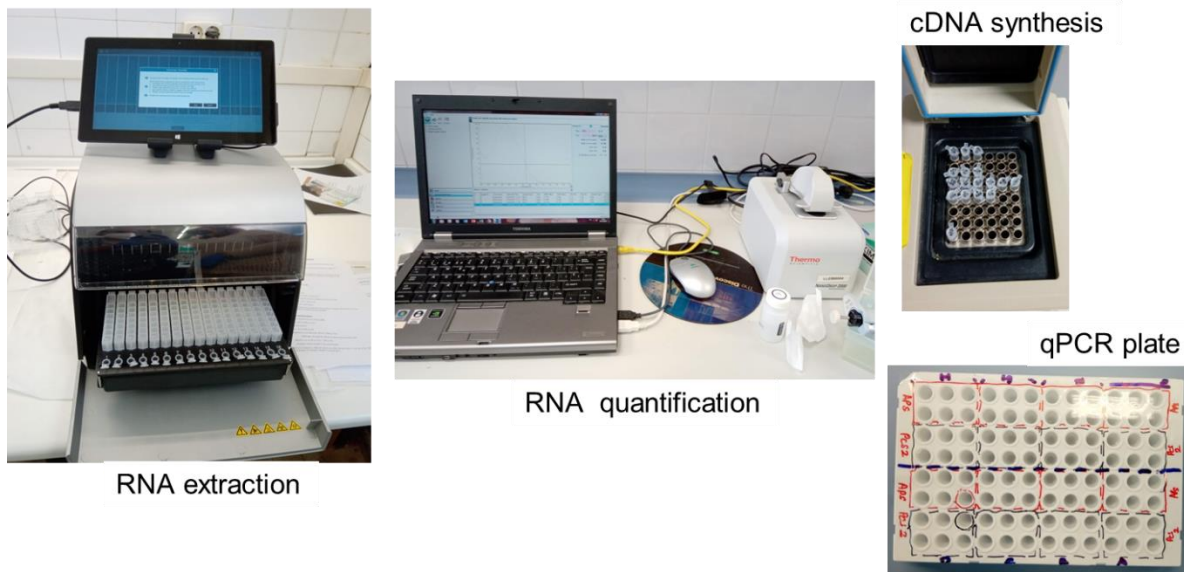


Figure 4: qPCR steps and characterization

## References

Appels, R., Eversole, K., Feuillet, C., Keller, B., Rogers, J., Stein, N., Pozniak, C.J., Choulet, F., Distelfeld, A., Poland, J., Ronen, G., Barad, O., Baruch, K., Keeble-Gagnère, G., Mascher, M., Ben-Zvi, G., Josselin, A.A., Himmelbach, A., Balfourier, F., Gutierrez-Gonzalez, J., Hayden, M., Koh, C.S., Muehlbauer, G., Pasam, R.K., Paux, E., Rigault, P., Tibbits, J., Tiwari, V., Spannagl, M., Lang, D., Gundlach, H., Haberer, G., Mayer, K.F.X., Ormanbekova, D., Prade, V., Wicker, T., Swarbreck, D., Rimbart, H., Felder, M., Guilhot, N., Kaithakottil, G., Keilwagen, J., Leroy, P., Lux, T., Twardziok, S., Venturini, L., Juhasz, A., Abrouk, M., Fischer, I., Uauy, C., Borrill, P., Ramirez-Gonzalez, R.H., Arnaud, D., Chalabi, S., Chalhoub, B., Cory, A., Datla, R., Davey, M.W., Jacobs, J., Robinson, S.J., Steuernagel, B., Van Ex, F., Wulff, B.B.H., Benhamed, M., Bendahmane, A., Concia, L., Latrasse, D., Alaux, M., Bartoš, J., Bellec, A., Berges, H., Doležel, J., Frenkel, Z., Gill, B., Korol, A., Letellier, T., Olsen, O.A., Šimková, H., Singh, K., Valárik, M., Van Der Vossen, E., Vautrin, S., Weining, S., Fahima, T., Glikson, V., Raats, D., Toegelová, H., Vrána, J., Sourdille, P., Darrier, B., Barabaschi, D., Cattivelli, L., Hernandez, P., Galvez, S., Budak, H., Jones, J.D.G., Witek, K., Yu, G., Small, I., Melonek, J., Zhou, R., Belova, T., Kanyuka, K., King, R., Nilsen, K., Walkowiak, S., Cuthbert, R., Knox, R., Wiebe, K., Xiang, D., Rohde, A., Golds, T., Čížková, J., Akpınar, B.A., Biyiklioglu, S., Gao, L., N'Daiye, A., Číhalíková, J., Kubaláková, M., Šafář, J., Alfama, F., Adam-Blondon, A.F., Flores, R., Guerche, C., Loaec, M., Quesneville, H., Sharpe, A.G., Condie, J., Ens, J., Maclachlan, R., Tan, Y., Alberti, A., Aury, J.M., Barbe, V., Couloux, A., Cruaud, C., Labadie, K., Mangenot, S., Wincker, P., Kaur, G., Luo, M., Sehgal, S., Chhuneja, P., Gupta, O.P., Jindal, S., Kaur, P., Malik, P., Sharma, P., Yadav, B., Singh, N.K., Khurana, J.P., Chaudhary, C., Khurana, P., Kumar, V., Mahato, A., Mathur, S., Sevanthi, A., Sharma, N., Tomar, R.S., Holušová, K., Plíhal, O., Clark, M.D., Heavens, D., Kettleborough, G., Wright, J., Balcárková, B., Hu, Y., Ravin, N., Skryabin, K., Beletsky, A., Kadnikov, V., Mardanov, A., Nesterov, M., Rakitin, A., Sergeeva, E., Kanamori, H., Katagiri, S., Kobayashi, F., Nasuda, S., Tanaka, T., Wu, J., Cattonaro, F., Jiumeng, M., Kugler, K., Pfeifer, M., Sandve, S., Xun, X., Zhan, B., Batley, J., Bayer, P.E., Edwards, D., Hayashi, S., Tulpová, Z., Visendi, P., Cui, L., Du, X., Feng, K., Nie, X., Tong, W., Wang, L., 2018. Shifting the limits in wheat research and breeding using a fully annotated reference genome. *Science* (80-). 361. <https://doi.org/10.1126/science.aar7191>

VanGuilder, H.D., Vrana, K.E., Freeman, W.M., 2008. Twenty-five years of quantitative PCR for gene expression analysis. *Biotechniques* 44, 619–626. <https://doi.org/10.2144/000112776>